Editor of *Geoscientific Model Development*

Dear Editor,

we received the Reviewers' reports on our manuscript entitled "Spatio-temporal dynamics of mercury concentration in the Augusta Bay (southern Italy): matching model and data" by G. Denaro, D. Salvagio Manta, A. Borri, M. Bonsignore, D. Valenti, A. Cucco, B. Spagnolo, M. Sprovieri, A. De Gaetano.

We thank you and the Reviewers for the constructive comments and criticisms, which definitively helped us to improve the model and the manuscript. We took into account all the specific points raised by the referees and submit a revised version of the manuscript. Detailed discussions and corrections are listed below. Please note that we highlighted in red words and/or sentences which we removed from the old version, and in blue words and/or sentences inserted in the revised version.

Reviewer 1

A.General

1. **Reviewer** wrote:
   Introduction: I am missing a more comprehensive overview of Hg modelling performed on the scale of the Mediterranean Sea and its parts. The authors do not report any of the 2D and 3D models developed and applied before this study. These models, although not as complex as the presented HR3DHG, were also supported by a hydrodynamic model and performed quite well at the scale of the entire Mediterranean and at smaller scale (Gulf of Trieste, Adriatic Sea) with regard to both transport and transformations of two or three Hg species. My suggestion to the authors would be to investigate the article by Zhu et al. (https://doi.org/10.1016/j.scitotenv.2018.04.397) and the references therein, and to include the previously developed multi-dimensional models into the section Introduction. The same comment is valid for the chapter Discussion: 2D and 3D models were used before the HR3DHG model.

   Authors answer:
   The Introduction section has been modified according to the reviewer's suggestions. Specifically, we inserted the following paragraph at page 3, lines 49-67, of the new version of manuscript:
   "In general, the appropriate modelling to reproduce the spatial and temporal variability of Hg species in highly heterogeneous marine ecosystems, such as Augusta Harbour, requires the use of a hydrodynamics model integrated with a biogeochemical model (Zagar et al., 2007, 2014). To this aim, Zagar et al. (2007) introduced a PCFLOW3D model upgraded with the biogeochemical module for simulating simultaneously velocity field of marine currents, suspended particles transport and mercury biogeochemical transformations for the whole Mediterranean Sea. (...) Among these, Zhang et al. (2014) reproduced the $[Hg_T]$ in oceans and calculated a Hg mass balance by using a 3D ocean tracer model (OFFTRAC) coupled with a general circulation model (GEOS-Chem) (Zhang et al., 2014). Here, the sinking flux of Hg bound to POM was calculated exploiting the remote sensing data for net primary production (NPP) and chlorophyll concentration, which are associated to phytoplankton abundance."
   We also added the following two new sentences at page 26 of Discussion section:
   "For comparison, the different approach used in the WASP models did not allow to reproduce the dynamics of mercury concentration distribution at 3D high resolution in polluted sites characterized by elevated spatial heterogeneity. (...) In general, only few models (Rajar et al., 2007; Zagar et al., 2007; Canu et al., 2017) were able to make forecasts about the mercury depletion time in the sediment compartment of highly polluted sites, such as Augusta Bay."

2. **Reviewer** wrote:
   Sensitivity analysis confirms high significance of circulation (Line 501). Is therefore the constant-density approach correct? Non-stratified conditions are acceptable in winter months, while the temperature stratification in the summer may significantly influence the circulation and the fluxes through the picnocline. Whether to use stratified or non-stratified conditions depends on temporal resolution applied: with seasonal (or finer temporal resolution) stratified conditions should be taken into account.

Authors answer:

We followed a constant-density approach being the water circulation in the bay mainly ruled by the wind and tidal forcing only. Density gradients and the stratification were not strongly affecting the bay water circulation. This was suggested in previous modelling works of De Marchis et al. (2014) and Lisi et al. (2009). The latter, in particular, suggested that the water circulation in the Augusta bay is influenced mainly by tides and wind and the harbour can be investigated as a lagoon.

In the Section S3.2 of the new version of Supplement, some paragraphs have been inserted to clarify and improve this point.

3. **Reviewer** wrote:

To proceed with the same concern: the temporal and spatial dynamics of the simulations are unclear. Several questions arose during reading:

a) How were data from various seasons (Fig 1) taken into account (for calibration/validation)? Particularly when the constant water-density was accounted for in the model.

b) What is the temporal resolution of hydrodynamics (real-time = hourly, or any other resolution) used in transport simulations, and how often was the velocity field changed in a long-term simulation? Was a perpetual year used or did the conditions change (using any of the possible IPCC scenarios for changing climate conditions or anything similar)? A 250-year simulation would require an explanation of the applied parameters.

c) When adapting hydrodynamics from the SHYFEM model to the HR3DHG grid, were the velocities interpolated to the HG grid or integrated over the cells of the HG grid? When using real-time hydrodynamics, the correct transport can only be achieved by integration.

d) A table with temporal dynamics of each of the variables and (environmental) parameters would be useful. I.e. how often are the input parameters changed (annually/seasonally/weekly) and in which way the results were obtained (re-initialisation with experimental data/a single long simulation for 250 years?)

Authors answer:

About the various points:

a) The calibration procedure, together with the experimental data involved, is reported in the Section 3.3 of main text at pages 17-18, lines 463-487. The experimental findings involved in the validation of model results, are listed at the ending of the Section 3.3 of main text.

b) The temporal resolution of hydrodynamics is set to three hours (see page 22 of Section S3.2 of Supplement), as a consequence the velocity field changes 2920 times for each simulation year.

In our simulations, we used a perpetual year (see the ending of Section S3.2 of Supplement).

The most part of parameters does not depend on environmental variables. However, we are aware that some parameters (biological rate constants in seawater, methylation/de-methylation rate constants in sediments, desorption rate etc) are strictly connected with environmental variables (NPP, temperature etc.). Although we know that the model results could change significantly if the effects of climate changes on our parameterization were considered, currently we could not enough and robust information to simulate the mercury dynamics for different future scenarios. Following suggestions from the second reviewer, we also removed any reference to the climate changes.

c) The velocities obtained by the SHYFEM model were interpolated to the HR3DHG grid. Specifically, the velocity field used as the dataset for the interpolation was derived from a time average procedure of the SHYFEM model output produced at hourly frequency in order to have a three-hours residual velocity field. The obtained dataset consisting in three-hours time averaged velocity field was then used as input data for the interpolation. Considering the circulation within the bay is mostly homogeneous and the spatial discretization used by the HR3DHG comparable to the spatial scale of the flow variability, the adopted interpolation procedure was sufficiently accurate to reproduce the original hydrodynamic model dataset time and space variability.

The detailed interpolation procedure is reported at page 22, lines 561-566, of the Supplement.

d) The Table S2 (environmental variables used in the model) has been modified according to the reviewer's indications. The model results were obtained by running a single long simulation for 250 years (see pages 16-17, lines 443-446, of

the new version of manuscript).

4. **Reviewer** wrote:
Another question is the agreement of simulated and experimental results:
a) The complexity of the model requires thorough verification, calibration and validation. In order to confirm an "excellent agreement of the model with experimental data", validation of the model should have been performed with calibrated parameters. Was such a procedure done and if yes, on which temporal scale? The latest available experimental data are from 2017, and the modelling results for 2017 can be reproduced from the initial 2005, 2011 or 2012 experimental data. How different would be the modelling results for 2017 using the same set of calibrated parameters? In any case, it is very difficult to justify results of a 250-year long simulation even without the climate and other environmental changes that may occur in such a long time interval.
b) Several statistical methods for evaluation of model efficiency (Nash-Sutcliffe, Kling-Gupta, rmse) can be applied in order to quantify the agreement with experimental data. The results of these tests would give a better impression on the model performance than qualitative description by using excellent/good/poor based on visual agreement between figures.

Authors answer:
About the various points:
a) The validation of model results with calibrated parameters has been performed (see Section 4.1 of the new version of manuscript). Specifically, the theoretical results for $[MeHg_D]$, $[Hg_D]$ and $[Hg_T]$ were validated with the respective experimental data measured in seawater between May 2011 and October 2017, while all annual Hg fluxes obtained by modelling were validated with those estimated empirically by Salvagio Manta et al. (2016) for the sampling period May 2011- June 2012.
All model results have been obtained by using the same set of calibrated parameters.
About climate changes, we know that the model results could change significantly if the effect of environmental changes was considered, however we would need more information to simulate the mercury dynamics for the different future scenarios. See comments reported in the previous point.
b) The results of some statistical checks performed on $[MeHg_D]$, $[Hg_D]$ and $[Hg_T]$ are reported at pages 19-20 of the new version of manuscript. Specifically, a statistical analysis based on the χ^2 test is now introduced for $[MeHg]$, while a quantitative comparison between the model results and field observations for the $[Hg_D]$ and $[Hg_T]$ is performed on the basis of observed experimental error. In fact, we could not make the χ^2 test for $[Hg_D]$ and $[Hg_T]$ since their magnitude were below the detention limit in many sampling points. Moreover, the most part of the experimental data for $[Hg_D]$ and $[Hg_T]$ were acquired only in two/three sampling points for each station. For these reasons, we chose to make an alternative statistical check for $[Hg_D]$ and $[Hg_T]$.

5. **Reviewer** wrote:
Mass balance (Table S9 and Conclusions lines 544-545):
a) In the section Conclusions (line 544) the authors discuss the mass balance, which has never been established and presented. A mass balance should consist of quantities of the species under consideration (inventories) and fluxes, and in most cases, (see the references in Zhu et al.) such balances are presented in graphical form.
b) What is the inventory of (at least HgT) in the domain and in each of the compartments (water/sediment)? How do the fluxes affect the inventory? All that is evident from the numbers in the Table S9 is the constant decrease of the fluxes. Is the presented mass balance obtained solely from the results of the model or is it supported by experimental results? Furthermore, is the annual balance closed or open? With steadily decreasing fluxes and the deposition remaining more or less unchanged (term AD in Table S9), the inputs and the outputs should balance once in the future. When?

Authors answer:
About the various points:

a) The mass balance for Hg_T is introduced in the Section 3.1.1 of the new version of manuscript, while the scheme of transport processes (fluxes) at the boundaries of domain is reported in the new Figure 3 (see also the new caption of Figure 3). Moreover, we recall that the annual fluxes of $MeHg$ are estimated by our model, even if they cannot validated with experimental findings on the contrary of Hg_T. For this reason, the mass balance for MeHg has been not reported in the paper.

b) The Hg_T mass balance is performed only for seawater compartment.

The effects of the fluxes on the mercury concentration are described throughout the Section 4.1 of the new version of the manuscript. For example, we reported at page 20 the following assertion:

" It should be noted that the model results suggest that the benthic Hg_D fluxes are mainly generated by the diffusion process at the seawater-sediment interface and that the amount of Hg_D release from the re-suspended particulate matter is negligible."

Also, we inserted the following sentence at page 24 of the new version of manuscript:

" In general, the contribute of AD is negligible in the mercury mass balance of the Augusta Bay. Indeed, the simulations indicate that a strong increase of atmospheric mercury deposition caused by environmental changes (dust fall increase and/or rainfall increase), would not affect on numerical results of our model significantly."

About the presented mass balance, we recall that the annual mercury fluxes obtained by our model are compared with those obtained by Salvagio Manta et al. (2016) using the experimental data collected during the sampling period May 2011- June 2012 (see pages 21-23 of the new version of manuscript). The results of this comparison indicates a good agreement only for the mercury evasion flux (V) at atmospheric-seawater interface.

The Hg_T mass balance is open. According to this, we inserted three new paragraphs at page 24 of the new version of manuscript:

"In this work, the annual recycled mercury flux (D) is calculated by subtraction using the mass balance equation (18), (...). Here, values calculated by our model (2.50 $kmol\ y^{-1}$ for the year 2011 and 2.46 $kmol\ y^{-1}$ for the year 2012) are larger and probably more realistic than those estimated in Salvagio Manta et al. (2016) (0.84 $kmol\ y^{-1}$). (...)

In order to reproduce the effects induced by scavenging process on the mercury dynamics, our model calculates the annual sinking mercury flux, whose results are shown in Fig. 6d. Here, a significant gap between the recycled flux (2.50 $kmol\ y^{-1}$ for the year 2011) and the sinking flux (0.07 $kmol\ y^{-1}$ for the year 2011) is observed probably due to the underestimation of the amount of mercury captured by POM (see Eqs. (4)-(5)). (...)

On the contrary, very high values of the annual Hg_T accumulation rate in surface sediment layer (12.07 $kmol\ y^{-1}$ for the year 2011), respect to those of the annual recycled flux (2.50 $kmol\ y^{-1}$ for the year 2011), are obtained by our model. (...) In fact, the results obtained by the sediment transport model indicate a low average sedimentation rate for the Augusta Bay."

The benthic mercury flux decreases slowly at quasi-steady state (0.12 percent for $t_{max} = 250\ years$). Therefore, it will remain quite high for a very long time (more than 250 years). As a consequence, we aspect that the balance between the inputs and the outputs may occur only after several centuries.

B. Details (manuscript):

6. **Reviewer** wrote:

Line 73: Rajar et al. (doi:10.1016/j.marchem.2006.10.001) and Zagar et al. (DOI 10.1007/s11356-013-2055-5) established two (annual) Hg mass balances in the Mediterranean Sea. There, the atmospheric deposition and the rivers contributions were found to be significantly more important than any of the point sources. In order to support the statement that "the Augusta Bay has a key role in Mediterranean Hg inventory" this role should be quantified and compared to the previously published values.

Authors answer:

According to the reviewer's indication, we inserted the following sentence at page 5, lines 121-123, of the new version of manuscript:

"The estimate of the Hg export from Augusta Bay to the open sea (0.54 $kmol\ y^{-1}$, Salvagio Manta et al., 2016), corresponds to about 4% of total input from coastal point/diffuse sources to the Mediterranean Sea (12.5 $kmol\ y^{-1}$, Rajar et al., 2007)."

7. **Reviewer** wrote:
Lines120-121: The sentence explaining why the results were unaffected by the chosen initial condition is not clear.

Authors answer:
The paragraph on the initial condition has been moved in the "Model and simulation setup" Section according to the second reviewer's indication. Moreover, we modified the sentence at page 16, lines 441-442, of the new version of manuscript, as follows:
" The numerical results were not affected by the chosen initial conditions, indeed the same spatial distribution of $[Hg]$ at nearly-steady state was obtained when higher initial Hg concentrations than detection limit were fixed."

8. **Reviewer** wrote:
Line 149: What is the temporal resolution of hydrodynamics? I.e., how many different velocity fields were used for computing transport?

Authors answer:
The temporal resolution of hydrodynamics is set to three hours (see page 22 of Section S3.2 of Supplement), as a consequence the velocity field changes 2920 times for each simulation year.

9. **Reviewer** wrote:
Lines 320-340: Were the results of the calibration procedure constant or variable (in time) input parameters? If temporally constant, for which period (set of measurements). Were the same constant coefficients used for another time interval between measurements? If variable, on what temporal scale?

Authors answer:
The input parameters obtained by the calibration procedure were temporally constant. Since the acquisitions of all experimental data were performed for time limited periods, we used for each calibrated parameter different set of measurements collected during different sampling periods. The same constant coefficients were used for the whole time simulation. Conversely, the photo-chemical and biological rate constants changed as a function of time due to the seasonal oscillations of RAD and NPP (see Section S1 of Supplement).

10. **Reviewer** wrote:
Figure 6: Shows a decreasing trend for all fluxes. The Hg inventory in the Bay is most probably decreasing as well (unfortunately the mass balance is not established in a way to either confirm or contradict this hypothesis). Were these results obtained by accounting for computed or measured deposition? There is a high discrepancy (factor2.5) between these two values. As reported by several previous modelling/mass balance studies (Zhu et al., and the references therein), deposition is a very important source of Hg in the Mediterranean. Including deposition into the performed sensitivity analysis would be very useful for clarification of this question.

Authors answer:
The reviewer is right. The Hg concentrations follow the same decreasing trend of all fluxes. The annual mass balance for mercury is now described in complete way throughout the Section 4.1 of new version of manuscript. In particular, we explain the reason of high discrepancy between our model result and that estimated in experimental work by Salvagio Manta et al. (2016), at page 22, lines 581-586, of new version of manuscript:
"This discrepancy is due to different calculation methods used in the two works. Specifically, in our model the AD is calculated by using both the atmospheric mercury concentrations and the average precipitations, measured for all months of the year. On the contrary, in Bagnato et al. (2013) the AD is calculated by averaging the experimental data acquired during a time limited sampling period (from 29^{th} August 2011 to 23^{th} April 2012), namely without considering the year period in which the amount of precipitation is very low. By this way, the AD obtained by Bagnato et al. (2013) is very higher than that of our model, even if it is probably overestimated due to calculation method used."
Moreover, a rough sensitivity analysis has been performed on the atmospheric deposition calculated in our model. According to this, we inserted at page 24, lines 586-589, of new version of manuscript the two following sentences:
" In general, the contribute of AD is negligible in the mercury mass balance of the Augusta Bay. Indeed, the simulations

indicate that a strong increase of atmospheric mercury deposition caused by environmental changes (dust fall increase and/or rainfall increase), would not affect on numerical results of our model significantly."

C. Details (Supplement):

11. **Reviewer** wrote:
References to Figs in the supplement should be noted as eg. Fig S5, not Fig 5.

    Authors answer:
    We modified the references to Figures in the Supplement.

12. **Reviewer** wrote:
In several equations the annual flux is debated. Were fluxes calculated also on seasonal (or finer) temporal scale?

    Authors answer:
    The fluxes were calculated for each node of 3D grid using a finer temporal scale. Specifically, the our code allowed to print all fluxes for each node of grid and for each month of year.

13. **Reviewer** wrote:
Equations S8 and S21: Where is the dry deposition, as the first term in line 59 and the most right-hand term in S21 only have the wet part, connected to precipitation P?

    Authors answer:
    Following the reviewer's suggestions, in new simulations we considered the dry deposition of Hg^{II} and $MeHg$ at atmosphere-seawater interface, while only the wet deposition is taken into account for Hg^0. According to this, we modified the text and the equations of Sections S1.1.1, S1.2.1 and S1.3.1 of Supplement.

14. **Reviewer** wrote:
Equations S23 (and S37): if tortuosity is not taken into account in neither Dw-in (or Dw-or) nor δ_w , please explain whether and how this is compensated in the equation.

    Authors answer:
    We better explained the relation between tortuosity and porosity at page 10, lines 230-231, of the new version of Supplement.

15. **Reviewer** wrote:
Tables S4, S10: The presented concentrations are given for 2011 and 2017. Any other comparison possible?

    Authors answer:
    No other comparison is possible.

Reviewer 2

1. **Reviewer** wrote:
L4-5: why is the sediment module presented as two different models?

    Authors answer:
    There is only one model for the sediment compartment. To clarify this point, we modified the sentence at page 1, lines 4-6, of Abstract as follows:
    "... an advection-diffusion-reaction model for the dissolved mercury in the seawater compartment coupled with a diffusion-reaction model for dissolved mercury in the pore water of sediments, in which the de-sorption process for the sediment total mercury is taken into account."

2. **Reviewer** wrote:
L5: an adsorption/desorption model would need an adsorption and desorption rate constants, while here do you have a desorption rate constant combined with the Kd. I am concerned about this approach, given that the Kd represents the ratio between adsorption and desorption rate constants at the equilibrium. Can you provide a theoretical background for the parameterization chosen?

Authors answer:
The purpose of diffusion-reaction model was to reproduce the spatio-temporal behaviour of dissolved mercury in the pore water of sediments in quasi-steady conditions (instead of the customary stationary conditions used in other models). To this aim, in the model differential equations we did need to consider both the sediment - pore water distribution coefficients and the desorption rate for the total mercury concentration in the sediment. The former described the ratio between adsorption and desorption rate constants at the steady state without considering pertubations induced by mercury concentration reduction in pore water. The latter reproduced the effects of these pertubations on the solid phase of the sediments. The sediment - pore water distribution coefficients were fixed by using the experimental data, while the desorption rate for the total mercury concentration in the sediment was calibrated to obtain the best fit with the experimental mercury concentrations in pore water.
According to this, we inserted three sentences at pages 3-4, lines 84-88, of the new version of manuscript.

3. **Reviewer** wrote:
L5-7 "the spatio-temporal variability of dissolved and total mercury concentration both in seawater ([HgD] and [HgT]) and first layers of bottom sediments ([HgsedD] and [HgsedT]), and the Hg fluxes at the boundaries of the 3D model domain have been theoretically reproduced, showing an excellent agreement with the experimental data". This sentence is not clear and misleading. It should be said what is simulated with the biogeochemical model (HgD) and what is estimated with other methods (HgT). Avoid claiming excellent agreement that is not supported by facts.

Authors answer:
To clarify this point, we modified the sentences at page 1, lines 5-10, of Abstract as follows:
"The spatio-temporal variability of mercury concentration both in seawater ($[Hg_D]$) and first layers of bottom sediments ($[Hg_D^{sed}]$ and $[Hg_T^{sed}]$), and the Hg fluxes at the boundaries of the 3D model domain have been theoretically reproduced, showing an acceptable agreement with the experimental data, collected in multiple field observations during six different oceanographic cruises. Also, the spatio-temporal dynamics of total mercury concentration in seawater have been obtained by using both model results and field observations." Moreover, the word "excellent" has been replaced by the word "acceptable" throughout the whole manuscript.

4. **Reviewer** wrote:
L8-9 "The mass-balance of the different Hg species in seawater has been calculated for the Augusta Harbour, improving previous estimations" I only found the budget for HgT, not for other Hg species.

Authors answer:
Only the budget for HgT is calculated. In accordance with the reviewer's comment, we modified the sentence as follows: "The mass-balance of the total Hg in seawater has been calculated for the Augusta Harbour, improving previous estimations."

5. **Reviewer** wrote:
L10-11 "The HR3DHG 10 model includes modules that can be implemented for specific and detailed exploration of the effects of climate change on the spatio-temporal distribution of Hg in highly contaminated coastal-marine areas." This is never shown or discussed in the manuscript, except for a couple of similar mentions at the end of the Introduction and Discussion, so I do not find it relevant nor true.

Authors answer:
The effects of climate changes were not discussed in the manuscript. We removed the sentence. Moreover, we modified the ending of the abstract as follows:

"The HR3DHG model could be used as an effective tool to predict the spatio-temporal distributions of dissolved and total mercury concentrations, while contributing to better assess the hazard for environment and therefore for human health in highly polluted areas."

6. **Reviewer** wrote:
L18: why sophisticated?

Authors answer:
We replaced the word "sophisticated" with the word "innovative".

7. **Reviewer** wrote:
L20: Among the references cited to support this sentence, only the work Melaku Canu et al., (2015) is based on the WASP model. Zhang et al., (2014) do not use a box model, but a 3D ocean tracer model (OFFTRAC) coupled with a general circulation model. Ciffroy et al., (2015) use the MERLIN-Expo model, as explained just below by the authors. Other works based on the WASP model are Canu and Rosati (2017) and Rosati et al., (2018). There are also other applications of biogeochemical models specific for mercury in water (and thus more relevant here than the MERLIN-Expo model) that are never mentioned. I suggest modifying the paragraph and correcting the references after carrying out a more systematic review.

Authors answer:
We correct the references throughout the paragraph. We also modified the paragraph as follows:
"Over the last few years some theoretical studies have offered innovative tools to reproduce the mass balance and the dynamics of $[Hg]$ in the marine environment by means of biogeochemical models based on interconnected zero dimensional boxes, representing water or sediment compartments: among these are the River MERLIN-Expo model (Ciffroy et al.,(2015)) and the WASP (Water Analysis Simulation Program) model (Melaku Canu et al., (2015), Canu and Rosati (2017) and Rosati et al., (2018)). (...) The WASP models have been used to simulate the Hg cycle within aquatic ecosystems characterized by well-mixed water layers and homogeneous sediment layers coupled through the boundary conditions at the water-sediment interface (Melaku Canu et al., 2015, Canu and Rosati, 2017, Rosati et al. 2018). In particular, a WASP model applied to a 1D domain and calibrated by using experimental data for dissolved Hg and $MeHg$, allowed to explore $[Hg]$ dynamics in the Black Sea (Rosati et al. 2018)."
Moreover, we inserted in page 3, lines 49-67, the following new paragraph:
"In general, the appropriate modelling to reproduce the spatial and temporal variability of Hg species in highly heterogeneous marine ecosystems, such as Augusta Harbour, requires the use of a hydrodynamics model integrated with a biogeochemical model (Zagar et al. (2007)). (...) Here, the sinking flux of Hg bound to POM was calculated exploiting the remote sensing data for net primary production (NPP) and chlorophyll concentration, which are associated to phytoplankton abundance."

8. **Reviewer** wrote:
L21: As before, the citation "Zhang et al., (2014)" is unrelated to the sentence.

Authors answer:
The reference has been removed. Moreover, we inserted the citation "Canu and Rosati (2017)".

9. **Reviewer** wrote:
L21: I suggest to change "WASP-based approach" with box model approach.

Authors answer:
We replaced " ‘WASP-based approach" with "box model approach".

10. **Reviewer** wrote:
L22-25: "Similarly, a box-model approach has been adopted by the River MERLIN Expo model (Ciffroy, 2015), which has been used to reproduce the spatio-temporal distribution of inorganic and organic contaminants in the abiotic compartments of rivers, and to calculate [Hg] mass balance for each of them." The reference here provided "Ciffroy et

al.,(2015)" seems to be the model documentation https://merlin-expo.eu/wpcontent/uploads/2015/10/Documentation-River-V2.1.pdf I could not find any case study for Hg in the reference provided.

Authors answer:
The cited paper "Ciffroy et al.,(2015)" have no case study for mercury. However, the River Model reproduces the 1-D distribution of inorganic and organic contaminants and calculates the mass balance for each of them. According to this, we modified the sentence as follows:
"The River MERLIN-Expo model (Ciffroy et al.,(2015)) has been used to reproduce the spatio-temporal distribution of inorganic and organic contaminants in the 1D domain of rivers, and to calculate the mass balance for each of them."
The sentence has been moved at the beginning of the paragraph.

11. **Reviewer** wrote:
L25-27: "Although the River model is able to describe many of the physical and chemical processes involved in freshwater and sediment, corresponding this model specifically targets environments characterized by (i) nearly-homogeneous water bodies and (ii) limited variations in landscape geometry." The Introduction begins stating the importance of "biogeochemical dynamics of Hg species in the marine environment", and then it goes on with the WASP model that is specific for Hg. Why does it now go back to a general model for contaminants in freshwater and sediment and neglect other existing models?

Authors answer:
The sentence has been moved at the beginning of the paragraph. Other existing models are presented now in the Introduction.

12. **Reviewer** wrote:
L27-28: "In general, models based on zero dimensional boxes do not deliver reliable concentration values of contaminants in highly heterogeneous environments." I suggest rewording this sentence. Zero dimensional boxes models can provide reliable concentrations as much as other models. Box models can be less or more accurate than other models depending on the parameterizations used and on the spatial resolution, which however could be very fine.

Authors answer:
The sentence has been modified as follows:
"In general, models based on zero dimensional boxes do not deliver reliable concentration values of contaminants in highly heterogeneous environments unless they provide high spatial resolution and a proper parameterization of the biogeochemical system."

13. **Reviewer** wrote:
L28-34: "[...] in more recent works (Yakushev et al., 2017; Pakhomova et al., 2018) the biochemistry of Hg in aquatic ecosystems has been studied using a 1D advection reaction-diffusion model: the Bottom RedOx Model (BROM) has been used to reproduce the vertical dynamics of the total dissolved Hg and MeHg in the marine coastal areas of the Etang de Berre lagoon (France) (Pakhomova et al., 2018). However, even the BROM includes some criticalities in the estimation of mercury dynamics [...]" Why should a1D model be better than a box model for highly heterogeneous environments? Also, the reference "Yakushev et al., 2017" refers to the original BROM model formulation for water and sediment biogeochemistry but not Hg, I think it doesn't need to be here.

Authors answer:
In accordance with the reviewer's comment, the paragraph has been modified as follows:
"For this reason, in a recent work (Pakhomova et al., 2018) the biochemistry of Hg in aquatic ecosystems has been studied using a high resolution (HR) 1D advection-reaction-diffusion model, in which a mercury module has been integrated with the Bottom RedOx Model (BROM) (Yakushev et al., 2017) to reproduce the vertical dynamics of the total dissolved Hg and $MeHg$ in the marine coastal areas of the Etang de Berre lagoon (France) (Pakhomova et al., 2018). However, even this model includes some criticalities in the estimation of mercury dynamics. For example, the temporal variations of mercury benthic fluxes, due to reaction and diffusion processes which involve mercury species present in sediments, are not taken into account in the boundary conditions of this model. On the other hand, the sediment

chemistry and diffusion were investigated recently by Soerensen et al. (2016), who implemented a high resolution 1D model for Hg species in the water and sediments of the Baltic Sea. In both HR models, however, the strong impact of the horizontal velocity field on the spatio-temporal distribution of $[Hg]$ could not be considered since the 1D modelling was used."

14. **Reviewer** wrote:
L35-38: "All these approaches forego the complete representation of the spatial variability by approximating the model domain as a set of interconnected boxes or by detailing only the vertical dynamics of the investigated chemical species. In the present work we report on results obtained using a 3D advection-diffusion-reaction biogeochemical model for three Hg species in seawater (Hg0, HgII , and MeHg), coupled with a diffusion-reaction model in sediments and connected pore water.". This part needs rewording. No model can achieve a "complete representation of the spatial variability".

Authors answer:
To clarify, we modified the paragraph as follows:
"All these approaches do not allow a fine representation of the spatial variability by approximating the model domain as a set of interconnected boxes or by detailing only in seawater compartment the spatio-temporal dynamics of the investigated chemical species. For these reasons, we devised a new model to reproduce the spatio-temporal dynamics of $[Hg]$ in polluted marine sites characterized by very high spatial heterogeneity, such as the Augusta Harbour. In the present work we report on results obtained using a 3D advection-diffusion-reaction biogeochemical model for three Hg species in seawater (Hg^0, Hg^{II}, and $MeHg$), coupled with a diffusion-reaction model for dissolved mercury in the pore water of sediments."

15. **Reviewer** wrote:
L43: has the model been validated? Where is this explained in the text?

Authors answer:
The explanation of the calibration and validation is reported in Section 3.3.

16. **Reviewer** wrote:
L46: how exactly can this model be useful "to explore the effects of sorption-desorption dynamics"?

Authors answer:
The word "sorption" has been deleted by the sentence. Indeed, the equation for the dynamics of total mercury concentration in sediments takes into account only the de-sorption process, which mimics the "response" of solid particles to a perturbation of sorption/de-sorption equilibrium, triggered by a slowly decrease of dissolved mercury concentration in the pore water. For more details, please refer to answer n. 2.

17. **Reviewer** wrote:
L47: how can this model addresses the "role played by the spatio-temporal behavior of phytoplankton and the potential mechanism responsible for the uptake of Hg within the cells"?

Authors answer:
The sentence has been modified as follows:
"Moreover, the role played by the spatio-temporal behaviour of phytoplankton and the mechanisms responsible for the uptake of Hg within cells is taken into account as specific contribution to the scavenging process and the Hg release process by POM, respectively."

18. **Reviewer** wrote:
L58-61: here I would like to read something more informative such as the paper aim.

Authors answer:
To clarify the paper aim we inserted new sentences in the main text, at page 4, lines 96-104 of Introduction:
"The main objectives of the HR3DHG model can be synthesized as following: (i) to accurately reproduce and localize

the peaks of $[Hg]$ within the 3D domain, (ii) to estimate the Hg fluxes at domain boundaries, and (iii) to predict the evolution of mercury in sediment of polluted sites. Moreover, the HR3DHG model offers the possibility to describe the $MeHg$ and Hg^{II} partition between the dissolved phase (both seawater and pore water) and the particulate phase (suspended particulate matter and sediment particles).Specifically, in the dissolved phase the model describes the overall behaviour of Hg in ionic form and complexed with Dissolved Organic Carbon (DOC). Finally, the HR3DHG model can be a useful tool to predict and prevent the risks for the human health in marine areas close to industrial sites affected by Hg pollution extended for very long time intervals."

19. **Reviewer** wrote:
L88-95: I suggest to use this part to better explain the general architecture of the work, explaining with a figure how the various part of the model(s) interact with each other.

Authors answer:
According to reviewer's indication, at page 7 of manuscript, we inserted a new figure (Figure 2) where the basic structure of HR3DHG model is described.
Moreover, in order to explain the general architecture of the work, we inserted new sentences at page 6, lines 138-152 of manuscript:
"As well as the PCFLOW3D model of Zagar et al., the module of biogeochemical model for the seawater compartment is integrated with a hydrodynamics module. Specifically, the SHYFEM model is used to calculate the spatio-temporal behaviour of the horizontal components of the velocity field in the seawater compartment, fixing to zero the vertical velocity according to the experimental data (see Section S3 of the Supplement for details).(....) By using the curve of mean vertical profile obtained by Brunet et al. the picoeukaryotes abundances are converted into the chlorophyll concentration, which allows to reproduce the spatio-temporal distribution of NPP. This is used in our model to calculate both the biological rate constants and the sinking flux of Hg adsorbed by POM. (...) The two modules are coupled with the advection-diffusion-reaction sub-model in order to reproduce the spatio-temporal behaviour of the load of dissolved Hg released by dead picoeukaryotes cells in the seawater compartment."

20. **Reviewer** wrote:
L90 why eukaryotes? You mean phytoplankton here (see comment on S4)

Authors answer:
The word "eukaryotes" has been replaced by the word "picoeukaryotes" throughout the whole manuscript. In our work, we considered the picoeukaryotes community (i.e. phytoplanktonic eukaryotes with size less than 3 μm) since it represents the set of most representative populations of oligotrophic waters of Augusta Bay.
According to this, we modified the first sentence of Section 4 of the Supplement as follows:
"Our study includes the analysis of the abundance of picoeukaryotes community (i.e. phytoplanktonic eukaryotes with size less than 3 μm), which represents the set of most representative populations of the Augusta Bay."

21. **Reviewer** wrote:
L91-92: too many references

Authors answer:
We removed some useless references.

22. **Reviewer** wrote:
L93: what is this reference "Radomyski and Ciffroy 2015"?

Authors answer:
The reference "Radomyski and Ciffroy 2015" recalls the paper on the Phytoplankton MERLIN-Expo Model.

23. **Reviewer** wrote:
L93: here is the first mention to Supplement material, with no section specified, which after a long search I found to be S5, at the end of the document, and part of S1.3. This issue occurs throughout the manuscript and must be fixed.

Authors answer:
We specified in more detail all the sections of the Supplement throughout the manuscript.

24. **Reviewer** wrote:
L98: the reference "Melaku Canu et al., 2015" is not necessary here.

Authors answer:
We removed the reference.

25. **Reviewer** wrote:
L102-103: "By solving the model equations, we obtain the spatio-temporal distributions of Hg0(x,y,z, t), HgII (x,y,z, t), and MeHg(x,y,z, t)." Redundant with the previous lines.

Authors answer:
The sentence has been deleted. The second sentence of subsection 3.1. has been modified as follows:
"Specifically, the model equations are solved to obtain the behaviour of the three main Hg species in seawater, (...) with the reaction terms of the Partial Differential Equations (PDEs)."

26. **Reviewer** wrote:
L119: "As initial conditions, we assumed an uniformly distributed concentration of HgD and HgT, set to 1.9 ng/l corresponding to the experimental detection limit". This part should be moved to the "Model and simulation setup" section. I am not sure to understand it well, is it HgT(t0)=HgD(t0)=1.9? It should be specified "experimental detection limit for HgT in our dataset (reference)" or something similar, as 1.9 ng/l (about 9.5 pM) is very high as a detection limit. See for comparison (Mason et al. 1999; Horvat et al. 2003; Han et al. 2007; Monperrus et al. 2007; Hammerschmidt and Bowman 2012; Lamborg et al. 2012) who have detection limits well below 1 pM. What about initial conditions for MeHg?

Authors answer:
The sentence has been moved to the "Model and simulation setup" section, where also the initial conditions for all mercury species are defined now. Detection limit for Hg_T and Hg_D is 1.9 ng/l. This value is higher than that reported in cited previous works [1 pM versus our 9.5 pM] but it is near more than one order of magnitude lower with respect to the regulation level for Italian country and also this well captures the dynamic of Hg in the studied area.

27. **Reviewer** wrote:
L126-138: a crucial process such as biotic demethylation is missing. The description of photo demethylation is inconsistent with Figure 2.

Authors answer:
The biotic demethylation is now included in PDEs of our model. According to this modification, the paragraph at page 8, lines 192-197 of Model description has been reviewed as follows:
"The model includes three reaction terms regulated by first-order kinetics, which describe the photo-demethylation of $MeHg$, the methylation of Hg^{II} and the biotic demethylation of $MeHg$, respectively. The first is the amount of Hg^{II} produced by the $MeHg$ through photochemical reactions. The second is the amount of $MeHg$ obtained by the Hg^{II} through biotic and abiotic pathways in seawater. The third is the amount of Hg^{II} produced by the $MeHg$ through reductive demethylation processes caused by activity of bacteria in contaminated environments. The rate constants of three reaction terms are fixed according to previous works" Moreover, the Figure 2 of the old version of manuscript (now Figure 3) has been modified according to the reviewer's comment.

28. **Reviewer** wrote:
L132: the sentence "All data to estimate the rate constants of the redox reactions are derived from remote sensing (see Supplement)." should be moved to the Model setup section, along with similar sentences appearing below in the text (I listed some but not all of them) and the reference to the Supplement must be more specific.

Authors answer:
The sentence has been moved to page 17, lines 453-455 of the Model setup section, and modified as follows:
"Furthermore, the photochemical and biological rate constants of the redox reactions have been calculated by using both the outputs of NP model and the data coming from remote sensing (see Section S1 of the Supplement)."

29. **Reviewer** wrote:
L142-144: "The vertical turbulent diffusivity is calibrated according with experimental data, which indicate highly stratified water column conditions during the whole year". So is there oxygen depletion in the water column? If so, it should be discussed in the paper. The value given for vertical diffusivity in Table S1 is not representative of stratified conditions, and the reference provided in the table is missing in the bibliography. (This part should be moved to model setup section)

Authors answer:
On the basis of the experimental data, there is not oxygen depletion in the water column of Augusta Bay. In the new simulations, we re-calibrated the vertical turbulent diffusivity (see Table S1), which is now representative of weakly mixed layers. According to this, the sentence has been modified and moved at the "Model and simulation setup" section. Finally, the quotation Pham Thi et al. (2005) is replaced by Denman et al. 1983.

30. **Reviewer** wrote:
L148: there are eight references for one model implementation, is confusing.

Authors answer:
We removed some less crucial references following the reviewer's comment.

31. **Reviewer** wrote:
L152: it is not clear to me how are "the dynamics of the dissolved HgII and MeHg species [estimated], considering effects due to (i) the adsorption by SPM (scavenging process)". Your equations 2 and 3 contain the terms for Hg and MeHg scavenging (S^{II}_{SPM} e S^{MeHg}_{SPM}). These terms, adopted from the work of Zhang (2014) and described in the Supplemental do not include SPM:

$$S^{II}_{SPM} = \quad -\frac{\partial}{\partial z}\left[NPP\cdot(peratio)\cdot\left(\frac{z}{z_0}\right)^{-0.9}\cdot\left(\frac{k_D}{f_{org}}\right)\cdot Hg^{II}(z)\right], \tag{1}$$

The equation should be moved to the main text.

Authors answer:
To clarify the meaning of sentence we inserted at page 10, lines 245-257, of the main text the equations for the sinking flux of the SPM-bound mercury for Hg^{II}_D and $MeHg_D$, respectively. Moreover, the contribute of silt to the scavenging process is taken into account in new simulations.

32. **Reviewer** wrote:
L153-154: How is "the scavenging process for both Hg_D species regulated by the gradient of mercury concentration along the water column"?

Authors answer:
The sentence is modified as follows:
"The scavenging process for both Hg_D species is regulated by the sinking flux of particle-bound mercury along the water column (see Section 1.3 of the Supplement)."

33. **Reviewer** wrote:
L155: this is a repetition of L90-92, please mention explicitly which parameter or variable you extract from which model and where it has been used in the Hg model, choose for each parameter one or two references that actually refer to the model implementation you used.

Authors answer:
To specify the variables extracted by each module to be used in the Hg model, we inserted the following sentences at

pag 8, lines 205-212, of the of Model description section:
"Specifically, the NP model provides the spatio-temporal distribution of picoeukaryotes abundance, which is used to get the chlorophyll concentration and the net primary production through suitable conversion functions (see Sections S1.1 and S4 of the Supplement). These two variables are then exploited to calculate the contribute of the sinking flux for POM-bound Hg within the suspended particulate matter (see Sections S1.2 and S1.3 of the Supplement). The Phytoplankton MERLIN-Expo Model gives the spatio-temporal dynamics of the Hg^{II} and $MeHg$ contents within the picoeukaryotes cells. These two variables are then used, together with the picoeukaryotes abundance, to get the amount of Hg^{II} and $MeHg$ released by the dead picoeukaryotes cells (see Sections S1.2 and S1.3 of the Supplement)."

34. **Reviewer** wrote:
L172-176: I don't think there is any wet deposition for Hg0, please provide one reference for each process and parameterization selected/excluded. It should be stated explicitly that dry deposition and MeHg deposition are neglected. Somewhere should be also mentioned that Me2Hg is not explicitly considered.

Authors answer:
In accordance with previous works (see Zagar et al. 2007 and Zagar et al. 2014) the wet deposition forHg^0 is considered in our model, even if this contribute is negligible with respect to that of the Hg^{II} . In particular, the Hg^0 wet deposition flux is about $1/20000$ of the total wet deposition flux in the Augusta Harbour.
According to reviewer's comment, we inserted at least one reference for each process and parameterization selected/excluded. In new simulations, we also include both the dry deposition of Hg^{II} and total $MeHg$ deposition. According to this, the mentioned paragraph at pages 11-12, lines 288-297, has been modified as follows:
"Specifically, we take into account for the three mercury species: i) the evasion and the deposition of Hg^0 at the water-atmosphere interface; ii) the lack of Hg^0 diffusion at the water-sediment interface; iii) the wet and dry deposition of Hg^{II} at the water-atmosphere interface; iv) the wet and dry deposition of $MeHg$ at the water-atmosphere interface; v) the diffusion of Hg^{II} and $MeHg$ at the water-sediment interface; vi) the constant fixed value of $[Hg_D]$ out of Augusta Bay (Ionian Sea); vii) the exchange of the elemental mercury, Hg^{II} and $MeHg$ between the Augusta basin and the Ionian Sea through the two inlets."
Moreover, we inserted a new sentence at page 6, lines 159-160, of the Model description section, to mention the fact that Me2Hg is not explicitly considered:
"Since the experimental data indicate that Me_2Hg concentration is very low in the Augusta Harbour, the behaviour of this Hg species is not reproduced in our model."

35. **Reviewer** wrote:
L175-176: the boundary conditions describing the diffusion of HgII and MeHg at the sediment-water interface are very important in your model, as they represent the only connection between the water and the sediment, but they are not explained. Saying that you simulate "the exchange of HgII and MeHg at the seawater-sediment interface due to particulate matter deposition and re-suspension mechanisms" is extremely misleading because the reader will likely understand that you simulate deposition and resuspension fluxes of particulate Hg species, while this is not the case. I suggest to separate these equations from atmospheric boundary conditions and spend more words to explain well how they are implemented.

Authors answer:
Initially, we attempted to calculate also the amount of dissolved mercury embedded/released by the pore water due to the particulate matter deposition/re-suspension mechanisms at the sediment-water interface. However, the sediment transport module did not reproduce correctly the sedimentation rate experimentally observed in the Augusta Harbour. Therefore, we removed this module by our model and, according to experimental data, we fixed a constant sedimentation rate for the whole Augusta Bay and the whole period investigated. As a consequence, the mentioned sentence has been removed by the manuscript as well as the terms in Eqs. (11)-(12) which describe the effects of particulate matter deposition/re-suspension mechanisms. Finally, the equations for the boundary conditions are better explained in the Section S1 of Supplement.

36. **Reviewer** wrote:
L182-196: maybe the equations can be distributed within the text describing them, or at least they must be recalled in the text when being described.

Authors answer:
The equations are now recalled in the manuscript when they are described.

37. **Reviewer** wrote:
L207: references?

Authors answer:
The references have been removed.

38. **Reviewer** wrote:
L212-214: "the mass transfer coefficients ($MTC^{II}_{sed-water}$ and $MTC^{MM}_{sed-water}$) at the water-sediment interface are calculated in order to fit the experimental findings and according to previous works (Schulz and Zabel,2006; Ciffroy,2015)(see Supplement)." I think that the equations for these MTC should stay in the main text. The fact that they are adjusted to fit experimental findings should be said in the Model setup section. The reference "Schultz and Zabel 2006" is incomplete, and so is "Ciffroy 2015".

Authors answer:
The description of the mass transfer coefficients is very long (see Sections S1.2.2 and S1.3.2 of the Supplement). Therefore, it cannot stay in the main text due to the reduced size imposed by the journal. The sentence at page 13, lines 329-335, is modified as follows:
"The spatio-temporal dynamics of pore water mercury concentrations (...), while the mass transfer coefficients ($MTC^{II}_{sed-water}$ and $MTC^{MM}_{sed-water}$) at the water-sediment interface are calculated by sediment porosity, molecular diffusion coefficient, boundary layer thickness above and below sediment according to previous works."
Moreover, we described the setup of the parameters for the mass transfer coefficients ($MTC^{II}_{sed-water}$ and $MTC^{MM}_{sed-water}$) at the water-sediment interface in the Model setup section, where the followings sentences have been added at page 17:
"Before to calculate the mass transfer coefficients at the water-sediment interface, the *boundary layer thickness above the sediment* was optimized to better reproduce the spatial distribution of mercury benthic flux observed experimentally. Unlike the *boundary layer thickness above the sediment*, the other parameters used to obtain $MTC^{II}_{sed-water}$ and $MTC^{MM}_{sed-water}$ were not calibrated. In fact, the *boundary layer thickness below the sediment* was estimated by using the relationship between this parameter and the average velocity of marine currents defined by Sorensen (2001), while the spatial distribution of the sediment porosity within Augusta Harbour was reproduced, according to previous works, by exploiting the measurements on the sediment samples performed by $ICRAM$ in 2005. Also, the molecular diffusion coefficient was that reported by Schulz and Zabel (2006)."
According to reviewer's comment, some references have been added.

39. **Reviewer** wrote:
L214-218: "The dynamics of the mercury benthic fluxes (phi_res) caused by particulate matter deposition and resuspension mechanisms (Neumeier et al., 2008; Ferrarin et al., 2008) is obtained by considering both the spatial distribution of sediment porosity and the spatio-temporal behaviour of removed/settled sediment thickness at the seawater-sediment interface. The sediment exchanges at the water-bottom interface are obtained from the application of the hydrodynamic model, which accounts for sediment transport processes induced by currents (see Supplement)." This part seems very confusing to me. The equation for $phi-res$ and Er should be defined in the main text and should be probably given different names. Moreover, the hydrodynamic SHYFEM model can not provide fluxes of sediment, if the SEDTRANS model or any other Sediment model has been run with SHYFEM to obtain sediment fluxes in the Augusta Bay,it should be described in detail in the Supplement (including the parameters used). Also, if you had run a sediment model, why did you adopt experimentally measured SPM concentrations for your eq. 13? If you had not run a sediment model, explain where the sediment fluxes come from and make it more evident throughout the text that they are not transporting particulate mercury. In Figure 2 there are thick arrows with an "R" that looks like re-suspension, which is misleading.

Authors answer:
This paragraph has been removed by the manuscript. In our work no sediment model is now used to describe the particulate matter deposition/re-suspension mechanisms at the sediment-water interface. In the new Figure 3 (ex Figure 2), as well as in the whole manuscript, the benthic flux from sediments to seawater is now named "B".

40. **Reviewer** wrote:
L219-220: repetition

Authors answer:
The reviewer is right. The sentence has been removed.

41. **Reviewer** wrote:
L221: this should appear before in the section

Authors answer:
The paragraph has been moved at page 11 (lines 277-286).

42. **Reviewer** wrote:
L223: same KD for Hg and MeHg? No units for the terms of this equation?

Authors answer:
No experimental data has been collected for the K_D of Hg^{II} and $MeHg$. On the contrary, the seawater-SPM partition coefficient (K_D) has been measured for the total Hg_D. According to this, we chose to use the same experimental K_D for both dissolved Hg species (i.e. Hg^{II} and $MeHg$).
The units for the terms of the equation are now inserted in the text.

43. **Reviewer** wrote:
L225-227: please change "in very good agreement with" with "within the range of"

Authors answer:
The sentence has been deleted, and the whole paragraph has been modified (see page 11 of the new version of manuscript).

44. **Reviewer** wrote:
L228-229: is then SPM kept constant in time? If so, it should be state

Authors answer:
The spatial distribution of SPM is constant in time. The sentence has been modified as follows:
"The spatial distribution of SPM was set according to the experimental information collected during the oceanographic cruise of October 2017, and assumed constant for the whole simulation time."

45. **Reviewer** wrote:
L230-242: This part should be elsewhere, is not part of the model.

Authors answer:
We inserted this paragraph in a new subsection of the Model description (section 3.1.1).

46. **Reviewer** wrote:
L242: Figure 2 should be mentioned before in the text, and used to help the reader in the model description. The caption does not explain the figure.

Authors answer:
The ex figure 2 (now figure 3) has been moved at the beginning of the Model description section. In the new Figure 3 caption, we inserted the following description for the scheme:
"The scheme describes the transformation processes (k_1- photo-oxidation , k_2- photo-reduction, k_3-biological oxidation, k_4-biological reduction, k_{Ph-de}-photo-demethylation, k_{deme}-demethylation, k_{me}-methylation, K_{demeth}-demethylation, K_{meth}-methylation) and the main transport processes (A-anthropogenic input, AD-atmospheric deposition, B-benthic

flux, D-net flux due to particulate deposition and settling, O-net outflow from basin, V-atmospheric evasion) which involve the dissolved and particulate-bound Hg species in seawater (Hg_D^{II}, $MeHg_D$, Hg_D^0, Hg_P^{II}, $MeHg_P$) and sediments (Hg_{pw}^{II}, $MeHg_{pw}$, Hg_T^{sed})."

47. **Reviewer** wrote:
L245: please recall the equations where needed, not in this aggregated form.

Authors answer:
The recalling to equations has been removed.

48. **Reviewer** wrote:
L249: Please motivate this choice. This is a strong assumption that I have never seen before.

Authors answer:
We attempted to model the mercury concentration by adopting a different order kinetic for Eq.(22), however the best agreement between theoretical results and experimental data was obtained when a first-order kinetic was used. According to this, the sentence is modified as follows:
"In order to better reproduce the experimental findings, we describe mercury desorption using an exponential equation, which accounts, in the absence of external sources, for the loss of mercury through the desorption mechanism. Since the mercury desorption has to depend on its instantaneous concentration, the mechanism is regulated by a first-order kinetic."

49. **Reviewer** wrote:
L259-260: This is already mentioned in the section for the water model. I think features are common to the water and sediment modules for Hg might be explained just once at the beginning of section 3 (same for L265-266, L278-279).

Authors answer:
The manuscript has been modified in section 3 according to the reviewer's suggestion.

50. **Reviewer** wrote:
L284-285: diffusion coefficients are not constant in time in Melaku Canu et al., (2015)

Authors answer:
The reference Melaku Canu et al. (2015) has been removed by the sentence.

51. **Reviewer** wrote:
L290, L291: while I understand the use of MeHg fraction (k_{MeHg}) in setting the initial conditions, I do not understand why it is used in the partial difference equations that also include Hg methylation and demethylation (eq.16 and 17). Can you explain the parameterization in the text? I suggest changing k_{MeHg} with f_{MeHg} so it is more intuitive.

Authors answer:
The fraction of methyl-mercury is used as parameter in one of terms of the partial differential equations since it is necessary to calculate the amount of $MeHg$ and Hg^{II} released to pore waters during the desorption process of mercury bound to sediment particles. k_{MeHg} is replaced by f_{MeHg} throughout the manuscript.

52. **Reviewer** wrote:
L296 and L301: I've never seen this approach based on a desorption rate () in mercury modeling. In this way, your sediment HgT decrease with time by assumption, as there are no source terms. By adopting a reductio ad absurdum logic, if your simulation would start in 1900 or before, which initial conditions HgT(0) would you need to achieve observed HgT concentrations for 2005? Can you provide any theoretical background for this parameterization? Also, you state "The desorption rate is fixed to a low value to fit the slow mercury release from the sediment particles to pore water according to experimental observations" but in Table S1 "no data" is given as a reference for the parameter.

Authors answer:
The choice of this modelling for the total mercury in sediments is connected to the industrial history of the Augusta Bay.

Specifically, it is necessary to recall that an important chlor-alkali plant discharged (legally and illegally) a great amount of mercury at the southernmost part of Augusta Bay until 2005, namely when the plant has been closed. Soon after the chlor-alkali plant closure, the ICRAM performed several samplings in the sediments of the Augusta Bay by providing a 3D spatial distribution of total mercury concentration in the surface sediment layer (from 0.1 to 1.9 m depth), which constitute the initial condition for our model. Since no mercury source was anymore present in Augusta Bay after the chlor-alkali plant closure (2005), except for the release by buried sediments, we assumed that the mechanism responsible of the high mercury concentration measured in seawater and pore water until last sampling (2017) was the desorption process of particle-bound mercury. The same approach could not be used before the ending of mercury discharge in the Augusta Bay when other mercury sources were still present within the basin. In conclusion, our model is valid since it reproduces the spatio-temporal dynamics of mercury after the plant closure, by fixing initial conditions for the sediments equal to the total mercury concentration measured in 2005. Analogously, the model can reproduce the mercury distribution in all basins where the industrial pollution is ceased recently.

About the sentence mentioned, the reviewer is right. In fact, it is mistaken. For this reason, we moved the sentence at page 17 of "Model and simulation setup" Section and rewrote it as follows:

"In the Eq. (22), the desorption rate α was calibrated to obtain the best fit between the theoretical results and experimental observations for $[Hg]$ in pore water"

Since the desorption rate has been calibrated in the model by using the experimental data of mercury concentration in the pore water, no reference cannot given for this parameter.

53. **Reviewer** wrote:
L298 "The spatial distribution of the fraction of methylmercury in the sediments is that obtained by field observations, while the two sediment-pore water distribution coefficients are calibrated, according to previous work (Oliveri et al., 2016)" move to model setup, provide a reference for the data/publication from where you derived the fraction of methylmercury and mention how much is this fraction.

Authors answer:
The sentence has been moved at page 17 of "Model and simulation setup" Section, and modified as follows:
"Specifically, in Eqs. (20)-(21) the sediment-pore water distribution coefficients were calibrated to guarantee the best theoretical $[Hg]$ in pore water in agreement with the value ranges experimentally observed in a previous work (Oliveri et a. 2016), whereas the fraction of methyl-mercury in sediments for the whole spatial domain was set to that obtained by field observations during the oceanographic survey of October 2017 (see Table S1)."

54. **Reviewer** wrote:
L306 why is the MTC parameterization not included in the boundary conditions for sediment? Are you assuming only one-way fluxes toward the water?

Authors answer:
Yes, in our model we assume only one-way fluxes toward the water. This assumption is in agreement with the experimental data (not reported in the manuscript) which indicate a negative gradient for dissolved mercury concentration from the pore water to seawater.

55. **Reviewer** wrote:
L338-339, L342: this is different from what is said in L142-144.

Authors answer:
The sentences on the turbulent diffusivities have been modified in the Model setup section. The two sentences in section 3.1 have been removed.

56. **Reviewer** wrote:
L338-344: please do not go back and forth from vertical to horizontal diffusivity, discuss one at a time and select a reference that is consistent with that given in Table S1.

Authors answer:
According to the reviewer's indication, the paragraph has been modified, as follows:
"The vertical turbulent diffusivity was calibrated according to experimental data, (...) during the whole year. Specifically, the vertical turbulent diffusivity was set (...) at the surface layer of the water column. The calibrated vertical diffusivity was in good agreement with (...) under the condition of weakly mixed waters. The horizontal turbulent diffusivity was assumed (...) the values obtained in Massel (1999). In particular, the horizontal turbulent diffusivities were optimized (...) the observed mercury evasion flux. The calibrated horizontal diffusivities were (...) to those of the Augusta Bay."

57. **Reviewer** wrote:
L351: it is not clear to me why you chose to run 250 years of simulation without varying the forcings.

Authors answer:
To clarify the sentence has been modified as follows:
"Finally, the calibrated model has been run by considering the seasonal oscillations of the environmental data (water currents, wind etc.) provided by hydrodynamic modelling (see Section S4 of the Supplement)."

58. **Reviewer** wrote:
L357-361: this part should not be in the Results section, Table S1 must be introduced much before in the text.

Authors answer:
According to the reviewer's indication, the most part of this paragraph has been moved in Model setup section.

59. **Reviewer** wrote:
Figure 3: you must show modeled vertical profiles against observations when available. I do not find useful or interesting what is currently shown in Figure 3.

Authors answer:
We moved the Figure 3 of the old version of manuscript in the Supplement. Afterwards, we inserted a new Figure 3 in the manuscript in which the comparison between the theoretical results and experimental data for dissolved mercury concentration is shown.

60. **Reviewer** wrote:
L364: please provide the values of these ratios and values for comparison to prove this excellent agreement (this applies to most of the Results section, show the numbers).

Authors answer:
The average concentration ratios among the three mercury species dissolved are now provided in the main text (see page 18). Moreover, a new table with the numerical values of the three species has been inserted in the Supplement (see Table S5).

61. **Reviewer** wrote:
L368-369: "In general, the mercury concentration is maximal at the seawater-sediment interface, where the main sources of HgII and MeHg are localized.". Do you mean in general in your model? While from your budget I see that diffusion flux appears to be the first HgT source, what supports this statement for MeHg? Especially in this model configuration without biological demethylation in the water column, I would expect water column methylation to be significant. Is the increase of Hg species at the bottom of the water column in agreement with your dataset? Please show and discuss it.

Authors answer:
According to the reviewer's indication, the paragraph has been modified as follows:
"The model results indicate that the dissolved mercury concentration is usually maximal at the seawater-sediment interface (see Fig.4), where the main sources of Hg^{II} and $MeHg$ are localized. These numerical results are in reasonable agreement with the field observations (see Tables S6-S7 of the Supplement). Moreover, taking into account the redox conditions of sediments in the area, we speculate that maxima in $MeHg$ production be confined to the seawater/sediments interface."

Moreover, the points raised by the reviewer are clarified both in other parts of this letter and in the revised version of the Introduction.

62. **Reviewer** wrote:
L369: I don't think (x,y) is useful here.

Authors answer:
(x,y) has been removed by text.

63. **Reviewer** wrote:
L370-371: "[...] peaks of mercury concentration occur at mid-depth of the water column possibly due to the effects of the velocity field of marine currents and the bathymetric features of Augusta basin.". I do not understand this explanation.

Authors answer:
The sentence has been modified as follows:
" (...) we observe that the peaks of mercury concentration occur at mid-depth of the water column possibly due to the distribution of marine currents velocity field within Augusta basin, which determines sometimes the presence of a $[Hg]$ maximum in the intermediate layers of seawater."

64. **Reviewer** wrote:
L372: specify "in our model"

Authors answer:
We specified "in our model" at the beginning of the sentence.

65. **Reviewer** wrote:
L375-377: please support this "good agreement" with statistical and visual tools. There is no comparison of modeled and observed vertical profiles of Hg and MeHg, which would be interesting to see and discuss, especially considering the emphasis put in the 3D model domain.

Authors answer:
A statistical analysis based on the χ^2 test for $[MeHg]$ is now present. In general, it is worth to point out that no experimental data for $[Hg^{II}]$ and $[Hg^0]$ were collected in the Augusta Bay during the oceanographic surveys. In fact, the most part of the experimental data concerns $[Hg_D]$ and $[Hg_T]$, which were measured only in two/three sampling points for each station. Moreover, the magnitude of $[Hg_D]$ and $[Hg_T]$ is below the detention limit in many sampling points. For these reasons, in the first version of the paper we chose to make neither graphs nor statistical checks for comparing theoretical results and experimental data.
The sentence at pages 19-20 of manuscript is modified as follows:
"A quantitative analysis, based on the reduced χ^2 test, indicates a good agreement between the model results and experimental findings for $[MeHg]$ in stations $A3$ ($\tilde{\chi}^2 = 0.0005$) and $A7$ ($\tilde{\chi}^2 = 0.0005$), while differences can be observed in the stations $A9$ ($\tilde{\chi}^2 = 0.0955$) and $A11$ ($\tilde{\chi}^2 = 0.1065$), where the theoretical concentrations appear overestimated at the bottom layer (see Table S6 of the Supplement)."

66. **Reviewer** wrote:
L377-378: "This result is probably due to the overestimation of the $MeHg$ benthic fluxes in these two stations." Can you support this statement? Other reasons would be possible as well.

Authors answer:
We have no experimental data on the $MeHg$ benthic fluxes to support this statement. However, the two stations ($A9$ and $A11$) are localized in sites where the theoretical $MeHg$ benthic fluxes are very high, and the effects of transport mechanisms on the $MeHg$ concentration are negligible respect to diffusion process from sediments.

67. **Reviewer** wrote:
L379-81: I think it must be highlighted that HgD is modeled while HgT is estimated assuming a linear correlation with

modeled HgD concentrations and SPM through equation 13 (which might be not representative of processes occurring in the field).

Authors answer:
According to the reviewer's indication, the sentence at page19 has been modified as follows:
"On the other hand, the dynamics of the spatial distribution of the $[Hg_T]$ is estimated according to Eq. (9), assuming a linear correlation between the modeled $[Hg_D]$ and the experimental SPM concentrations."

68. **Reviewer** wrote:
L383-384: same comment as for L375-377

Authors answer:
Please, see the previous answer for $[MeHg]$. To clarify the magnitude of the difference between theoretical results and experimental data, we added the following sentences at page 20:
"Specifically, the difference between the model result and field observation for the $[Hg_D]$ is less than the experimental error ($\sigma = 3.2\ ng/l$) in 59% of sampling points, while it exceeds 2σ in only 17% of sampling sites. As a conclusion, the comparison between experimental data and theoretical results for the $[Hg_D]$ shows mostly small discrepancies except in some of the most contaminated areas, where concentration hot spots are hard to capture due to the resolution grid used in the present work."

69. **Reviewer** wrote:
L387: same comment as for L375-377 and 383-384

Authors answer:
Please, see the previous answer for $[MeHg]$ and$[Hg_D]$. To clarify the magnitude of the difference between theoretical results and experimental data, we added the following sentence at page 20:
"As a whole, the discrepancy for the $[Hg_T]$ is less than σ in 44% of cases, while it exceeds 2σ in 32% of sampling sites."

70. **Reviewer** wrote:
L391-395: the reader knows nothing about your modeled concentrations and spatial distribution of SPM since they are not shown.

Authors answer:
The modeled concentrations are shown in the Supplement, while the experimental data of SPM (acquired recently and never published) can be put in a repository if needed.

71. **Reviewer** wrote:
L399-400: "The model reliably reproduces the high benthic mercury fluxes also in the part of the south-east sector close to the inlets of the Augusta Bay, where intensive ship traffic and the relatively high velocity field of the marine currents cause sediment resuspension and intensive transport of SPM." is the high sediment resuspension induced by ship traffic considered in your model? How does it relate to your modeled benthic fluxes? From figure 4, I find modeled fluxes to be one order of magnitude higher than fluxes reported by (Salvagio Manta et al. 2016). Please explain what I am missing or what is going on.

Authors answer:
The resuspension induced by ship traffic is not considered in our model. Therefore, there is no relation between the modeled benthic fluxes and the sediment resuspension induced by ship traffic. According to this, we removed the second part of the sentence at page 20, lines 548-549, of the main text.
Since the experimental findings on benthic fluxes have been acquired in different sites than those mentioned by referee, the comparison between the theoretical results and experimental data cannot performed in these highly polluted sites. In general, it is possible to assert only that very high benthic fluxes modeled in some sites of Augusta Harbour are strictly connected to the high total mercury concentrations measured in sediments of the same sites. According to this, we added the following sentence at page 20, lines 553-555, of the new version of manuscript:

"Moreover, the model results confirm that the spatial heterogeneity of benthic fluxes observed experimentally is strictly connected to that of Hg_T concentration in sediments."

72. **Reviewer** wrote:
Figure 4: probably you don't need to show fluxes for both inorganic Hg and HgT, as they look the same. Why available data are not shown on the map,or in another figure?

Authors answer:
The maps on the inorganic flux are now removed by the Figure 5 (ex Figure 4). A map of the experimental total benthic fluxes cannot to be reproduced due to the reduced number of measurements (three for sampling) performed in the two periods investigated. Experimental data are reported in Table S9 of Supplement for a direct comparison.

73. **Reviewer** wrote:
L407-409: "In general, the theoretical distribution of the mercury evasion fluxes is in a very good agreement with the experimental results for the investigated periods". Same comment as for L375-377,383-384 and 387. From figure 5, I see that modeled evasion (up to 100 ug/m2d) is about 100 times as high as evasion modeled by Bagnato et al. 2013.

Authors answer:
In this case, no significant comparison between theoretical results and experimental data is possible to make on the basis of statistical tests. Indeed, only three experimental measurements (in three different sites) have been acquired for each sampling period. Too much few to perform a significant statistical check.
Moreover, the assertion "I see that modeled evasion (up to 100 ug/m2d) is about 100 times as high as evasion modeled by Bagnato et al. 2013" is not correct. In fact, also Bagnato et al. (2013) obtained high evasion fluxes $72\ \mu g \cdot m^{-2} \cdot d^{-1}$ in the coastal zones at the south-west of the Augusta Bay. Therefore, our model results are not so different than those obtained by Bagnato et al..
According to the reviewer's indication, the paragraph at the ending of page 20 has been modified as follows:
"In general, the theoretical distribution of the mercury evasion fluxes is in acceptable agreement with the experimental results for the investigated periods (see Table S10 of the Supplement). Specifically, small discrepancies are observed in the most part of the stations (four over six), while larger difference emerge in stations 3 (November 2011) and 5 (June 2012). From a qualitative point of view, (...)"

74. **Reviewer** wrote:
L416-419: "The modeled HgD benthic fluxes (...) are significantly larger than those estimated for both sampling periods on the basis of the field observations (...) (Salvagio Manta et al., 2016)." Why do you go back to benthic fluxes, which are already discussed from L396 to L404, contradicting your previous statements (L399 and 403)?

Authors answer:
No contradiction is present in this sentence. Indeed, in this part of section we discuss over the annual mass balance for the whole basin, while previous statements described the model results for benthic fluxes in each site. To clarify, we inserted at the beginning of the paragraph the following sentence:
"In this work, we make the annual mass balance of the Augusta Bay to study the fate of Hg coming from sediments, and to estimate the Hg outflows at the inlets of basin."

75. **Reviewer** wrote:
L419-420: "This probably depends on the limited number of sampling sites available in the experimental work with a consequent extremely coarse capacity to capture reliable estimates of benthic fluxes." Six sites for measuring benthic fluxes within the Augusta Bay is a lot. Other work of this kind I came across only had 2-3 sampling stations for larger study areas, I thus disagree with the statement that they provide an "extremely coarse representation".

Authors answer:
To clarify, we modified the sentence at page 22 as follows:
"This probably depends on (...) with a consequent limited capacity to capture reliable estimates of benthic fluxes within a basin, such as Augusta Bay, where the spatial distribution of sediment mercury is highly heterogeneous."

76. **Reviewer** wrote:
L421-423: I do not follow why this should ensure that your model results for a specific period are better than values experimentally detected under conditions that are representative of that period.

Authors answer:
The sentence has been removed.

77. **Reviewer** wrote:
L424-429: you have already discussed evasion fluxes before, so the two parts should go together. Be careful of the references.

Authors answer:
Please, see the previous answer for benthic fluxes. The two references have been removed.

78. **Reviewer** wrote:
L439-440: "The model results for the annual recycled mercury flux are shown in Fig.6d. In this case, values calculated (2.45 kmol y-1 for the year 2011 and 2.41 kmol y-1 for the year 2012) are larger and more realistic than those estimated in Salvagio Manta et al. (2016) by simple linear subtraction of the available fluxes in the mass-balance equation (0.84 kmol y-1).". How do you support this statement that your estimate is more realistic? Isn't the mercury recycling calculated by subtraction also in this work (equation 14)? How do you argue the significant gap that is shown in Figure 6d between the "Total recycled" and the "Scavenged recycled"? How large is your estimated HgT reservoir in the water and sediment of Augusta Bay?

Authors answer:
To answer the referee's questions, we modified the last paragraph of section 4.1 (see page 24) as follows:
" In this work, the annual recycled mercury flux is calculated by subtraction using the mass balance equation (18), as well as it was done in previous works on the Augusta Bay. The model results for the recycled mercury flux are shown in Fig.7d. Here, values calculated by our model (2.50 $kmol\ y^{-1}$ for the year 2011 and 2.46 $kmol\ y^{-1}$ for the year 2012) are larger and probably more realistic than those estimated in Salvagio Manta et al. (2016) (0.84 $kmol\ y^{-1}$). Indeed, the former are obtained by considering the seasonal oscillations of all other mercury fluxes during the year, while the latter are calculated without considering the seasonal changes of mercury fluxes.
In order to reproduce the effects induced by scavenging process on the mercury dynamics, our model calculates the annual sinking mercury flux, whose results are shown in Fig. 7d. Here, a significant gap between the recycled flux (2.50 $kmol\ y^{-1}$ for the year 2011) and the sinking flux (0.07 $kmol\ y^{-1}$ for the year 2011) is observed probably due to the underestimation of the amount of mercury captured by POM (see Eq. (4)-(5)). More specifically, this behaviour could be caused by the underestimation of NPP, which is calculated by using a conversion function calibrated for oceans rather than for coastal zones.
On the contrary, very high values of the annual Hg_T accumulation rate in surface sediment layer (12.07 $kmol\ y^{-1}$ for the year 2011), respect to those of the annual recycled flux (2.50 $kmol\ y^{-1}$ for the year 2011), are obtained by our model. This result is caused by the high sedimentation rate (11.7 $mm\ y^{-1}$) estimated experimentally and used in our calculations for annual Hg_T accumulation rate. However, the sedimentation rate could be overestimated due to sampling methods used. In fact, the results obtained by the sediment transport model indicate a low average sedimentation rate for the Augusta Bay."

79. **Reviewer** wrote:
L447: 50 cm is not shallow for sediment. Why did you choose to represent about 2 m of sediment with a coarse resolution (10 cm layers)?

Authors answer:
We recall that experimental findings in sediments constitute the initial conditions of model. According to this, in our work the choice of investigated sediment layer thickness is bound to the maximum depth of sediment samplings, while the grid resolution is imposed by the distance between the sampling points of total mercury concentration.
According to the Referee's indication, the sentence at page 25 has been modified as follows:

"(...) the vertical profiles of mercury concentration in the sediments (...) reach their maximum value within the surface layer of the sediments ($< 0.5\ m$ of depth)."

80. **Reviewer** wrote:
L459: you should make it clear which data are used for calibration and which are used for validation.

Authors answer:
To clarify, the section "Model and simulation setup" has been modified according to the reviewer's requests.

81. **Reviewer** wrote:
L465-466: "This "integrated" model, which allows to give a description of the mercury dynamics in the whole system (seawater, pore water, and particulate phase of the sediment), represents an absolute novelty in the landscape of the mathematical modelling of spatio-temporal dynamics in a biogeochemical context". This is not true, as you can realize with a thorough review of the mercury modelling at the state of the art. Besides, the parameterization chosen in your model for Hg species dynamics in water and sediment is overall questionable and not well supported by theoretical knowledge at the state of the art. Even correcting major oversights mentioned in other comments, this model still neglects the dynamics of Hg in the particulate phase. It thus does not provide a "description of the mercury dynamics in the whole system", and is probably less advanced than other existing models.

Authors answer:
According to the reviewer's indications, the sentence at page 26 has been modified as follows:
"This "integrated" model, which allows to give a description of the mercury dynamics in highly polluted marine sites, introduces some novelties in the landscape of the mathematical modelling of spatio-temporal dynamics in a biogeochemical context."

82. **Reviewer** wrote:
L480-482: "the different approach used in the WASP models and River MERLIN-Expo model allowed neither to reproduce the dynamics of the vertical profiles of mercury concentration in the seawater compartment, nor to obtain the spatio-temporal behaviour of mercury concentration in the sediments". Again, the River MERLIN model does not seem to be relevant here, and it is not true that the previous approaches could not reproduce the vertical dynamics nor the spatio-temporal evolution of Hg species. For example in Rosati et al.,(2018) the WASP model has been used to simulate the vertical profile of Hg and MeHg in the water column and sediments of the Black Sea; this has been done in 1D but it could have been done in 3D as well. Sorensen et al., (2016) also implemented a 1D model for Hg species in the water and sediments of the Arctic Sea. As for the spatio-temporal evolution of Hg and MeHg in water and sediment, an example can be found in Canu and Rosati (2017).

Authors answer:
According to the reviewer's comment, the sentence at page 26 has been modified as follows:
"For comparison, the different approach used in the WASP models did not allow to reproduce the dynamics of mercury concentration distribution at 3D high resolution in polluted sites characterized by elevated spatial heterogeneity. Similar criticalities came out from the study of HR-1D models (Soerensen et al., (2016), Pakhomova et al., (2018)), in which the effects of horizontal velocity field on the mercury dynamics could not be taken into account."
Moreover, the point raised by the reviewer is clarified in the revised version of the Introduction.

83. **Reviewer** wrote:
L484: "In general, no forecast about the mercury depletion time in the sediment compartment of Augusta Bay was possible by other models." See Canu and Rosati, 2017.

Authors answer:
According to the reviewer's indication, the sentence at page 26 has been modified as follows:
"In general, only few models (Rajar et al., (2007), Zagar et al. (2007), Canu and Rosati (2017)) were able to make forecasts about the mercury depletion time in the sediment compartment of highly polluted sites, such as Augusta Bay."

84. **Reviewer** wrote:
L486-490: "Finally, the biogeochemical models introduced in previous publications included neither the Nutrient-Phytoplankton model (Dutkiewicz et al., 2009; Morozov et al., 2010; Valenti et al., 2012; Denaro et al., 2013a, c, b; Valenti et al., 2015, 2016a, b, c, 2017) nor the Phytoplankton MERLIN-Expo model for the mercury content in eukaryotes cells (Pickhardt and Fischer, 2007; Radomyski and Ciffroy, 2015). All the aforementioned aspects are therefore an element of novelty in the context of 3D biogeochemical modelling." The model here presented do not include a plankton model, the two tools are used together but not integrated. Moreover, there has been previous work integrating phyto- and zooplankton in a biogeochemical model for marine Hg cycle (e.g. Soerensen et al., 2016).

Authors answer:
Actually both the Nutrient-Phytoplankton (NP) model and the Phytoplankton MERLIN-Expo (PME) model for the mercury content in eukaryotes cells are integrated with the biogeochemical (BG) model. Specifically, the NP and MPE model interact with the BG model through the load of Hg_D released by POM. Moreover, in the new version of the manuscript we inserted results obtained in the presence of a new interaction term (sinking fluxes of organic and inorganic mercury) between the BG and NP model, which makes "stronger" the integration among the three models. Specifically, in the new version of model the NPP coming from the NP model is used to calculate the sinking fluxes of the BG model. According to reviewer's indications and related model modifications, we replaced the first sentence with the following one: "Finally, the biogeochemical models introduced in previous works (Soerensen et al., 2016) provided neither the NPP coming from the Nutrient-Phytoplankton model (...), nor the load of POM-relseased Hg_D obtained using the Phytoplankton MERLIN-Expo model (...) (see Section 3.1)."

85. **Reviewer** wrote:
L491-492 "The HR3DHG model considers the effects of the seasonal changes of the environmental variables on the mercury out flows to wards the atmosphere and the open sea, and this also is a new feature in biogeochemical model." The seasonal effects are never discussed in the manuscript, and anyways this is clearly not a new feature.

Authors answer:
The seasonal changes of the environmental variables are discussed only in the Supplement. We deleted the second part of the sentence: "and this also is a new feature in biogeochemical model".

86. **Reviewer** wrote:
L495 "Firstly, the mass transfer coefficients at the water-sediment interface are highly sensitive to the layer thickness above the sediment and their variation could cause significant changes of mercury benthic fluxes." Why is this relevant? Which are the environmental implications?

Authors answer:
To explain the environmental implications, we modified this paragraph as follows:
"Firstly, the mass transfer coefficients at the water-sediment interface are highly sensitive to the *layer thickness above the sediment*. Specifically, for each mercury species in sediments, a small decrease of this parameter causes a great increase of benthic fluxes, with a consequent strong enhancement of dissolved mercury concentration in seawater."

87. **Reviewer** wrote:
L497 "Sensitivity analysis performed on the sediment compartment indicates that the spatio-temporal dynamics of the benthic mercury flux strongly depends on the spatial distribution of the sediment porosity and of the initial total mercury concentration in the top-sediments". Sensitivity analysis is never discussed in the manuscript but should be.

Authors answer:
The sensitivity analysis has been not performed for the sediment porosity and the initial total mercury concentration in the top-sediments. These two spatial variables were fixed by using experimental findings. On the other hand, in the sentence we intended to stress only that the benthic mercury fluxes strongly depend on these two spatial variables. According to this, we modified the sentence as follows:
"The model framework for the sediment compartment causes that the spatio-temporal dynamics of the benthic mercury

flux strongly depends on the spatial distribution of the sediment porosity and of the initial total mercury concentration in the top-sediments, which were fixed using the experimental data."

88. **Reviewer** wrote:
L500 "Sensitivity analysis performed on the environmental parameters and variables used in the seawater compartment indicates that the spatio-temporal dynamics of [HgT] and [HgD] primarily depends on the velocity field of the marine currents obtained from the hydrodynamic model (Burchard and Petersen, 1999; Umgiesser et al., 2004; Umgiesser, 2009; Umgiesser et al., 2014; Ferrarin et al., 2014; Cucco et al., 2016a, b, 2019), even if the role played by the vertical and horizontal diffusivities (Pacanowski and Philander, 1981; Massel, 1999; Katz et al., 1979; Denman and Gargett, 1983; Peters et al.,1988; Valenti et al.,2015,2017)". How did you perform sensitivity analysis on HgT that is not modeled but assumed to be linearly correlated to HgD (eq.13)? From my experience, HgD and HgT dynamics are likely to have different drivers. If sensitivity analysis has been carried out, it should be described. There are too many references.

Authors answer:
We removed $[Hg_T]$ and some references from the sentence.
The sensitivity analysis is quite difficult to perform because of the variations of velocity field and/or diffusivities. The spatial distributions of the dissolved mercury indeed are strongly affected by these non-stationary conditions, which make hard to evaluate correctly the effects of a parameter and its variations.
In order to describe the performed sensitivity analysis , we inserted the following sentences at page 27:
"Specifically, the spatio-temporal behaviour of $[Hg_D]$ changed significantly when alternative velocity fields for the Augusta Bay were used in the biogeochemical module, confirming a feature already observed in previous models. Conversely, limited changes in the spatial distribution of $[Hg_D]$ were observed when different values of vertical and horizontal diffusivities were set in our model."

89. **Reviewer** wrote:
L508 if both data and model suggest Hg is mostly in the particulate phase, why is your model designed around the dynamics of dissolved Hg species?

Authors answer:
Our model has been designed to reproduce the dynamics of dissolved Hg species since we could not calibrate a sediment transport model with sufficient reliability to reproduce the spatio-temporal behaviour of suspended particulate matter.

90. **Reviewer** wrote:
L510 "the amount of mercury dissolved in pore water is negligible with respect to the total amount in the sediments" this is not a finding of this work.

Authors answer:
According to reviewer's indication and new simulations, we deleted the sentence at page 27 and modified the rest part of paragraph as follows:
"According to the available experimental data, the theoretical results obtained with the HR3DHG model suggest that the amount of mercury bound to the particulate matter is quite high in seawater compartment (about 47% of the Hg_T on average). Because of the exponential decay of $[Hg_T]$ in sediments, (...)".

91. **Reviewer** wrote:
L511-L512 "In general, the concentration of the three mercury species dissolved in seawater decreases slowly as a function of time, whereas their concentration ratios remain approximately constant" this happens due to the exponential decay of Hg parameterized for sediment and the absence of inputs in your system (except atmospheric deposition, which is set to be very low, about 3 times lower than observations in Bagnato et al. 2013).

Authors answer:
According the reviewer's comment, we modified the sentence at page 27 as follows:
"Because of the exponential decay of $[Hg_T]$ in sediments, the concentration of the three mercury species dissolved in seawater decreases slowly as a function of time, whereas their concentration ratios remain approximately constant."

92. **Reviewer** wrote:
L526-528 "the amount of mercury absorbed by the phytoplankton, and recycled in seawater, is negligible. In this last respect, it is however important to underscore that even a reduced amount of MeHg entering phytoplankton cells can be very dangerous for the health of human beings due to the bio-accumulation processes which occur throughout the food chain." this seems to be pointless in the discussion. Can you quantify the amount of Hg adsorbed and released?

Authors answer:
These theoretical findings are reported in the manuscript since they represent secondary results of model. In our simulations we could quantify only the Hg adsorbed by POM (see text at page 28) and the content of Hg^{II} (on average $0.000166\ mg/Kg$ in 2011) and $MeHg$ (on average $0.000021\ mg/Kg$ in 2011) within the picoeukaryotes cells. According to this, the paragraph at page 28 has been modified as follows:
" More specifically, in the quasi-stationary condition, the model results indicate that most of the recycled mercury returns to the sediments where is re-buried, and that the amount of mercury absorbed by the POM (0.008 $kmol\ y^{-1}$ for the year 2011), and recycled in seawater, is negligible. In this last respect, it is however important to underscore that even a reduced amount of $MeHg$ entering living phytoplankton cells can be very dangerous for the health of human beings due to the bio-accumulation processes which occur throughout the food chain."

93. **Reviewer** wrote:
L529 "The dynamics of the particulate matter deposition-resuspension process (Neumeier et al., 2008; Ferrarin et al., 2008) does not significantly modify the spatial distribution of the HgT recycled at the surface layer of the sediments" the dynamics of particulate matter are not included in the Hg model, and never presented in the manuscript, so where does this statement come from? (see comments on L214-218)

Authors answer:
This sentence has been removed by the manuscript. In our work no sediment model is now used to describe the dynamics of particulate matter deposition/re-suspension process at the sediment-water interface.

94. **Reviewer** wrote:
L530-533 "Moreover, the theoretical results show that the recycled mercury flux in the Augusta Bay can only partially be described by the scavenging process of organic particles, which however needs further experimental investigations. In fact, improved knowledge of the scavenging process would be necessary to obtain a better estimation of the HgT removed from the water column". Which are other processes affecting the "recycled mercury"? I argue that here, rather than more experimental investigation, you would need a model that can reproduce particulate Hg dynamics.

Authors answer:
According to reviewer's indications, we modified the paragraph at page 28 as follows:
"The theoretical results show that the recycled mercury flux in the Augusta Bay is only partially described by the scavenging process. In particular, an underestimation of the sinking flux for POM-bound mercury is observed when the NPP coming from the NP model is used in Eqs. (4)-(5). Probably, this behaviour is due to the $chl-a$ concentration conversion equation of Baines et al.(1994), which has been calibrated for oceans instead of coastal zones. For this reason, the NPP estimation would need further experimental and theoretical investigations. Moreover, a deeper knowledge of the scavenging process, which determines the particulate Hg dynamics, would be necessary, from a theoretical point of view, to obtain a better estimation of the Hg_T removed from the water column."

95. **Reviewer** wrote:
L537 I do not think is relevant talking about climate change here, at the very end of discussion.

Authors answer:
According to the reviewer's indication, we removed the second-last sentence of Discussion section. Moreover, we modified the last sentence of section as follows:
"Finally, for its features, the HR3DHG model may represent a useful tool to explore and predict the effects of environmental changes on the mercury dynamics for several possible forthcoming environmental scenarios."

96. **Reviewer** wrote:
L551 why should this model be a promising tool to explore and predict the effects of climate changes on Hg dynamics?

Authors answer:
We deleted the last sentence of Conclusion section.

Supplement material

97. **Reviewer** wrote:
S1.1 All the parts that are repetition of section 3.1 in the main text must be removed.

Authors answer:
All repetitions of section 3.1 in the main text have been removed.

98. **Reviewer** wrote:
L49 why is Net Primary Production obtained from satellite if you have a NP model run for the area?

Authors answer:
The Net Primary Production (NPP) is now calculated by using the NP model and conversion equation of Baines et al.(1994). According to this, the definition of NPP at page 3 of Supplement has been modified as follows:
"(...) where NPP is the net primary production obtained by the NP model, (...)"

99. **Reviewer** wrote:
L51-52: this seems to be a misunderstanding of the concept of euphotic layer. If equation S7 is not used must be removed.

Authors answer:
In our work, the euphotic zone depth ($z_0 = 75\ m$) is that arbitrarily fixed by Zhang et al.(2014) for equation S6. To clarify the concept of euphotic layer in this case, we modified the sentence at page 3 of Supplement as follows:
"Since the bathymetry of the Augusta Bay indicates that the water column depth in the whole basin is less than the theoretical euphotic zone depth ($z_0 = 75\ m$) fixed by Zhang et al.(2014), in our model we use only the equation for $z < z_0$"
Moreover, the equation S7 has been removed from the Supplement.

100. **Reviewer** wrote:
L54 why is chlorophyll concentrations obtained from measurements if you have a NP model run for the area? How should the reference Zhang be related to this sentence?

Authors answer:
The chlorophyll concentrations are now calculated by using the NP model and conversion curve of Brunet et al.(2007). To answer the reviewer's questions, the last paragraph of the Section S1.1 has been modified as follows:
"Here, the NPP is calculated by using the conversion equation for $chl\ a$ concentration, as follows:

$$log(NPP(x,y,z,t)) \quad = \quad 2.09 + 0.81 \cdot log(chl\ a(x,y,z,t)), \tag{2}$$

where $chl\ a$ is the chlorophyll concentration $[\mu g \cdot l^{-1}]$ obtained by the NP model (see Section S4).
On the other hand, the $peratio$ is obtained by using the following equation (Zhang et al.,2014):

$$peratio(x,y,z,t) \quad = \quad -0.0081 \cdot T + 0.0806 \ln chl\ a(x,y,z,t) + 0.426, \tag{3}$$

where T is the surface atmospheric temperature $[C]$ coming from remote sensing."

101. **Reviewer** wrote:
S1.1.1 $\phi_{dep} = \frac{Hg_{gas-atm} \cdot Pr}{\Delta t}$ is not dry+wet deposition of Hg, and is a questionable parameterization.

Authors answer:
We consider only the wet deposition for Hg^0. According to this, we modified the text of Supplement at page 4.

About parameterization, we used the equation of Bagnato et al. (2013) to calculate the wet deposition both for Hg^0 and Hg^{II}. Therefore, we do not understand why this parameterization is questionable.

102. **Reviewer** wrote:
S1.1.2 "The lateral fluxes for all variables are set up equal to zero at the boundaries of Augusta basin (Valenti et al., 2017) except where inlets, rivers and sewerage are localized." In this work, only inlets are considered while inputs from rivers and sewerage are assumed to be negligible, but this is not mentioned in the text (it can only be seen from the equations S13 and S14).

Authors answer:
To clarify this point, we modified the sentence at page 5, line 95, of Supplement as follows:
"Since the direct Hg^0 loads from rivers and sewerage are assumed to be negligible for the whole basin, we set:(...)"

103. **Reviewer** wrote:
S1.2 equation S17 is already in the main text (eq.2). Equation S18 should be moved in the main text. In the definition of PHg should be specified that it is estimated externally with the plankton model and is not coupled with the Hg model. It should be explained that is the nutrient recycling efficiency coefficient, which is assumed to be the same for mercury. Equation S19 should be also presented in the main text. The definition given for forg is inconsistent. How are the units for S^{II}_{SPM}? The name S^{II}_{SPM} is misleading, this is an estimate of Hg scavenged by phytoplankton, not SPM.

Authors answer:
According to reviewer's indications, the equations S18 has been moved in the main text, where PHg and λ are better defined. However, it is worth to stress that the Hg model and the Phytoplankton MERLIN-Expo Model are coupled. In fact, the PHg^{II} ($PMeHg$) is obtained by the Phytoplankton MERLIN-Expo Model using dissolved Hg^{II} ($MeHg$) concentration in the seawater (see Section 5 of the Supplement). At the same time, the Hg model uses the PHg^{II} ($PMeHg$) to calculate the load of the dissolved inorganic mercury released by the POM, which is necessary to reproduce the dynamics of dissolved Hg^{II} ($MeHg$) concentration in the seawater (see Section 3.1 of the main text).
The equation S19 has been modified according to reviewer's indications, and moved in the main text.
The S^{II}_{SPM} and S^{MM}_{SPM} have been redefined at page 10 of the revised manuscript. Moreover, all units of parameters and variables are now reported throughout the main text and the Supplement.

104. **Reviewer** wrote:
S1.2.1 equation S21 is only for wet deposition, differently from what is stated

Authors answer:
We modified the equation S21 according to the reviewer's indication. Moreover, the surface dry deposition flux of contaminated particles is now considered in the model. Therefore, we inserted the following sentence at the beginning of page 9 of Section S1.2.1:
"The $Drydep_{part}$ is set equal to that estimated by Rajar et al. (2007) for the whole Mediterranean basin."

105. **Reviewer** wrote:
S1.2.2 The definition for ϕ^{II}_{res} is misleading, why not keeping only the extended version of eq. S22 (which is eq. 7 in the main text)? Is not $Hg^{II}_{dis-water}$ the same as your modeled Hg^{II} with z=zb? Why using a different name?

Authors answer:
The sediment transport module is not included in our model anymore. As a consequence, the terms ϕ^{II}_{res} and ϕ^{MM}_{res} have been removed by Eqs. S22 and S36, respectively.
The Eqs. 7 and 8 of main text are recalled in the Supplement to better define mass transfer coefficients at the water-sediment interface, and to better describe the connections between benthic mercury fluxes and mercury concentrations in the pore water of sediment.
To clarify the terms used in Eq. S22, we replaced $Hg^{II}_{dis-water}$ with $Hg^{II}|_{z=z_b}$. A similar replacement has been done in Eq. S36 between $MeHg_{dis-water}$ and $MeHg|_{z=z_b}$.

106. **Reviewer** wrote:
L212 Why do the values of the "boundary layer thickness above sediment" for Hg and MeHg differ in Table S1? Why are their values so low (0.009 cm for HgII and 0.03 cm for MeHg)? And why are they lower than the "boundary layer thickness below sediment" that is 0.01 for both Hg and MeHg? Equations S22 and S25 is already given in the main text (eq. 16 and 18), refer to that. Equation S25 is not in agreement with Melaku Canu et al., 2015 as stated in L228.

Authors answer:
We recall that the *boundary layer thickness above sediment* for Hg^{II} and $MeHg$ are calibrated separately according to the procedure of Section 3.3, while the *boundary layer thickness below sediment* has been estimated for both mercury species by the average velocity of marine currents.
The Eqs. 16, 17 and 18 of main text are recalled in the Supplement to better describe the parameter setting of these equations. The reference Melaku Canu et al., (2015) in L228 has been removed.

107. **Reviewer** wrote:
S1.2.3 is already in the main text (eq.15).

Authors answer:
The Eq. 15 of main text is recalled in the Supplement to better describe the setting of $Hg_T^{sed}(0)$ coming from experimental data.

108. **Reviewer** wrote:
S1.2.5 eq. S27 is eq. 9 in the main text. Equations S28-S29 are the same as S13-S14, and S42-S43, I think they can be written in a more general formula without repeating them for each Hg species, especially considering that they are set to 0 for your implementation.

Authors answer:
According to reviewer's indications, we removed Sections S1.2.5 and S1.3.4 of the Supplement, and modified the last paragraph of Section S1.1.2 as follows:
"The same boundary conditions (lateral fluxes) are also valid for Hg^{II} , $MeHg$ and Hg_T. The annual net outflow of elemental mercury from (...) and for the whole year. Similarly, the annual net outflows of Hg^{II} and $MeHg$ are calculated.
In order to perform the mass balance for the Augusta Bay, we calculate the annual net outflow of total mercury (O) from the basin towards (...)."

109. **Reviewer** wrote:
S1.3 Equation S32 is already in the main text (eq.3).

Authors answer:
The whole text of Section S1.3 has been removed from the Supplement.

110. **Reviewer** wrote:
L295-296 why all these references?

Authors answer:
See previous answer of authors.

111. **Reviewer** wrote:
L304-307 the text is already in the main text.

Authors answer:
The text at page 13 lines 304-307 has been removed.

112. **Reviewer** wrote:
L308 "The rate constant for the methylation of inorganic mercury is fixed according to Monperrus et al. (2007) (Batrakova et al.,2014; Monperrus et al., 2007b)." Why are references reported in this way? There are other cases.

Authors answer:
The references are now reported in correct way throughout the manuscript.

113. **Reviewer** wrote:
L311-317 same comments as for S1.2 (and it can be explained just once for both Hg and MeHg) .

Authors answer:
The text at page 13 lines 311-317 has been removed.

114. **Reviewer** wrote:
S1.3 Almost the entire section is a repetition of information already given in the main text or in S1.2. The only difference with section S1.2 is the substitution of "HgII" with "MeHg", there must be a better way.

Authors answer:
All repetitions of Section 1.3 have been removed from the text.

115. **Reviewer** wrote:
S1.3.1 MeHg atmospheric deposition is > 0, although low (e.g. Mason et al., 2012).

Authors answer:
The boundary condition for MeHg atmospheric deposition has been changed according to Mason et al., (2012). As a consequence, the text of Section S1.3.1 has been rewritten as follows:
"According to Mason et al. (2012), the methyl-mercury flux at the water-atmosphere interface (z=0) is estimated to be 0.5 % of total Hg deposition flux ($\simeq 0.5\%$ of Hg^{II} deposition flux). Therefore, in our model we set: (...)
The annual atmospheric deposition of the methyl-mercury is calculated by integrating Eq. (S36) for the whole horizontal surface of the basin and for the whole year. The annual total atmospheric mercury deposition (AD) is equal to the sum of the amounts of elemental, inorganic and methyl mercury deposited on the surface of the Augusta basin in one year."

116. **Reviewer** wrote:
S2 "Since the direct loads of SPM (Ciffroy, 2015; Melaku Canu et al., 2015) for the Augusta basin were unknown, the SPM concentration dynamics could not be reproduced correctly. Therefore, we reproduced the spatial distribution of SPM concentration at the steady state by interpolating the experimental data observed in recent samplings (October 2017) performed in the site investigated." You obtained SPM values by interpolating observations and assume steady state conditions, thus why do you present a dynamic model for SPM that is not used (eq.S46)? What about the references? Besides, at a first and second reading is not clear why you need SPM if adsorption of particulate Hg species is based on NPP obtained from satellite data. At some point, I realized that this is only used in eq. 13 to estimate HgT.

Authors answer:
The equation for the SPM dynamics has been removed by Section S2, as well as the references. Moreover, to clarify why the experimental SPM concentrations need, we added at the ending of Section S2 the following sentences:
"The experimental SPM and POM concentrations were used to reproduce the spatial distribution of the fraction of suspended particulate matter as organic carbon (f_{oc}), which was necessary to obtain the sinking fluxes of Hg^{II} and $MeHg$. Afterwards, the SPM concentrations were used to calculate the $[Hg_T]$ in seawater (see Section 3.1)."

117. **Reviewer** wrote:
S2.1 the definition given for f_{org} "organic fraction of suspended particulate matter in dissolved-phase" is meaningless.

Authors answer:
We removed the words "in dissolved phase" from the f_{org} definition. Moreover, we defined the fraction of suspended particulate matter as organic carbon at the ending of Section S2.1, as follows:
"Since we assumed that 52% of organic matter was carbon, the fraction of suspended particulate matter as organic carbon was calculated by using the following equation: (...)"

118. **Reviewer** wrote:
S3 and S3.1 These sections should present the site-specific implementation of SHYFEM model for Augusta Bay, rather

than providing a general description of the model, which is available elsewhere in the literature. The reader should be able to understand how the hydrodynamic and sediment models have been run (add values used for parameters and coefficients, show the calibration). The title for S3.1 is incomplete.

Authors answer:
According to the reviewer's indications, we modified Section S3 of the Supplement. Specifically, a new paragraph entitled " Hydrodynamic model validation" has been added describing the comparison between the model results and ones obtained from previous application in the bay. See in the text from line 567 to line 611.

119. **Reviewer** wrote:
S4 Be aware that eukariotes are not a planktonic population, thus line 566 is meaningless. The term eukariotes is much broader than phytoplankton, which is what is actually simulated here; this must be corrected throughout the text.
The NP model is already described in many publications reported here and is not a central part of this work, so as for the hydrodynamic and sediment models I do not think the model theory should be explained in detail here. Probably a description of the implementation for the Augusta Bay (linked to Table S3) clarifying which are site specific parameters and which parameters are adopted from other areas, would be more useful. I would also like to see calibration, or a map of the output.

Authors answer:
The word "eukaryotes" has been replaced by the word "picoeukaryotes" in the Section S4. We recall that the picoeukaryotes domain is the set of most representative phytoplankton populations of oligotrophic waters of Mediterranean Sea.
To clarify which are site-specific parameters of NP model, we inserted at page 25, lines 661-664, the two following sentences:
"The half-saturation constants for growth of picoeukaryotes, used in the the Michaelis-Menten formulas, depend on the environmental conditions of investigated site. Since the *chlorophyll-a* concentrations, measured in the Augusta Bay, are those typical of oligotrophic waters of the Mediterranean Sea, the half-saturation constants are set equal to values previously obtained in the Southern Sicily by Valenti et al. (2017) adopting an accurate calibration procedure." Moreover, we modified the sentence at page 25, lines 664-667, as follows:
"All other parameters are set in accordance with the methods described in previous works, while the temporal behaviour of incident light intensity, $I_{in}(t)$, is obtained for the Augusta Bay by using the remote sensing data."

120. **Reviewer** wrote:
Table S1 all parameters where "no data" is reported are set to 0. Is it possible to make assumptions and estimate them?

Authors answer:
We cannot estimate the parameters where "no data" is reported. However, we can speculate that these parameters are negligible according to field observations.

121. **Reviewer** wrote:
Table S2 why is it separated from S1? The caption is the same. Do you have 0 porosity value?

Authors answer:
The caption is not the same. In fact, Table S1 describes the parameters of biogeochemical model, while Table S2 reports the range of the variables of model. Finally, the minimum value of porosity has been corrected.

122. **Reviewer** wrote:
Table S9 It should be explained in the main text why your modeled value of atmospheric deposition is 2.5 lower than the deposition measured at your study site in 2011-2012 (Bagnato et al. 2013; Salvagio Manta et al. 2016). How would affect your results the increase atmospheric deposition to the observed rate? It should be also explained in the main text why all inputs different from atmospheric deposition are set to 0.
Why is the term "MeHg released from sediment" in this HgT budget? Here only the total is needed. Why is MeHg budget not estimated?

Authors answer:
According to reviewer's indications, we inserted the following new paragraphs at the ending of page 22 of the main text: "This discrepancy is due to different calculation methods used in the two works. Specifically, in our model the AD is calculated by using both the atmospheric mercury concentrations and the average precipitations, measured for all months of the year. On the contrary, in Bagnato et al. (2013) the AD is calculated by averaging the experimental data acquired during a time limited sampling period (from 29^{th} August 2011 to 23^{th} April 2012), namely without considering the year period in which the amount of precipitation is very low. By this way, the AD obtained by Bagnato et al. (2013) is very higher than that of our model, even if it is probably overestimated due to calculation method used. In general, the contribute of AD is negligible in the mercury mass balance of the Augusta Bay. Indeed, the simulations indicate that a strong increase of atmospheric mercury deposition caused by environmental changes (dust fall increase and/or rainfall increase), would not affect on numerical results of our model significantly.
The annual net mercury inflows (A) from rivers and sewerage to basin are assumed to be negligible in agreement with field observations. Specifically, the flow rate of Marcellino river is equal to zero for the most part of year, while the inflow from the sewerage is low. Moreover, it is fair to speculate that the Hg concentration in fresh waters discharged in the Augusta Bay was decreased significantly after the chlor-alkali plant closure."
According to reviewer's indication, the "MeHg released from sediment" has been removed by Hg_T budget in Table S11. Moreover, it is worth to underline that the annual fluxes of MeHg are estimated by our model, even if they cannot validated with experimental findings. For this reason, the MeHg budget has been not reported in the paper.

123. **Reviewer** wrote:
Table S5-S6-S7-S8-S10. To improve readability, I would move the station/longitude/latitude information for data and model in a separate table and keep here only Station | Period | Depth | Hg.

Authors answer:
According to reviewer's indication, the station/longitude/latitude information for data have been moved in a separate table (see Table S4 of Supplement).

124. **Reviewer** wrote:
Figure S3. I don't see a good agreement here. I took the effort to copy your Hg_D data from Table S5 and found an average relative error of 86% (median 62%) between model and observations, this could even be fine if you acknowledge it and properly discuss it.

Authors answer:
The goodness of agreement between the theoretical results and experimental data is now discussed at pages 19-20 of the main text.

125. **Reviewer** wrote:
Figure S4. The scale (up to 140) is almost two time as high as the maximum value shown, so almost everything appears in blue.

Authors answer:
The color scale of Figure S4 has been changed to make comparable the experimental and theoretical data maps.

Best regards.

On behalf of all authors

Alessandro Borri

HR3DHG version 1: modelling the spatio-temporal dynamics of mercury in the Augusta Bay (southern Italy)

Giovanni Denaro[1], Daniela Salvagio Manta[2], Alessandro Borri[3], Maria Bonsignore[4], Davide Valenti[1,5], Enza Quinci[4], Andrea Cucco[6], Bernardo Spagnolo[5,7,8], Mario Sprovieri[4], and Andrea De Gaetano[3]

[1]CNR-IRIB, Consiglio Nazionale delle Ricerche - Istituto per la Ricerca e l'Innovazione Biomedica, Via Ugo La Malfa 153, I-90146 Palermo, Italy
[2]CNR-IAS, National Research Council of Italy – Institute of Anthropic Impacts and Sustainability in marine environment, ex Complesso Roosevelt, Lungomare Cristoforo Colombo, 4521, Loc. Addaura, Palermo, Italy
[3]CNR-IASI Biomathematics Laboratory, Consiglio Nazionale delle Ricerche - Istituto di Analisi dei Sistemi ed Informatica "A. Ruberti", Via dei Taurini 19, I-00185 Rome, Italy
[4]CNR-IAS, National Research Council of Italy – Institute of Anthropic Impacts and Sustainability in marine environment, U.O.S di Capo Granitola, Via del Faro 3, I-91020 Campobello di Mazara (TP), Italy
[5]Dipartimento di Fisica e Chimica "Emilio Segrè", Università di Palermo, Group of Interdisciplinary Theoretical Physics and CNISM, Unità di Palermo, Viale delle Scienze, Ed. 18, I-90128 Palermo, Italy
[6]CNR-IAS, Consiglio Nazionale delle Ricerche - Istituto per lo studio degli impatti Antropici e Sostenibilità in ambiente marino, U.O.S. di Oristano, località Sa Mardini, I-09072 Torregrande (OR), Italy
[7]Radiophysics Department, National Research Lobachevsky State University of Nizhni Novgorod, 23 Gagarin Avenue, Nizhni Novgorod 603950, Russia
[8]Istituto Nazionale di Fisica Nucleare, Sezione di Catania, Via S. Sofia 64, I-90123 Catania, Italy

Correspondence: Alessandro Borri (alessandro.borri@iasi.cnr.it)

Abstract. The biogeochemical dynamics of Hg, and specifically of its three species Hg^0, Hg^{II}, and $MeHg$ (elemental, inorganic, and organic, respectively) in the marine coastal area of Augusta Bay (southern Italy) have been explored by the high resolution 3D Hg (HR3DHG) model, namely an advection-diffusion-reaction model for the dissolved mercury in the seawater compartment coupled with i) a diffusion-reaction model for dissolved mercury in the pore water of sediments and ii) a sorption/de-sorption model for total mercury in the sediments, in which the de-sorption process for the sediment total mercury is taken into account. The spatio-temporal variability of dissolved and total mercury concentration both in seawater ($[Hg_D]$ and $[Hg_T]$) and first layers of bottom sediments ($[Hg_D^{sed}]$ and $[Hg_T^{sed}]$), and the Hg fluxes at the boundaries of the 3D model domain have been theoretically reproduced, showing an excellent acceptable agreement with the experimental data, collected in multiple field observations during six different oceanographic cruises. Also, the spatio-temporal dynamics of total mercury concentration in seawater have been obtained by using both model results and field observations. The mass-balance of the different total Hg species in seawater has been calculated for the Augusta Harbour, improving previous estimations. The HR3DHG model includes modules that can be implemented for specific and detailed exploration of the effects of climate change on the spatio-temporal distribution of Hg in highly contaminated coastal-marine areas. The HR3DHG model could be used as an effective tool to predict the spatio-temporal distributions of dissolved and total mercury concentrations, while contributing to better assess the hazard for environment and therefore for human health in highly polluted areas.

1 Introduction

The investigation of biogeochemical dynamics of Hg species in the marine environment addresses the need to accurately model sources and pathways of this priority contaminant within and among the different abiotic and biotic compartments of the aquatic ecosystem (Driscoll et al., 2013; Batrakova et al., 2014) . Over the last few years some theoretical studies have offered sophisticated innovative tools to reproduce the mass balance and the dynamics of $[Hg]$ in the marine environment by means of biogeochemical models based on interconnected zero dimensional boxes, representing water or sediment compartments: among these is are the River MERLIN-Expo model (Ciffroy, 2015) and the WASP (Water Analysis Simulation Program) model (Melaku Canu et al., 2015; Canu and Rosati, 2017; Rosati et al., 2018). Similarly, a box-model approach has been adopted by In particular, the River MERLIN-Expo model (Ciffroy, 2015) has been used to reproduce the spatio-temporal distribution of inorganic and organic contaminants in the 1D domain of rivers, and to calculate $[Hg]$ the mass balance for each of them. Although the River model is able to describe many of the physical and chemical processes involved in freshwater and sediment, corresponding this model specifically targets environments characterized by (i) nearly-homogeneous water bodies and (ii) limited variations in landscape geometry. The WASP models have been used to simulate the Hg cycle within aquatic ecosystems characterized by well-mixed water layers and homogeneous sediment layers coupled through the boundary conditions at the water-sediment interface (Melaku Canu et al., 2015; Canu and Rosati, 2017; Rosati et al., 2018). In particular, a WASP model applied to a 1D domain and calibrated by using experimental data for dissolved Hg and $MeHg$, allowed to explore $[Hg]$ dynamics in the Black Sea (Rosati et al., 2018). Similarly, the WASP-based box model approach has been adopted in 2D configuration (Melaku Canu et al., 2015; Canu and Rosati, 2017) to calculate Hg mass balance in the coastal areas of the Marano-Grado lagoon (northern Italy), where heterogeneous spatial distributions of Hg species have been observed experimentally. In general, models based on zero dimensional boxes do not deliver reliable concentration values of contaminants in highly heterogeneous environments unless they provide high spatial resolution and a proper parameterization of the biogeochemical system.

For these reasons, in a recent work (Pakhomova et al., 2018) the biochemistry of Hg in aquatic ecosystems has been studied using a high resolution (HR) 1D advection-reaction-diffusion model, in which a mercury module has been integrated with the Bottom RedOx Model (BROM) (Yakushev et al., 2017) has been used to reproduce the vertical dynamics of the total dissolved Hg and $MeHg$ in the marine coastal areas of the Etang de Berre lagoon (France) (Pakhomova et al., 2018). However, even this model includes some criticalities in the estimation of mercury dynamics. For example, the temporal variations of mercury benthic fluxes, due to reaction and diffusion processes which involve mercury species present in sediments, are not taken into account in the boundary conditions of this model. On the other hand, sediment chemistry and diffusion were investigated recently by Soerensen et al. (2016), who devised a high resolution 1D model for Hg species present in water and sediments of the Baltic Sea (Soerensen et al., 2016). In both HR models, however, the strong impact of the horizontal velocity field on the spatio-temporal distribution of $[Hg]$ could not be considered since the 1D modelling was used.

In general, the appropriate modelling to reproduce the spatial and temporal variability of Hg species in highly heterogeneous marine ecosystems, such as Augusta Harbour, requires the use of a hydrodynamics model integrated with a biogeochemical model (Zagar et al., 2007, 2014). For this aim, Zagar et al. (2007) introduced a PCFLOW3D model upgraded with the biogeochemical module for simulating simultaneously velocity field of marine currents, suspended particles transport and mercury biogeochemical transformations for the whole Mediterranean Sea. The modified PCFLOW3D is a non-stationary 3D model, which consists of four real-time integrated modules: i) hydrodynamic module and ii) transport-dispersion module, both based on the finite volume method and implemented for obtaining the velocity field of marine currents and the turbulent diffusivities; iii) sediment-transport module used to simulate the transport, sedimentation and re-suspension of solid particles; iv) biogeochemical module to reproduce the advection, diffusion and reaction processes of Hg species. Although the used grid did not guarantee a high spatial resolution, the modified PCFLOW3D model allowed to obtain, for all the Hg species, theoretical vertical profiles of $[Hg]$ in acceptable agreement with experimental data for most part of the Mediterranean Sea (Zagar et al., 2007), and to improve the fluxes estimation of Hg mass balance for the whole Mediterranean basin (Rajar et al., 2007). By following the same modelling approach of Zagar et al. (2007), over the last decade several authors used 3D advection-diffusion- reaction models to simulate the spatio-temporal dynamics of $[Hg_D]$ and $[Hg_T]$ in oceans, lakes and estuaries (Zhu et al., 2018). However, the Hg partition mechanisms between the liquid phase and the (biotic and abiotic) particulate organic matter (POM) were explicitly included only in few studies. Among these, Zhang et al. (2014) reproduced the $[Hg_T]$ in oceans and calculated a Hg mass balance by using a 3D ocean tracer model (OFFTRAC) coupled with a general circulation model (GEOS-Chem) (Zhang et al., 2014). Here, the sinking flux of Hg bound to POM was calculated exploiting the remote sensing data for net primary production (NPP) and chlorophyll concentration, which are associated to phytoplankton abundance.

All these approaches forego the complete representation of the spatial variability by approximating the model domain as a set of interconnected boxes or by detailing only the vertical dynamics of the investigated chemical species. All these approaches do not allow a fine representation of the spatial variability by approximating the model domain as a set of interconnected boxes or by detailing only in seawater compartment the spatio-temporal dynamics of the investigated chemical species. For these reasons, we developed a new model to reproduce the spatio-temporal dynamics of $[Hg]$ in polluted marine sites characterized by very high spatial heterogeneity, such as the Augusta Harbour. In the present work we report on results obtained using a 3D advection-diffusion-reaction biogeochemical model for three Hg species in seawater (Hg^0, Hg^{II}, and $MeHg$), coupled with a diffusion-reaction model for dissolved Hg in the pore water of sediments in sediments and connected pore water. The model, named HR3DHG, has been applied to the investigation of the mercury dynamics in Augusta Bay (southern Italy, see Fig. 1) and specifically in its harbour, a highly polluted coastal site. In this area, a substantial experimental dataset has been collected and improved upon in recent years (Sprovieri et al., 2011; Bagnato et al., 2013; Sprovieri, 2015; Oliveri et al., 2016; Salvagio Manta et al., 2016): oceanographic cruises and data on key physical and chemical parameters from atmosphere, seawater and sediments are used to verify and validate the modules of HR3DHG for reliable and accurate high-resolution investigation of spatio-temporal dynamics of Hg in highly contaminated coastal-marine sites. The HR3DHG model has been designed to predict the biogeochemical behaviour of Hg in seawater and sediments, specifically in confined and highly-polluted marine-coastal areas. It offers the opportunity to explore the effects both of sorption/de-sorption dynamics of total mercury (Hg_T^{sed}) in

sediments, and of Hg_D^{sed} diffusion dynamics in pore water in nearly-steady conditions. To this aim, in the model we consider both the sediment - pore water distribution coefficients and the desorption rate for the total mercury concentration in the sediment. The former described the ratio between adsorption and desorption rate constants at the steady state without considering pertubations induced by mercury concentration reduction in pore water. The latter reproduced the effects of these pertubations on the solid phase of the sediments.

Moreover, the role played by the spatio-temporal behaviour of phytoplankton (La Barbera and Spagnolo, 2002; Fiasconaro et al., 2004; Valenti et al., 2004, 2008; Dutkiewicz et al., 2009; Morozov et al., 2010; Valenti et al., 2012; Denaro et al., 2013a, c, b; Valenti et al., 2015, 2016a, b, c, 2017; Morozov et al., 2019) and the mechanisms responsible for the uptake of Hg within cells (Pickhardt and Fischer, 2007; Radomyski and Ciffroy, 2015; Lee and Fischer, 2017; Williams et al., 2010) are taken into account as specific contribution to the scavenging process and the Hg release process by POM, respectively. Also seasonal oscillations of key environmental variables (velocity of marine currents, amount of precipitation, elemental and inorganic mercury concentration in atmosphere, etc.) are taken into account.

The main objectives of the HR3DHG model can be synthesized as following: (i) to accurately reproduce and localize the peaks of $[Hg]$ within the 3D domain, (ii) to estimate the Hg fluxes at domain boundaries, and (iii) to predict the evolution of mercury in sediment of polluted sites. Moreover, the HR3DHG model offers the possibility to describe the $MeHg$ and Hg^{II} partition between the dissolved phase (both seawater and pore water) and the particulate phase (suspended particulate matter and sediment particles). Specifically, in the dissolved phase the model describes the overall behaviour of Hg in ionic form and complexed with Dissolved Organic Carbon (DOC). Given all these features, Finally, the HR3DHG model can be a useful tool to predict and prevent the risks for the human health in marine areas close to industrial sites affected by Hg pollution extended for possible effects of climate changes (e.g. increase of temperature, dust inputs, etc.) on mercury dynamics in the environment for very long time intervals.

The paper is organized as follows: a brief overview of the study site is provided in section 2. The description of the HR3DHG model and the model simulation setup are described in Section 3, referring to the Supplement for further details. In Section 4 the obtained results are reported and compared with experimental data. In Section 5 the model and the results are discussed and, finally, conclusions are drawn in Section 6.

2 The study area

The Augusta Bay (Fig.1) is a semi-closed marine area which occupies a surface of about 30 km^2 on the eastern coast of Sicily (southern Italy). The location of one of the most important harbours of the Mediterranean overtime since the early 1960s, the Augusta site also hosts several industrial plants, which have adversely affected the whole area with the diffusion of several priority pollutants. In particular, huge amount of Hg from one of the largest European chlor-alkali plant (Syndial Priolo Gargallo), was discharged into the sea without any treatment until the 1970s, when waste treatment became operational (Bellucci et al., 2012). Although discharge activities were definitively stopped in 2005, the Hg contamination from the chlor-alkali plant remains a critical environmental threat, with extremely high $[Hg]$ in the bottom sediments (ICRAM, 2008; Sprovieri et al.,

2011; Oliveri et al., 2016), significant Hg evasion fluxes from sediments to seawater (Salvagio Manta et al., 2016) and to the atmosphere (Bagnato et al., 2013; Sprovieri, 2015), and evident and recently documented risks for the ecosystem (Tomasello et al., 2012; Bonsignore et al., 2013) and for human health (Bianchi et al., 2006; Bonsignore et al., 2015, 2016). The geographical position, together with its geological and oceanographic features, assign to this area a key role in the Hg inventory at Mediterranean scale. The estimate of the Hg export from Augusta Bay to the open sea (0.54 $kmol\ y^{-1}$, Salvagio Manta et al., 2016), corresponds to about 4% of total input from coastal point/diffuse sources to the Mediterranean Sea (12.5 $kmol\ y^{-1}$, Rajar et al., 2007). A very narrow shelf develops down to 100-130 m with a mean gradient of about 1.0 degree and a next steep slope characterized by a dense net of canyons dropping to the deep Ionian basin (Budillon et al., 2008). The Augusta Harbour covers a surface of 23.5 km^2 with two main inlets connecting with the open sea: the Scirocco (300 m wide and 13 m deep) and the Levante inlets (400 m wide and 40 m deep). The bottom is mainly flat with an average depth of 15 m, with the exception of a deeper channel about 30 m deep connecting the inner part of the harbour with the Levante inlet. Water circulation inside the port and the exchanges through the inlets are mainly ruled by the wind and tidal forcing. Tidal fluctuations are generally low, with amplitudes ranging between 10 to 20 cm and the winds are generally from Northwest and Northeast with an average speed around 3 m/s (De Marchis et al., 2014). Water circulation in the outer coastal areas is also mainly affected by wind and tidal forcing and only weakly influenced by the outer baroclinic ocean circulation, which takes place mainly from the shelf break area offshore.

3 Model description

The HR3DHG model has been designed and implemented to reconstruct, at high spatio-temporal resolution, the behaviour of $[Hg_T]$ and $[Hg_D]$. The model consists of an advection-diffusion-reaction model for the seawater compartment, coupled with a diffusion-reaction sub-model for pore water, in which the dynamics of the sorption/de-sorption of $[Hg_T^{sed}]$ between the solid (sediments) and liquid phase (pore water) is considered.

As well as the PCFLOW3D model of Zagar et al. (Zagar et al., 2007), the module of biogeochemical model for the seawater compartment is integrated with a hydrodynamics module (see Fig.2). Specifically, the SHYFEM model is used to calculate the spatio-temporal behaviour of the horizontal components of the velocity field in the seawater compartment (Burchard and Petersen, 1999; Umgiesser et al., 2004; Umgiesser, 2009; Umgiesser et al., 2014; Ferrarin et al., 2014; Cucco et al., 2016a, b, 2019), fixing to zero the vertical velocity according to the experimental data (see Section S3 of the Supplement for details). In the HR3DHG model, the mercury exchange between the abiotic and biotic compartments is also taken into account. For this purpose, the spatio-temporal behaviour of picoeukaryotes abundance is reproduced by using the Nutrient-Phytoplankton (NP) model (Denaro et al., 2013a, c; Valenti et al., 2015, 2016a, b, 2017) (see Section S4 of the Supplement for details). By using the curve of mean vertical profile obtained by Brunet et al. (2007) the picoeukaryotes abundances are converted into the chlorophyll concentration, which allows to reproduce the spatio-temporal distribution of NPP. This is used in our model to calculate both the biological rate constants and the sinking flux of Hg adsorbed by POM. The amount of Hg absorbed and released by each picoeukaryote cell in seawater is calculated by using the Phytoplankton MERLIN-Expo Model (Ciffroy, 2015;

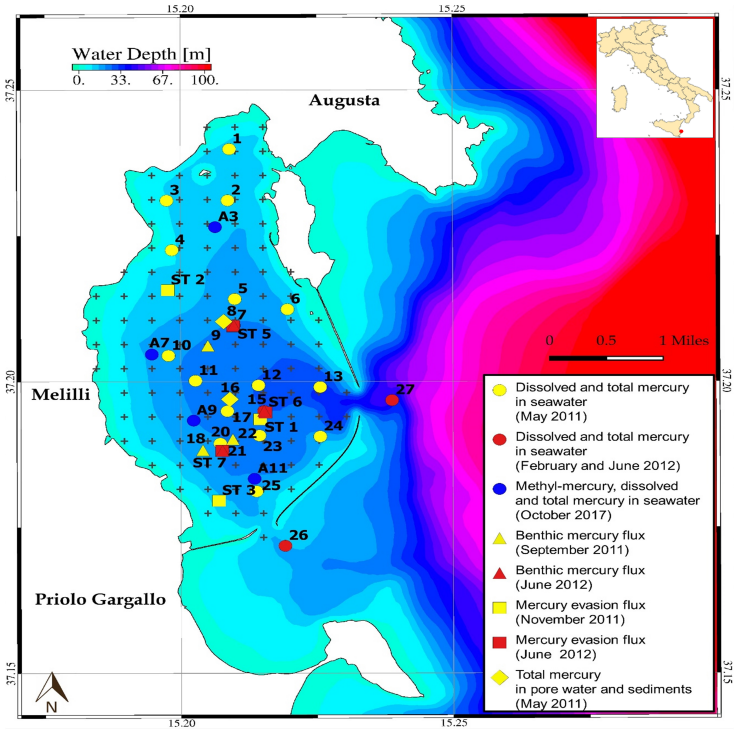

Figure 1. Map of the area under investigation including the Augusta Bay and the eponymous harbour. The sampling sites of each oceanographic survey are indicated with different symbols.

Radomyski and Ciffroy, 2015) (see Section S5 of the Supplement for details). The two modules are coupled with the advection-diffusion-reaction sub-model in order to reproduce the spatio-temporal behaviour of the load of dissolved Hg released by dead picoeukaryotes net amount of mercury incorporated by phytoplankton cells in the seawater compartment (see Fig.2).

3.1 The advection-diffusion-reaction model for the Hg species in seawater

The dynamics of the $[Hg_D]$ in the Augusta Bay has been reproduced using an advection-diffusion-reaction model. Specifically, the model represents equations are solved to obtain the behaviour of the three main Hg species in seawater, indicated by $Hg^0(x,y,z,t)$, $Hg^{II}(x,y,z,t)$, and $MeHg(x,y,z,t)$, which denote the concentrations of each Hg species in the position (x,y,z) within the three-dimensional domain at a specific time t, and whose reciprocal interactions are modeled with the reaction terms of the Partial Differential Equations (PDEs). Since the experimental data indicate that Me_2Hg concentration is very low in the Augusta Harbour (Sprovieri, 2015), the behaviour of this Hg species is not reproduced in our model. By solving the model equations, we obtain the spatio-temporal distributions of $Hg^0(x,y,z,t)$, $Hg^{II}(x,y,z,t)$, and $MeHg(x,y,z,t)$. The spatial domain is composed by the sum of several sub-domains (regular parallelepipeds), which cover the bathymetric map of

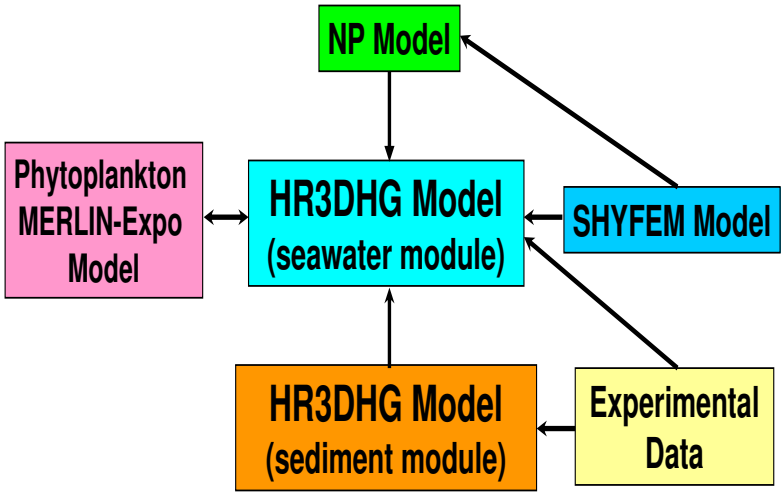

Figure 2. Basic structure of the HR3DHG model.

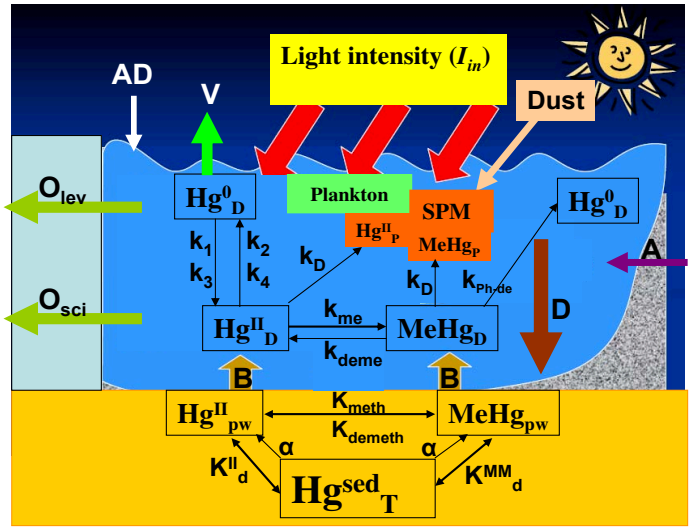

Figure 3. Basic scheme used for implementing the HR3DHG model. The scheme describes the transformation processes (k_1- photo-oxidation , k_2- photo-reduction, k_3-biological oxidation, k_4-biological reduction, k_{Ph-de}-photo-demethylation, k_{deme}-demethylation, k_{me}-methylation, K_{demeth}-demethylation, K_{meth}-methylation) and the main transport processes (A-anthropogenic input, AD-atmospheric deposition, B-benthic flux, D-net flux due to particulate deposition and settling, O-net outflow from basin, V-atmospheric evasion) which involve the dissolved and particulate-bound Hg species in seawater (Hg^{II}_D, $MeHg_D$, Hg^0_D, Hg^{II}_P, $MeHg_P$) and sediments (Hg^{II}_{pw}, $MeHg_{pw}$, Hg^{sed}_T).

the Augusta Bay (Sprovieri et al., 2011). Specifically, z represents the depth of the barycenter of each sub-domain, localized between the surface ($z = 0$) and the bottom ($z = z_b$), while x and y indicate the distance in meters measured from a reference point (Lat. $37^o14.618$ N, Long. $15^o11.069$ E) located at North-West of the town of Augusta.

The model for both compartments is coded in C++ and adopts a finite volume scheme in explicit form with spatial and temporal discretizations treated separately. The approach followed allows the combination of various types of discretization procedures for solving the diffusion, advection and reaction terms. Specifically, the differential equations are solved by performing centered-in-space differencing for the diffusion terms and first-order upwind-biased differencing for the advection terms.

The model domain in seawater is constituted by a mesh of 10 and 18 elements regularly spaced of 454.6 m in both x- and y-direction, and with a variable number of vertical layers of 5 m depth in the z-direction. The mesh covers the whole Augusta Harbour and part of the adjacent coastal area. In Fig.1 the model domain is shown along with the location of the open boundaries in correspondence of the two port inlets. In both compartments (seawater and sediment), a fixed time step of 300 sec has been chosen to satisfy the several stability conditions and constrains associated with the numerical method adopted (Tveito and Winther, 1998). Stability analysis, performed according to previously published methods (Roache, 1998; Tveito and Winther, 1998; Thi et al., 2005), indicates that the convergence of our algorithm is guaranteed.

As initial conditions, we assumed an uniformly distributed concentration of Hg_D and Hg_T, set to 1.9 ng/l corresponding to the experimental detection limit. However, the results appear substantially unaffected by the chosen initial conditions, since the same $[Hg]$ are obtained at nearly-steady state when higher initial Hg concentrations are hypothesized.

The dynamics of the Hg species in seawater is represented through five processes (Zhang et al., 2014; Melaku Canu et al., 2015): i) photochemical and biological redox transformations (reaction terms); ii) methylation/demethylation reactions (reaction terms); iii) movement due to turbulence (diffusion terms); iv) passive drift due to marine currents (advection terms); v) organic and inorganic particle scavenging; vi) organic particle re-mineralization.

The photochemical and biological redox transformations between Hg^0 and Hg^{II} have been described as reaction terms with a first-order kinetic (Batrakova et al., 2014; Zhang et al., 2014; Melaku Canu et al., 2015). In particular, the rate constants of photochemical redox reactions are directly proportional to the short-wave radiation flux at sea surface then attenuated along the water column due to the dissolved organic carbon (DOC) and suspended particulate matter (SPM) (Han et al., 2007; Zhang et al., 2014). At the same time, the rate constants of biological redox reactions are proportional to the organic carbon re-mineralization rate (OCRR), which depends on the net primary production at sea surface (NPP), surface chlorophyll concentration and surface atmospheric temperature (Zhang et al., 2014). All data to estimate the rate constants of the redox reactions are derived from remote sensing (see Section S1 of the Supplement).

The model includes three reaction terms regulated by first-order kinetics, which describe the photo-demethylation of $MeHg$, the methylation of Hg^{II} and the biotic demethylation of $MeHg$, respectively (Batrakova et al., 2014; Melaku Canu et al., 2015). The first is the amount of Hg^0 produced by the $MeHg$ through photochemical reactions. The second is the amount of $MeHg$ obtained by the Hg^{II} through biotic and abiotic pathways in seawater. The third is the amount of Hg^{II} produced by the $MeHg$ through reductive demethylation processes caused by activity of bacteria in contaminated environments. The rate constants of three reaction terms are fixed according to previous works (Monperrus et al., 2007b, a; Lehnherr et al., 2011;

Batrakova et al., 2014; Melaku Canu et al., 2015).

The PDEs include terms of advection and diffusion for each dimension of the 3D domain. In particular, the diffusion terms reproduce the effects of turbulence on the 3D distribution of Hg_D through horizontal (D_x and D_y) and vertical (D_v) turbulent diffusivities, which are fixed as constant (see Section S1 of the Supplement). The horizontal turbulent diffusivity is assumed isotropic in the horizontal water plane (D_x=D_y), and calibrated by considering the values obtained in Massel (1999) (Massel, 1999). The vertical turbulent diffusivity is calibrated according with experimental data, which indicate highly stratified water column conditions during the whole year.

The advection terms describe the effects on the Hg distributions induced by (i) the horizontal velocity components ($v_x(x,y,z,t)$ and $v_y(x,y,z,t)$) of the marine currents along the x- and y- directions, and (ii) the vertical velocity component ($v_z(x,y,z)$) along the z-direction. The horizontal velocities are calculated using results achieved by applying a hydrodynamic model to the area (Umgiesser et al., 2004; Umgiesser, 2009; Cucco et al., 2016a, 2019) (see Section S3 of the Supplement), and change as a function of space and time. The vertical velocity is fixed to zero according to available experimental data.

Moreover, we estimated the dynamics of the dissolved Hg^{II} and $MeHg$ species, also considering effects due to (i) the adsorption by SPM (scavenging process) and (ii) the release by particulate organic matter. The scavenging process for both Hg_D species is regulated by the sinking flux of particle-bound mercury mercury concentration along the water column (Zhang et al., 2014), which depends on variables calculated by using the NP model.The amount of Hg released by particulate organic matter is primarily estimated through parameters and variables defined in the NP model and Phytoplankton MERLIN-Expo Model (Valenti et al., 2012; Denaro et al., 2013a, c, b; Valenti et al., 2015, 2016a, b, c, 2017; Radomyski and Ciffroy, 2015) (see Sections S4 and S5 of the Supplement). Specifically, the NP model provides the spatio-temporal distribution of picoeukaryotes abundance, which is used to get the chlorophyll concentration and the net primary production through suitable conversion functions (Brunet et al., 2007; Baines et al., 1994) (see Sections S1 and S4 of the Supplement). These two variables are then exploited to calculate the contribute of the sinking flux for POM-bound Hg within the suspended particulate matter. The Phytoplankton MERLIN-Expo Model gives the spatio-temporal dynamics of the Hg^{II} and $MeHg$ contents within the picoeukaryotes cells (Radomyski and Ciffroy, 2015). These two variables are then used, together with the picoeukaryotes abundance, to get the amount of Hg^{II} and $MeHg$ released by the dead picoeukaryotes cells (see Sections S1.2 and S1.3 of the Supplement).

Thus, the advection-diffusion-reaction model for the Hg species in seawater is defined by the following coupled partial differential equations:

$$\frac{\partial Hg^0}{\partial t} = \frac{\partial}{\partial x}\left[D_x \frac{\partial Hg^0}{\partial x}\right] - \frac{\partial}{\partial x}(v_x Hg^0) + \frac{\partial}{\partial y}\left[D_y \frac{\partial Hg^0}{\partial y}\right] - \frac{\partial}{\partial y}(v_y Hg^0) + \frac{\partial}{\partial z}\left[D_z \frac{\partial Hg^0}{\partial z}\right] - \frac{\partial}{\partial z}(v_z Hg^0) + k_{Ph-de} \cdot MeHg - (k_1 + k_3) \cdot Hg^0 + (k_2 + k_4) \cdot Hg^{II} + S_L^0 \quad (1)$$

$$\frac{\partial Hg^{II}}{\partial t} = + \frac{\partial}{\partial x}\left[D_x \frac{\partial Hg^{II}}{\partial x}\right] - \frac{\partial}{\partial x}(v_x Hg^{II}) + \frac{\partial}{\partial y}\left[D_y \frac{\partial Hg^{II}}{\partial y}\right] - \frac{\partial}{\partial y}(v_y Hg^{II}) + \frac{\partial}{\partial z}\left[D_z \frac{\partial Hg^{II}}{\partial z}\right] - \frac{\partial}{\partial z}(v_z Hg^{II}) + (k_1 + k_3) \cdot Hg^0 - (k_2 + k_4) \cdot Hg^{II} - k_{me} \cdot Hg^{II} + k_{deme} \cdot MeHg + S_L^{II} + S_{DOM}^{II} - S_{SPM}^{II} \quad (2)$$

$$\frac{\partial MeHg}{\partial t} = +\frac{\partial}{\partial x}\left[D_x \frac{\partial MeHg}{\partial x}\right] - \frac{\partial}{\partial x}(v_x MeHg) + \frac{\partial}{\partial y}\left[D_y \frac{\partial MeHg}{\partial y}\right] - \frac{\partial}{\partial y}(v_y MeHg) + \frac{\partial}{\partial z}\left[D_z \frac{\partial MeHg}{\partial z}\right]$$
$$-\frac{\partial}{\partial z}(v_z MeHg) - K_{Ph-de} \cdot MeHg + k_{me} \cdot Hg^{II} - k_{deme} \cdot MeHg + S_L^{MM} + S_{DOM}^{MM} - S_{SPM}^{MM} \quad (3)$$

Here, k_1, k_2, k_3 and k_4 are the rate constants for the photo-oxidation of Hg^0, the photo-reduction of Hg^{II}, the biological oxidation of Hg^0 and the biological reduction of Hg^{II}, respectively $[h^{-1}]$; k_{Ph-de} is the rate constant for the photo-demethylation of $MeHg$ $[h^{-1}]$; k_{deme} and k_{me} are the rate constants for the biotic demethylation of $MeHg$ and the methylation of Hg^{II}, respectively $[h^{-1}]$; S_L^0, S_L^{II} and S_L^{MM} are the direct loads for Hg^0, Hg^{II} and $MeHg$, respectively $[\mu g \cdot m^{-3} \cdot h^{-1}]$; S_{DOM}^{II} and S_{DOM}^{MM} are the loads of Hg_D^{II} and $MeHg_D$, respectively, released by POM $[\mu g \cdot m^{-3} \cdot h^{-1}]$; S_{SPM}^{II} and S_{SPM}^{MM} are the sinking fluxes of the SPM-bound mercury for Hg^{II} and $MeHg$, respectively $[\mu g \cdot m^{-3} \cdot h^{-1}]$.

The photo-chemical rate constants (k_1 and k_2) are directly proportional to the short-wave radiation flux (RAD) at the water-atmosphere interface (Zhang et al., 2014; Soerensen et al., 2010; Qureshi et al., 2010; Batrakova et al., 2014), while the biological rate constants (k_3 and k_4) are calculated by the organic carbon remineralization rate ($OCRR$) of the microbial reactions (Zhang et al., 2014) (see Section S1 of the Supplement). The k_{me} and k_{deme} are fixed according to Lehnherr et al. (2011), while the k_{Ph-de} is set according to to Melaku Canu et al. (2015).

The two sinking fluxes (S_{SPM}^{II} and S_{SPM}^{MM}) are obtained according to previous works (Zhang et al., 2014; Rosati et al., 2018), as follows:

$$S_{SPM}^{II} = S_{POM}^{II} + S_{silt}^{II} = -\frac{\partial}{\partial z}\left[NPP \cdot (pe-ratio) \cdot \left(\frac{z}{z_0}\right)^{-0.9} \cdot \left(\frac{k_D}{f_{oc}}\right) \cdot Hg^{II}\right] - v_{silt} \cdot k_{Dsilt}^{II} \cdot SPIM \cdot Hg^{II} \quad (4)$$

$$S_{SPM}^{MM} = S_{POM}^{MM} + S_{silt}^{MM} = -\frac{\partial}{\partial z}\left[NPP \cdot (pe-ratio) \cdot \left(\frac{z}{z_0}\right)^{-0.9} \cdot \left(\frac{k_D}{f_{oc}}\right) \cdot MeHg(z)\right] - v_{silt} \cdot k_{Dsilt}^{MM} \cdot SPIM \cdot MeHg \quad (5)$$

where S_{POM}^{II} and S_{POM}^{MM} are the sinking fluxes of the POM-bound Hg for the Hg^{II} and $MeHg$ $[\mu g \cdot m^{-3} \cdot h^{-1}]$, respectively; S_{silt}^{II} and S_{silt}^{MM} are the sinking fluxes of the silt-bound Hg for the Hg^{II} and $MeHg$ $[\mu g \cdot m^{-3} \cdot h^{-1}]$, respectively; NPP is the net primary production $[g\ C \cdot m^{-2} \cdot h^{-1}]$; $pe-ratio$ is the ratio of particulate organic carbon (POC) export to NPP out of the euphotic zone $[dimensionless]$; z_0 is the depth of euphotic zone $[m]$; k_D is the seawater-SPM partition coefficient for Hg_D $[l \cdot Kg^{-1}]$; f_{oc} is the fraction of suspended particulate matter as organic carbon $[dimensionless]$; v_{silt} is the silt settling velocity $[m \cdot h^{-1}]$; k_{Dsilt}^{II} is the partition coefficient of Hg^{II} to silt $[l \cdot Kg^{-1}]$; k_{Dsilt}^{MM} is the partition coefficient of $MeHg$ to silt $[l \cdot Kg^{-1}]$; $SPIM$ is the suspended particulate inorganic matter $[Kg \cdot l^{-1}]$. The NPP is obtained by Baines et al.(1994) using the conversion equation for the $chl-a$ concentration (Baines et al., 1994). This is calculated by the picoeukaryotes abundance using the conversion curve of Brunet et al. (2007). The $pe-ratio$ is calculated by the surface atmospheric temperature, coming from remote sensing, and the $chl-a$ concentration obtained by the NP model (Zhang et al., 2014). The k_D has been

measured within the Augusta Harbour during the last oceanographic survey, while the spatial distributions of f_{oc} and $SPIM$ at the steady state have been reproduced by using the experimental findings for the suspended particulate matter (see Section 2.1 of the Supplement). The v_{silt}, k^{II}_{Dsilt} and k^{MM}_{Dsilt} for marine environments with silty $SPIM$ are fixed according to Rosati et al. (2018).

The loads of Hg^{II}_D and $MeHg_D$ released by POM are calculated by using the following equations:

$$S^{II}_{DOM} = \lambda \cdot m \cdot b \cdot PHg^{II}, \tag{6}$$

$$S^{MM}_{DOM} = \lambda \cdot m \cdot b \cdot PMeHg, \tag{7}$$

where PHg^{II} and $PMeHg$ are, respectively, the Hg^{II} content and $MeHg$ content in each cell of picoeukaryotes $[\mu g/cell]$; b is the picoeukaryotes abundance $[cell \cdot m^{-3}]$; m is the mortality of picoeukaryotes $[h^{-1}]$; λ is the Hg recycling coefficient for picoeukaryotes $[dimensionless]$. The spatio-temporal dynamics of PHg^{II} and $PMeHg$ are obtained by solving the ODEs of Phytoplankton MERLIN-Expo Model for Hg^{II} and $MeHg$, respectively (Radomyski and Ciffroy, 2015)(see Section 5 of the Supplement). The spatio-temporal distribution of b is reproduced by using the NP model (Valenti et al., 2017)(see Section 4 of the Supplement). The parameter m is set according to Valenti et al.(2017), while λ is fixed equal to the nutrient recycling coefficient for picoeukaryotes (Valenti et al., 2015, 2017).

The concentrations $[Hg_D]$ and $[Hg_T]$ are calculated as a function of position (x, y, z) and time t, as follows:

$$Hg_D = Hg^0 + Hg^{II} + MeHg \tag{8}$$

$$Hg_T = Hg_D + k_D \cdot SPM \cdot (Hg^{II} + MeHg). \tag{9}$$

Here, k_D is the seawater-SPM partition coefficient for Hg_D (only Hg^{II} and $MeHg$) $[l \cdot Kg^{-1}]$, and SPM is the Suspended Particulate Matter concentration $[Kg \cdot l^{-1}]$. The partition coefficient k_D is set to the value experimentally observed in seawater samples collected within the Augusta Bay recently. The partition coefficient k_D has been calibrated to fit experimental data for $[Hg_T]$ and $[Hg_D]$ in the seawater compartment, thus obtaining a value that is in very good agreement with those reported by Melaku Canu et al. (2015), Covelli et al. (2008) and Hines et al. (2012), for the Marano-Grado Lagoon (Melaku Canu et al., 2015; Covelli et al., 2008; Hines et al., 2012). The spatial distribution of SPM was set according to the experimental information collected during the oceanographic cruise of October 2017, and assumed constant for the whole simulation time.

The advection-diffusion-reaction model is completed by a set of ordinary differential equations (ODEs), which describe the mercury fluxes at the boundaries of Augusta Harbour. Specifically, we take into account for the three mercury species: i) the evasion and the deposition of Hg^0 at the water-atmosphere interface (Bagnato et al., 2013; Zagar et al., 2007); ii) the lack of Hg^0 diffusion at the water-sediment interface (Ogrinc et al., 2007); iii) the wet and dry deposition of Hg^{II} at the water-atmosphere interface (Rajar et al., 2007; Zagar et al., 2007); iv) the wet and dry lack of deposition of $MeHg$ at the water-atmosphere interface (Mason et al., 2012); v) the diffusion of Hg^{II} and $MeHg$ at the water-sediment interface; vi) the exchange of Hg^{II} and $MeHg$ at the seawater-sediment interface due to particulate matter deposition and re-suspension

mechanisms; vi) the constant fixed value of $[Hg_D]$ out of Augusta Bay (Ionian Sea) (Horvat et al., 2003); vii) the exchange of the elemental mercury, Hg^{II} and $MeHg$ between the Augusta basin and the Ionian Sea through the two inlets (Salvagio Manta et al., 2016). Since the Augusta Bay is considered as a semi-closed basin, the lateral fluxes at the boundaries of the domain are set to zero except for the two inlets (Salvagio Manta et al., 2016). Here, the lateral fluxes depend on the direction of horizontal velocities, and therefore change as a function of depth and time (see Sections S1.1.2 of the Supplement). The boundary conditions for the three mercury species are defined by the following equations:

$$\left[D_z \frac{\partial Hg^0}{\partial z} - v_z Hg^0\right]\Big|_{z=0} = \frac{Hg_{gas-atm} \cdot Pr}{\Delta t} + MTC_{water-atm} \cdot \left(Hg_{gas-atm} - H \cdot Hg^0|_{z=0}\right) \tag{10}$$

$$\left[D_x \frac{\partial Hg^0}{\partial x} - v_x Hg^0\right] = \left[D_y \frac{\partial Hg^0}{\partial y} - v_y Hg^0\right] = \left[D_z \frac{\partial Hg^0}{\partial z} - v_z Hg^0\right]\Big|_{z=z_b} = 0 \tag{11}$$

$$\left[D_z \frac{\partial Hg^{II}}{\partial z} - v_z Hg^{II}\right]\Big|_{z=0} = \frac{Hg^{II}_{atm} \cdot Pr}{\Delta t} + Drydep_{Hg^{II}}, \qquad \left[D_z \frac{\partial MeHg}{\partial z} - v_z MeHg\right]\Big|_{z=0} = 0.005 \cdot \left[D_z \frac{\partial Hg^{II}}{\partial z} - v_z Hg^{II}\right]\Big|_{z=0} \tag{12}$$

$$\left[D_z \frac{\partial Hg^{II}}{\partial z} - v_z Hg^{II}\right]\Big|_{z=z_b} = MTC^{II}_{sed-water} \cdot \left(Hg^{II}_{pore-water} - Hg^{II}|_{z=z_b}\right) \tag{13}$$

$$\left[D_z \frac{\partial MeHg}{\partial z} - v_z MeHg\right]\Big|_{z=z_b} = MTC^{MM}_{sed-water} \cdot \left(MeHg_{pore-water} - MeHg|_{z=z_b}\right) \tag{14}$$

$$\left[D_x \frac{\partial Hg^{II}}{\partial x} - v_x Hg^{II}\right] = \left[D_y \frac{\partial Hg^{II}}{\partial y} - v_y Hg^{II}\right] = 0 \tag{15}$$

$$\left[D_x \frac{\partial MeHg}{\partial x} - v_x MeHg\right] = \left[D_y \frac{\partial MeHg}{\partial y} - v_y MeHg\right] = 0 \tag{16}$$

$$Hg^0(x_{inlet}, y_{inlet}, z) = Hg^0_{ext}, \quad Hg^{II}(x_{inlet}, y_{inlet}, z) = Hg^{II}_{ext}, \quad MeHg(x_{inlet}, y_{inlet}, z) = MeHg_{ext} \tag{17}$$

where $Hg_{gas-atm}$ is the gaseous elemental mercury (GEM) concentration in atmosphere $[ng \cdot m^{-3}]$; Pr is the amount of precipitation $[mm]$; Δt is the exposition time to precipitations $[h]$; $Drydep_{Hg^{II}}$ is the atmospheric dry deposition of Hg^{II} $[ng \cdot m^{-2} \cdot h^{-1}]$; $MTC_{water-atm}$ is the gas phase overall mass transfer coefficient $[m \cdot h^{-1}]$; H is the Henry's law constant $[dimensionless]$; $Hg^0|_{z=0}$ is the $[Hg^0]$ at the sea surface $[\mu g \cdot m^{-3}]$; Hg^{II}_{atm} is the $[Hg^{II}]$ in atmosphere $[ng \cdot m^{-3}]$;

$MTC^{II}_{sed-water}$ is the mass transfer coefficient for Hg^{II} at the water-sediment interface $[m \cdot h^{-1}]$; $Hg^{II}_{pore-water}$ is the $[Hg^{II}]$ in the pore water of the surface layer (upper 10 cm) of the sediments $[\mu g \cdot m^{-3}]$; $Hg^{II}|_{z=z_b}$ is the dissolved $[Hg^{II}]$ at the deepest layer of the water column ($z = z_b$) $[\mu g \cdot m^{-3}]$; ϕ^{II}_{res} is the Hg^{II} flux at the seawater-sediment interface produced by particulate matter deposition and re-suspension processes; $MTC^{MM}_{sed-water}$ is the mass transfer coefficient for $MeHg$ at the water-sediment interface $[m \cdot h^{-1}]$; $MeHg_{pore-water}$ is the $[MeHg]$ in the pore water in the surface layer (upper 10 cm) of the sediments $[\mu g \cdot m^{-3}]$; $MeHg|_{z=z_b}$ is the dissolved $[MeHg]$ in the deepest layer of the water column ($z = z_b$) $[\mu g \cdot m^{-3}]$; ϕ^{MM}_{res} is the $MeHg$ flux at the seawater-sediment interface caused by the particulate matter deposition and re-suspension processes; Hg^0_{ext}, Hg^{II}_{ext} and $MeHg_{ext}$ are the average $[Hg^0]$, $[Hg^{II}]$ and $[MeHg]$, respectively, reported from the Ionian Sea $[\mu g \cdot m^{-3}]$. The dynamics of the GEM and Hg^{II} concentrations in the atmosphere ($Hg_{gas-atm}$ and Hg^{II}_{atm}) is reproduced using the experimental data collected in the Augusta Bay between August 2011 and June 2012 (Bagnato et al., 2013), whereas rainfall is derived from the remote sensing (see http://eosweb.larc.nasa.gov/sse/RETScreen/). The spatio-temporal dynamics of pore water mercury concentrations ($Hg^{II}_{pore-water}$ and $MeHg_{pore-water}$) at the sediment surface layer are obtained with the diffusion-reaction model for the sediment compartment, while the mass transfer coefficients ($MTC^{II}_{sed-water}$ and $MTC^{MM}_{sed-water}$) at the water-sediment interface are calculated by sediment porosity, molecular diffusion coefficient, boundary layer thickness above and below sediment in order to fit the experimental findings and according to previous works (Covelli et al., 1999; Sørensen et al., 2001; Schulz and Zabel, 2006; Ogrinc et al., 2007; Bryant et al., 2010; Ciffroy, 2015) (see Sections S1.2.2 and S1.3.2 of the Supplement). The dynamics of the mercury benthic fluxes (ϕ^{II}_{res} and ϕ^{MM}_{res}) caused by particulate matter deposition and re-suspension mechanisms (Neumeier et al., 2008; Ferrarin et al., 2008) is obtained by considering both the spatial distribution of sediment porosity and the spatio-temporal behaviour of removed/settled sediment thickness at the seawater-sediment interface. The sediment exchanges at the water-bottom interfase are obtained from the application of the hydrodynamic model, which accounts for sediment transport processes induced by currents (see Section S3 of the Supplement).

Eqs. (1)-(17) represent the 3D advection-diffusion-reaction model used to describe and reproduce the spatio-temporal dynamics of the three mercury species dissolved in seawater.

3.1.1 Mass balance of Hg in Augusta Bay

The annual mass balance for the total Hg in the seawater compartment can be estimated, using the boundary conditions given in Eqs. (10)-(16), according to the following equation (Sprovieri et al., 2011; Salvagio Manta et al., 2016):

$$A + AD + B = O + D + V \tag{18}$$

where A is the input of the Hg_D from anthropogenic activities; AD is the atmospheric mercury deposition; B is the mercury flux from sediments to seawater due to diffusion processes; O is the net mercury outflow from the Augusta Harbour to the Ionian Sea; D is the amount of mercury recycled in the Augusta Bay (or the net mercury deposition for settling and burial); V is the GEM evasion from the Augusta Bay to the atmosphere.

By integrating Eqs. (10)-(16), we obtain the terms of the annual mass balance referred to the mercury fluxes exchanged at

the interfaces (AD,B,V), and the net mercury outflow from the Augusta Bay to the Ionian Sea (O), while the input of the anthropogenic activities (A) is set to zero according to literature sources (Sprovieri et al., 2011; Salvagio Manta et al., 2016). Finally, we estimate the total amount of mercury recycled (D) from the other terms, and compare it with the amount of mercury recycled by scavenging (S). A simple scheme of the fluxes exchanged in the mercury biogeochemical cycle of the Augusta Bay is shown in Fig. 3.

3.2 The diffusion-reaction model for Hg species in pore water

The dynamics of $[Hg_D^{sed}]$ and $[Hg_T^{sed}]$ in the Augusta sediments (average thickness of $1.9\ m$) has been studied using a diffusion-reaction model (see the next Eqs. (20), (21), (22)). In particular, we investigated the behaviour of the two mercury species dissolved in pore water, i.e. Hg^{II} ($Hg^{II}_{pore-water}$) and $MeHg$ ($MeHg_{pore-water}$), which interact with each other directly through the reaction terms of the two PDEs. Moreover, in the model we took into account the variations of mercury concentrations in pore water due to the slow desorption of the fraction bound to particulate sediments. In order to better reproduce the experimental findings, we describe mercury desorption using an exponential equation, which accounts, in the absence of external sources, the loss of mercury through the desorption mechanism. Since the mercury desorption has to depend on its instantaneous concentration, the mechanism is regulated by a first-order kinetic.

The model provides solutions for the spatio-temporal behaviour of mercury concentration, both for the two species dissolved in pore water, i.e. inorganic mercury ($Hg^{II}_{pore-water}(x',y',z',t)$) and methyl-mercury ($MeHg_{pore-water}(x',y',z',t)$), and the total mercury concentration in the sediments ($Hg_T^{sed}(x',y',z',t)$). Here, the coordinates (x', y', z') indicate the position within the irregular three-dimensional domain of the sediment compartment. Since the surface sediment slope is very low for the whole basin, the domain is approximated as the sum of several sub-domains shaped as regular parallelepipeds, which reproduce the sediment columns in each position (x',y',z') of the Augusta Bay. Specifically, z' represents the depth of the barycenter of each subdomain, localized between the top ($z'=0$) and the bottom ($z'=1.9\ m$) of the surface sediment layer, while the other coordinates ($x'=x$ and $y'=y$) indicate the distance in meters measured from the same reference point used for the seawater compartment.

In the sediment compartment, the adopted numerical method uses a finite volume scheme in explicit form, where space and time discretization are considered separately. In particular, the PDEs of the model are solved by performing a centered-in-space differencing for the diffusion terms. The sea bottom is discretized in the horizontal plane using the same regular mesh adopted for simulating the dissolved mercury distribution in the seawater compartment (see Fig.1) with 454.6 m regularly spaced elements. In this case, the vertical discretization is constituted by equally spaced layers of 0.2 m depth, with the exception of the interface layer between water and sediment, whose depth is set at 0.1 m. This choice has been made in order to best adapt the 3D grid of the model to the scheme used to interpolate available experimental data. The same fixed time step of 300 sec is adopted to guarantee stability conditions (Roache, 1998; Tveito and Winther, 1998; Thi et al., 2005).

The initial conditions for $[Hg_T^{sed}]$ and $[Hg_D^{sed}]$ are fixed on the basis of experimental findings. As a first step we reproduced the spatial distribution of Hg_T^{sed} at time $t=0$ by interpolating the experimental data collected by ICRAM in 2005 (ICRAM, 2008) (see Section S1.2.4 of the Supplement). We then calculated both $[Hg^{II}]$ and $[MeHg]$ in pore water using the following

equations:

$$Hg^{II}_{pore-water}(0) = (1 - f_{MeHg}) \cdot \frac{Hg^{sed}_T(0)}{K^{II}_d}, \;\; MeHg_{pore-water}(0) = f_{MeHg} \cdot \frac{Hg^{sed}_T(0)}{K^{MM}_d} \tag{19}$$

where $Hg^{sed}_T(0)$ represents the spatial distribution of $[Hg_T]$ in the sediments at initial time$[mg \cdot Kg^{-1}]$, f_{MeHg} is the fraction of $MeHg$ in the sediments $[dimensionless]$, K^{II}_d is the sediment-pore water distribution coefficient for Hg^{II} $[l \cdot Kg^{-1}]$, and K^{MM}_d is the sediment-pore water distribution coefficient for $MeHg$ $[l \cdot Kg^{-1}]$.

In pore water, the dynamics of $[Hg^{II}]$ and $[MeHg]$ are modeled by considering three chemical-physical processes (Schulz and Zabel, 2006; Melaku Canu et al., 2015; Oliveri et al., 2016): i) methylation and de-methylation (reaction terms); ii) passive movement due to the Brownian motion of each chemical species (diffusion terms); iii) desorption of mercury bound to sediment particles (desorption term).

The methylation and de-methylation processes involved in the dynamics of the Hg^{II} and $MeHg$ are considered in the model through reaction terms describing first-order kinetics. The rate constants of these reactions are fixed according to previous works (Hines et al., 2012).

The diffusion terms reproduce the effects of the Brownian motions on the spatial distribution of the $[Hg^{sed}_D]$ in pore water. In particular, the magnitude of the Brownian motions is described by the molecular diffusion coefficients for Hg^{II} ($D^{in}_{sed}(x', y', z')$) and $MeHg$ ($D^{or}_{sed}(x', y', z')$), which change in each position of the domain as a function of porosity and tortuosity (see Sections S1.2.2 and S1.3.2 of the Supplement). The molecular diffusion coefficients are assumed isotropic in all directions, and are set as constant functions of time according to previous works (Schulz and Zabel, 2006; Melaku Canu et al., 2015).

The desorption term estimates the increase of $Hg^{II}_{pore-water}$ and $MeHg_{pore-water}$ due to the mercury release from the sediment particles to pore water. The desorption process is regulated by the temporal gradient of $[Hg^{sed}_T]$ ($\partial dHg^{sed}_T / \partial dt$), which changes as a function of position and time (see Section S1.2.2 and S1.3.2 of the Supplement).

Thus, the module for the sediment compartment is defined by the following coupled partial differential equations:

$$\begin{aligned}\frac{dHg^{II}_{pore-water}}{dt} = &+K_{demeth} \cdot MeHg_{pore-water} - K_{meth} \cdot Hg^{II}_{pore-water} + \frac{\partial}{\partial x}\left[D^{in}_{sed} \cdot \frac{\partial Hg^{II}_{pore-water}}{\partial x}\right] \\ &+\frac{\partial}{\partial y}\left[D^{in}_{sed} \cdot \frac{\partial Hg^{II}_{pore-water}}{\partial y}\right] + \frac{\partial}{\partial z}\left[D^{in}_{sed} \cdot \frac{\partial Hg^{II}_{pore-water}}{\partial z}\right] - \frac{(1 - f_{MeHg})}{K^{II}_d} \cdot \frac{dHg^{sed}_T}{dt}\end{aligned} \tag{20}$$

$$\begin{aligned}\frac{dMeHg_{pore-water}}{dt} = &-K_{demeth} \cdot MeHg_{pore-water} + K_{meth} \cdot Hg^{II}_{pore-water} + \frac{\partial}{\partial x}\left[D^{or}_{sed} \cdot \frac{\partial MeHg_{pore-water}}{\partial x}\right] \\ &+\frac{\partial}{\partial y}\left[D^{or}_{sed} \cdot \frac{\partial MeHg_{pore-water}}{\partial y}\right] + \frac{\partial}{\partial z}\left[D^{or}_{sed} \cdot \frac{\partial MeHg_{pore-water}}{\partial z}\right] - \frac{f_{MeHg}}{K^{MM}_d} \cdot \frac{dHg^{sed}_T}{dt}\end{aligned} \tag{21}$$

$$\frac{dHg^{sed}_T}{dt} = -\alpha \cdot Hg^{sed}_T \Rightarrow Hg^{sed}_T(t) = Hg^{sed}_T(0) \cdot exp(-\alpha \cdot t) \tag{22}$$

where K_{demeth} is the rate constant for the de-methylation of $MeHg$ $[h^{-1}]$; K_{meth} is the rate constant for the methylation of Hg^{II} $[h^{-1}]$; α is the desorption rate for the $[Hg_T^{sed}]$ bound to the sediment particles $[h^{-1}]$. The spatial distribution of the fraction of methyl-mercury in the sediments is that obtained by field observations, while the two sediment-pore water distribution coefficients are calibrated, according to previous work (Oliveri et al., 2016), in order to fit the experimental data. The desorption rate α is fixed to a low value to fit the slow mercury release from the sediment particles to pore water according to experimental observations.

As boundary conditions, we assume a null value of mercury flux at the bottom of the sediment column (1.9 m depth), mainly due to the measured very low porosity, while the vertical gradient of $[Hg_T^{sed}]$ and $[Hg_D^{sed}]$ are set to zero at the water-sediment interface, according to field observations. The mercury concentration in sediments is fixed to zero at the lateral boundaries (x'_b, y'_b) of the 3D domain. The boundary conditions for dissolved and total mercury concentrations in sediments are described by the following equations:

$$\left[D_{sed}^{in}\frac{\partial Hg^{II}_{pore-water}}{\partial z}\right]\Big|_{z'=0} = \left[D_{sed}^{in}\frac{\partial Hg^{II}_{pore-water}}{\partial z}\right]\Big|_{z'=1.9m} = 0 \tag{23}$$

$$\left[D_{sed}^{or}\frac{\partial MeHg_{pore-water}}{\partial z}\right]\Big|_{z'=0} = \left[D_{sed}^{or}\frac{\partial MeHg_{pore-water}}{\partial z}\right]\Big|_{z'=1.9m} = 0 \tag{24}$$

$$\left[\frac{\partial Hg_T^{sed}}{\partial z}\right]\Big|_{z'=0} = \left[\frac{\partial Hg_T^{sed}}{\partial z}\right]\Big|_{z'=1.9m} = 0 \tag{25}$$

$$Hg^{II}_{pore-water}|_{(x'_b,y'_b)} = 0, \;\; MeHg_{pore-water}|_{(x'_b,y'_b)} = 0, \;\; Hg_T^{sed}|_{(x'_b,y'_b)} = 0 \tag{26}$$

Eqs. (20)-(26) represent the three-dimensional diffusion-reaction model used to describe and reproduce the spatio-temporal dynamics of $[Hg^{II}]$ and $[MeHg]$ in pore water, and of $[Hg_T^{sed}]$ in sediments. It is to be noticed that equations (13)-(14), (20)-(21) and (19), which reproduce the spatio-temporal distributions of the mercury concentrations in both compartments (seawater and sediment), strongly depend on the initial condition for the total mercury concentration observed in the sediments.

3.3 Model and simulation setup

In our model, as initial conditions we assumed an uniformly distributed concentration of Hg_D and Hg_T, set to 1.9 ng/l corresponding to the experimental detection limit. Specifically, the initial concentration of each Hg species was fixed according to the percentage observed in seawater samples of Ionian Sea (Horvat et al., 2003), in such a way to respect the detection limit for total $[Hg_D]$. The numerical results were not affected by the chosen initial conditions, indeed the same spatial distribution of $[Hg]$ at nearly-steady state was obtained when higher initial Hg concentrations than detection limit were fixed.

The model results were obtained by running a single long simulation. To reproduce the spatial mercury distributions at near-steady-state, we integrated the model equations over a time interval ($t_{max} > 7$ $years$) long enough to reach an annual decrease

of mercury concentration of less than 2 percent. This percentage value progressively declines for longer time intervals down to an annual decrease of 0.12 percent for $t_{max} = 250\ years$.

All environmental parameters and variables used in the model are reported in Tables S1-S3 of the Supplement. Most of the environmental parameters have been set to values experimentally observed in sites contaminated by mercury (Horvat et al., 2003; Schulz and Zabel, 2006; Monperrus et al., 2007b, a; Strode et al., 2010; Lehnherr et al., 2011; Melaku Canu et al., 2015; Sprovieri et al., 2011; Salvagio Manta et al., 2016; Sunderland et al., 2006; Zhang et al., 2014; Batrakova et al., 2014), while other parameters, among which are those most sensitive for the model, have been calibrated so as to correctly reproduce the experimental data collected during the six oceanographic surveys (Sprovieri et al., 2011; ICRAM, 2008; Bagnato et al., 2013; Salvagio Manta et al., 2016; Oliveri et al., 2016). Furthermore, the photochemical and biological rate constants of the redox reactions have been calculated by using both the outputs of NP model and the data coming from remote sensing (see Section S1 of the Supplement).

Experimental measurements were carried out during the period between 2005 and 2017 in several stations inside and outside Augusta Harbour (see Fig. 1). Mercury concentration as well as mercury fluxes were measured both in sediments and seawater (see Tables S6-S10, S12 of Supplement). We refer to Bagnato et al. (2013), Salvagio Manta et al. (2016) and Oliveri et al. (2016) for a detailed description of the measured parameters, of the related dynamics and of the analytical methods used (ICRAM, 2008; Bagnato et al., 2013; Salvagio Manta et al., 2016; Oliveri et al., 2016). These experimental data were used to identify the most sensitive parameters for the model and to compare them with the theoretical results in order to estimate the model accuracy in reproducing Hg dynamics.

Concerning the calibration procedure, we first focused on the best values of the parameters for the sediment compartment (i.e. sediment-pore water distribution coefficients, desorption rate and boundary layer thickness above the sediment) in such a way as to optimize the match between theoretical results and experimental observations. Specifically, in Eqs. (20)-(21) the sediment-pore water distribution coefficients were calibrated to guarantee the best theoretical $[Hg]$ in pore water in agreement with the value ranges experimentally observed in a previous work (Oliveri et al., 2016), whereas the fraction of methyl-mercury in sediments for the whole spatial domain was set to that obtained by field observations during the oceanographic survey of October 2017 (see Table S1). In the Eq. (22), the desorption rate α was calibrated to obtain the best fit between the theoretical results and experimental observations for $[Hg]$ in pore water. Before to calculate the mass transfer coefficients at the water-sediment interface, the *boundary layer thickness above the sediment* was optimized to better reproduce the spatial distribution of mercury benthic flux observed experimentally. Unlike the *boundary layer thickness above the sediment*, the other parameters used to obtain $MTC^{II}_{sed-water}$ and $MTC^{MM}_{sed-water}$ were not calibrated. In fact, the *boundary layer thickness below the sediment* was estimated by using the relationship between this parameter and the average velocity of marine currents defined by Sørensen (2001), while the spatial distribution of the sediment porosity within Augusta Harbour was reproduced, according to previous works (Covelli et al., 1999; Ogrinc et al., 2007), by exploiting the measurements on the sediment samples performed by $ICRAM$ in 2005. Also, the molecular diffusion coefficient was that reported by Schulz and Zabel (2006).

As a second step, we calibrated model parameters for the seawater compartment (i.e. vertical and horizontal diffusivities) in order to better reproduce the spatio-temporal dynamics of the dissolved mercury concentration. The vertical turbulent

diffusivity was calibrated according to experimental data, which indicate weakly mixed water column conditions within the Augusta Bay during the whole year. Specifically, the vertical turbulent diffusivity was set in such a way as to obtain the best match with experimentally observed dissolved mercury concentration at the surface layer of the water column. The calibrated vertical diffusivity was in good agreement with previously reported values (Denman and Gargett, 1983) under the condition of weakly mixed waters. The horizontal turbulent diffusivity was assumed isotropic in the horizontal water plane (D_x=D_y), and calibrated by considering the values obtained in Massel (1999). In particular, the horizontal turbulent diffusivities were optimized to get the best possible match with the observed mercury evasion flux. The calibrated horizontal diffusivities were in accordance with the values estimated by other authors (Massel, 1999) for basins similar in size to those of the Augusta Bay. As a third step, we calibrated the seawater-SPM partition coefficient in order to obtain theoretical distributions of the total mercury concentration in agreement with experimental ones. The partition coefficient obtained was in very good agreement with that previously reported (Hines et al., 2012; Melaku Canu et al., 2015).

In our analysis, no comparison between the calibrated desorption rate and experimental data was possible. However, the other calibrated environmental parameters were in good agreement with those obtained experimentally both in the Augusta Bay and in other sites contaminated by mercury (Melaku Canu et al., 2015; Oliveri et al., 2016; Liu et al., 2012; Cossa and Coquery, 2005; Ciffroy, 2015).

Finally, the calibrated model has been run by considering the seasonal oscillations of the environmental data (water currents, wind etc.) provided by hydrodynamic modelling (see Section S3 of the Supplement). The model results were validated using the other experimental findings acquired in the Augusta Bay: $[MeHg_D]$, $[Hg_D]$ and $[Hg_T]$ measured in seawater; all annual Hg fluxes estimated for the mass balance.

4 Results

In the following the simulation results obtained for the seawater and sediment compartments are described and compared with experimental data.

4.1 Mercury in seawater

The spatial distribution of the three mercury species dissolved in seawater is obtained by solving Eqs. (1)-(17), together with the equation system (20)-(26) for the sediment compartment. The theoretical concentrations of the three mercury species dissolved in seawater are reported in the Table S5 of Supplement. Here, we observe the average concentration ratios among the three mercury species dissolved in seawater ($[Hg^{II}]/[[Hg_D] = 0.790$, $[MMHg]/[[Hg_D] = 0.022$ and $[Hg^0]/[[Hg_D] = 0.188$) are in good agreement with both experimental and theoretical values reported in recent publications (Zhang et al., 2014; Melaku Canu et al., 2015). Moreover, the theoretical results for the vertical profiles of the mercury concentration show a similar shape for the whole simulated period (2005-2254), while the magnitude of the concentrations in the whole water column decreases slowly as a function of time (see Fig. S1 of the Supplement).

The model results indicate that the dissolved mercury concentration is usually maximal at the seawater-sediment interface (see

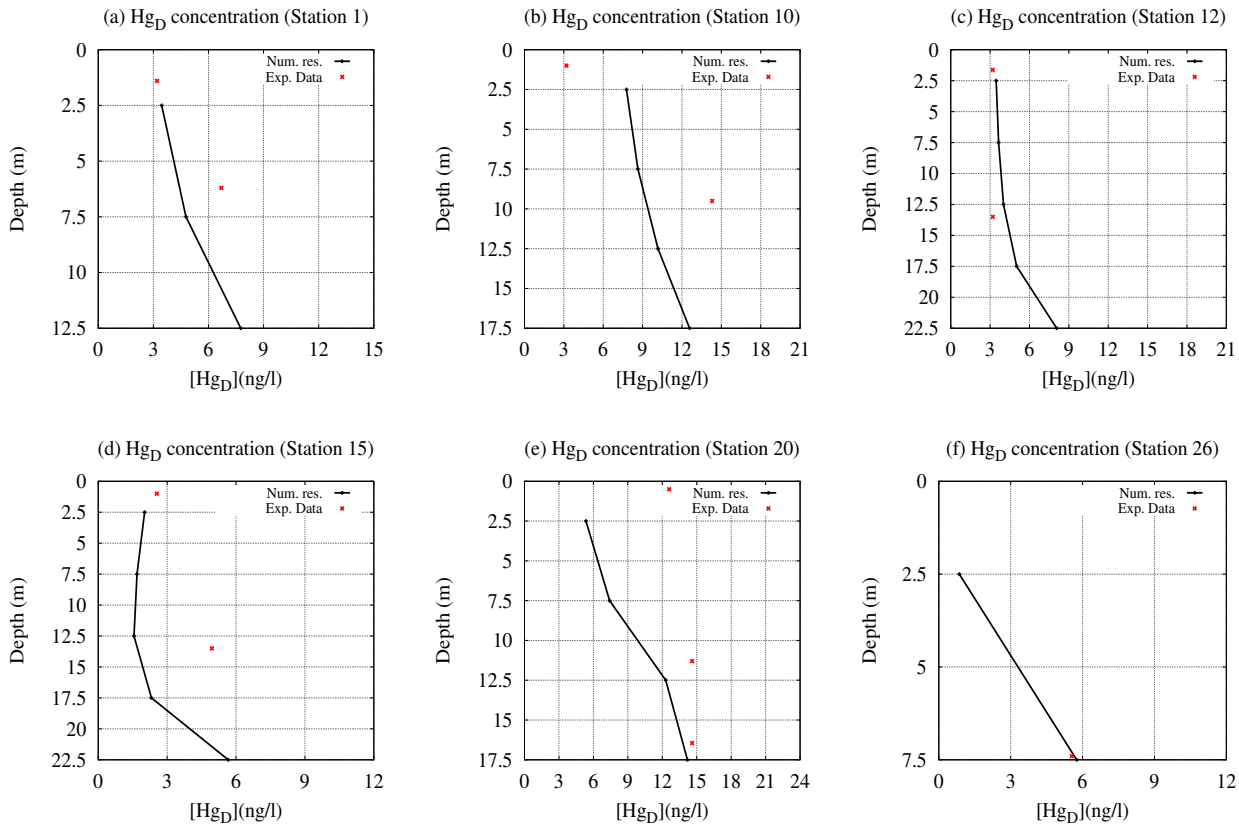

Figure 4. Comparison between the experimental data (red points) and the theoretical results (black lines) for the dissolved mercury concentration in six stations of the Augusta Bay. The vertical profiles of $[Hg_D]$ are obtained by model for the sites closest to stations 1, 10, 12 and 20 (sampling May 2011), station 15 (sampling June 2012) and station 26 (sampling February 2012).

Fig.4), where the main sources of Hg^{II} and $MeHg$ are localized. These numerical results are in reasonable agreement with the field observations (see Tables S6-S7 of the Supplement). Moreover, taking into account the redox conditions of sediments in the area, we speculate that maxima in $MeHg$ production be confined to the seawater/sediments interface.

Conversely, in some (x,y) sites of the calculation grid (see Fig.1) we observe that the peaks of mercury concentration occur at mid-depth of the water column possibly due to the distribution of marine currents velocity field within Augusta basin, which determines sometimes the presence of a $[Hg]$ maximum in the intermediate layers of seawater. In general, in our model the dynamics of mercury concentration in seawater is strictly connected with the behaviour of the benthic mercury fluxes, which decrease slowly as a function of time due to the slow molecular diffusion process of mercury within the pore waters of the sediments.

A quantitative analysis, based on the reduced χ^2 test, indicates a good agreement between the model results and experimental findings for $[MeHg]$ in stations $A3$ ($\tilde{\chi}^2 = 0.0005$) and $A7$ ($\tilde{\chi}^2 = 0.0005$), while differences can be observed in the stations $A9$

($\tilde{\chi}^2 = 0.0955$) and $A11$ ($\tilde{\chi}^2 = 0.1065$), where the theoretical concentrations appear overestimated at the bottom layer (see Table S6 of the Supplement). This result is probably due to the overestimation of the $MeHg$ benthic fluxes in these two stations. In our analysis, the spatio-temporal behaviour of $[Hg_D]$ is obtained as sum of the three dissolved mercury species. On the other hand, the dynamics of the spatial distribution of the $[Hg_T]$ is estimated according to Eq. (9), assuming a linear correlation between the modeled $[Hg_D]$ and the experimental SPM concentrations. The spatial distributions of $[Hg_D]$ and $[Hg_T]$ are reported for May 2011 in Fig.S2-S5 of the Supplement.

In general, The numerical results for the $[Hg_D]$ are in good agreement with the experimental findings for the four investigated periods (see Table S7 of the Supplement). Specifically, the difference between the model result and field observation for the $[Hg_D]$ is less than the experimental error ($\sigma = 3.2\ ng/l$) in 59% of sampling points, while it exceeds 2σ in only 17% of sampling sites. As a conclusion, the comparison between experimental data and theoretical results for the $[Hg_D]$ shows mostly small discrepancies except in some of the most contaminated areas, where concentration hot spots are hard to capture due to the resolution grid used in the present work.

The model results for $[Hg_T]$ show some discrepancies with experimental data in most of the sites investigated during the first sampling period (May 2011), while in general they evidence a acceptable agreement for the other sampling periods (see Table S8 of the Supplement). As a whole, the discrepancy for the $[Hg_T]$ is less than σ in 44% of cases, while it exceeds 2σ in 32% of sampling sites. The differences (larger than $\sigma = 3.2\ ng/l$) can be mainly explained by the significant distance between the sampling sites and the model calculation grid nodes (see Fig.1). Additionally, we cannot neglect the role played by the theoretical spatial distribution of the SPM concentration (see Eq. (9)), which could significantly affect the spatio-temporal dynamics of the total mercury concentration in seawater. In particular, the spatial distribution of SPM concentrations, used in the model, probably is not appropriate for the first sampling period investigated (May 2011), while it produces a good agreement for the other three sampling periods.

The theoretical distributions of the benthic mercury fluxes simulated by the model for the two investigated periods (September 2011 and June 2012) are shown in Fig. 5. Here very high benthic Hg^{II} and $MeHg$ fluxes are documented in the south-west sector of Augusta Harbour, where the chlor-alkali plant discharged high amounts of contaminants until the late 1970s. The model reliably reproduces the high benthic mercury fluxes also in the part of the south-east sector close to the inlets of the Augusta Bay, where intensive ship traffic and the relatively high velocity field of the marine currents cause sediment re-suspension and intensive transport of SPM. The benthic mercury fluxes are very low in the coastal zones at the north of the basin, while intermediate values have been calculated in the central part of the bay. As a whole, the estimated benthic mercury fluxes are in good agreement with the experimental data collected during the two sampling periods (see Table S9 of the Supplement). It should be noted that the model results suggest that the benthic Hg_D fluxes are mainly generated by the diffusion process at the seawater-sediment interface and that the amount of Hg_D release from the re-suspended particulate matter is negligible. Moreover, the model results confirm that the spatial heterogeneity of benthic fluxes observed experimentally is strictly connected to that of Hg_T concentration in sediments.

In general, the theoretical distribution of the mercury evasion fluxes is in acceptable agreement with the experimental results for the investigated periods (see Table S10 of the Supplement). Specifically, small discrepancies are observed in the most part

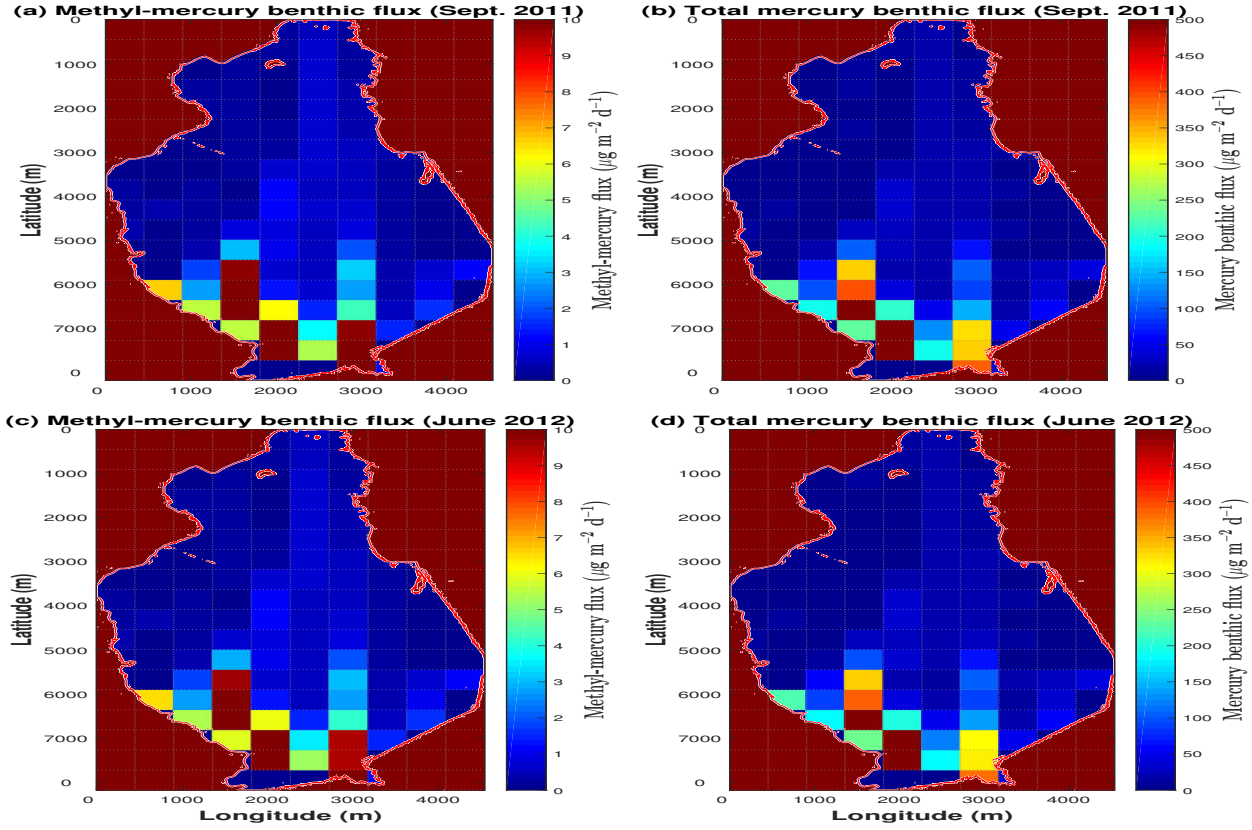

Figure 5. Distribution of $MeHg$ and Hg_D fluxes, calculated at the seawater-sediment interface. The maps reproduce the spatial distribution of the benthic flux in the Augusta Bay during the two sampling periods, i.e. 19-21 September 2011 (panels a, b) and 23-26 June 2012 (panels c, d).

of the stations (four over six), while larger difference emerge in stations 3 (November 2011) and 5 (June 2012). From a qualitative point of view, the model results for the elemental mercury evasion confirm that a high flux is present in the coastal zones at the south-west of the Augusta Bay (Bagnato et al., 2013), while a reduced evasion flux is observed at the northern sector of the basin (see Fig. 6).

In this work, we make the annual mass balance of the Augusta Bay to study the fate of Hg coming from sediments, and to estimate the Hg outflows at the inlets of basin. In Fig. 7, we show the temporal behaviour of the annual mercury fluxes used for mass balance calculation (see also Table S11 of the Supplement). The results of the annual benthic mercury fluxes (B) show that most of the mercury coming up from sediments is in inorganic form (see Fig.7a), while the benthic $MeHg$ flux appears to be one to two order of magnitudes lower. The model results are compared with experimental information reported by Salvagio Manta et al.(2016) for three different sampling sites and in two different periods (September 2011 and June 2012). The modeled Hg_D benthic fluxes (2.65 $kmol\ y^{-1}$ for the year 2011 and 2.61 $kmol\ y^{-1}$ for the year 2012) are significantly

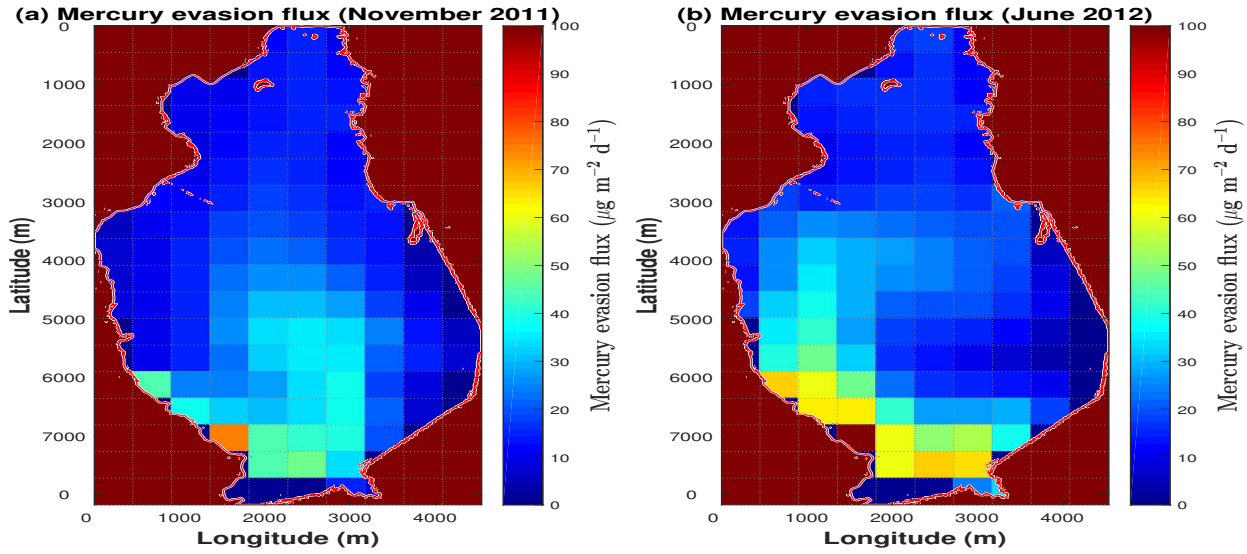

Figure 6. Distribution of Hg^0 flux calculated at the seawater-atmosphere interface. The maps reproduce the spatial distribution of the evasion flux in the Augusta Bay during the two sampling periods, i.e. 29-30 November 2011 (panel a) and 23-25 June 2012 (panel b).

larger than those estimated for both sampling periods on the basis of the field observations (1.1 $kmol\ y^{-1}$ in September 2011 and 1.4 $kmol\ y^{-1}$ in June 2012) (Salvagio Manta et al., 2016). This probably depends on the limited number of sampling sites available in the experimental work with a consequent extremely limited capacity to capture reliable estimates of benthic fluxes within a basin, such as Augusta Bay, where the spatial distribution of sediment mercury is highly heterogeneous. Also, the model takes into account seasonal variations of mercury concentrations in seawater as well as the effects of marine circulation, thus significantly improving the reliability of the results. Moreover, the higher resolution of the grid used in our model guarantees a better estimation of the annual benthic mercury fluxes once the spatio-temporal integration is performed.

The model results for the dynamics of the annual mercury evasion fluxes are shown in Fig.7b. The comparison with experimental findings indicates that the mercury evasion fluxes (V) obtained from the model ($1.93 \cdot 10^{-2}\ kmol\ y^{-1}$ for the year 2011 and $1.90 \cdot 10^{-2}\ kmol\ y^{-1}$ for the year 2012) are in good agreement with those estimated by Salvagio Manta et al.(2016) for each year ($1.70 \cdot 10^{-2}\ kmol\ y^{-1}$) (Sprovieri, 2015; Salvagio Manta et al., 2016). Conversely, a significant discrepancy is observed between the annual atmospheric mercury deposition (AD) obtained by our model ($0.22 \cdot 10^{-2}\ kmol\ y^{-1}$), and that estimated in the experimental work ($0.42 \cdot 10^{-2}\ kmol\ y^{-1}$) (Salvagio Manta et al., 2016). This discrepancy is due to different calculation methods used in the two works. Specifically, in our model the AD is calculated by using both the atmospheric mercury concentrations and the average precipitations, measured for all months of the year. On the contrary, in Bagnato et al. (2013) the AD is calculated by averaging the experimental data acquired during a time limited sampling period (from 29^{th} August 2011 to 23^{th} April 2012), namely without considering the year period in which the amount of precipitation is very low. By this way, the AD obtained by Bagnato et al. (2013) is very higher than that of our model, even if it is probably overestimated due

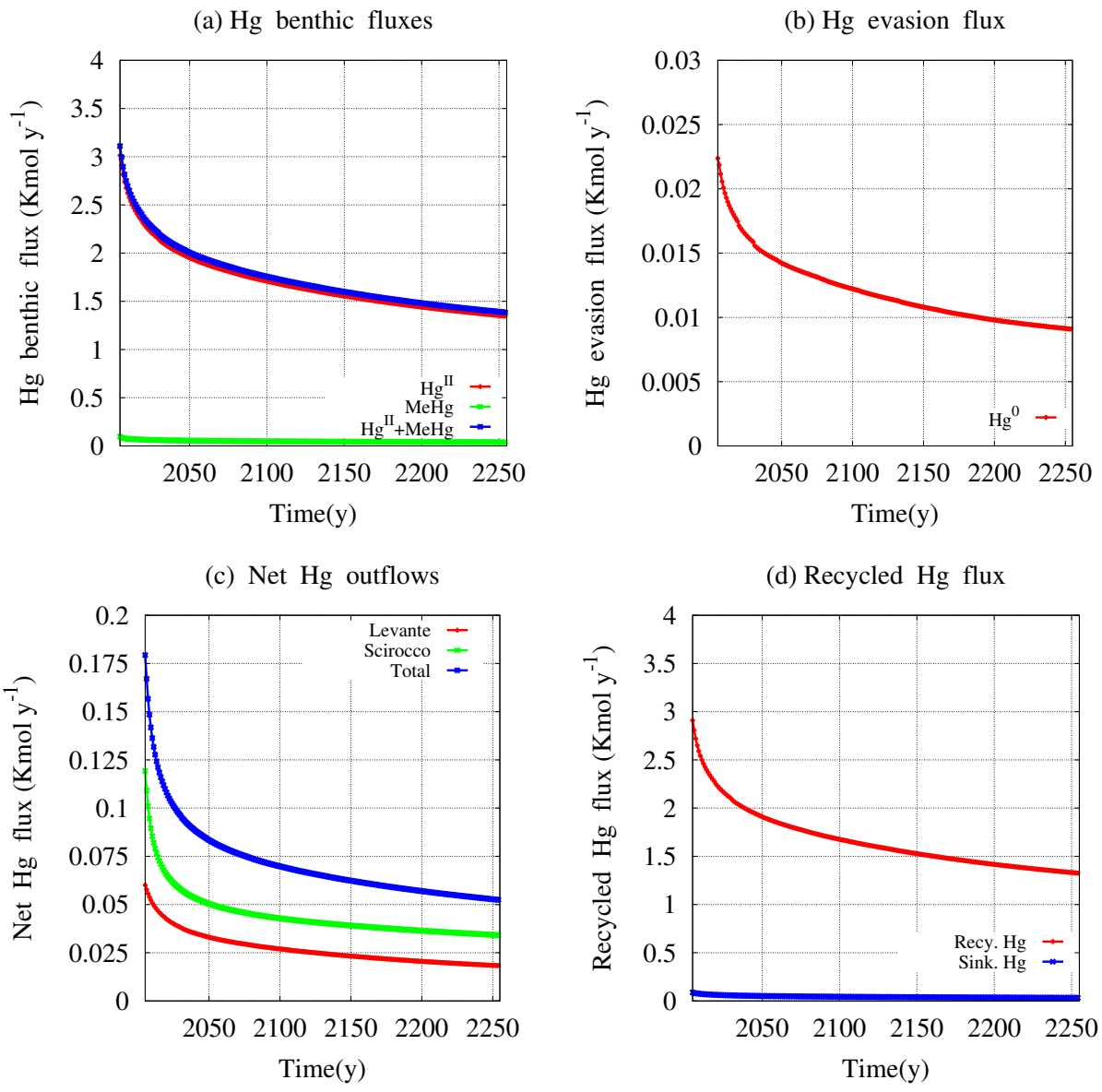

Figure 7. Mercury benthic fluxes (panel a), evasion flux to the atmosphere (panel b), net outflows at the inlets (panel c) and recycling fluxes (panel d).

to calculation method used. In general, the contribute of AD is negligible in the mercury mass balance of the Augusta Bay. Indeed, the simulations indicate that a strong increase of atmospheric mercury deposition caused by environmental changes (dust fall increase and/or rainfall increase), would not affect on numerical results of our model significantly.

The annual net mercury inflows (A) from rivers and sewerage to basin are assumed to be negligible in agreement with field observations. Specifically, the flow rate of Marcellino river is equal to zero for the most part of year, while the inflow from the sewerage is low. Moreover, it is fair to speculate that the Hg concentration in fresh waters discharged in the Augusta Bay was decreased significantly after the chlor-alkali plant closure.

The dynamics of the annual net mercury outflow (O) at the Levante and Scirocco inlets is described in Fig.7c. The results encompass both inflow and outflow of the water mass in each inlet for the whole year, and the associated Hg_T contribution. In Fig.7c, we show the annual Hg_T outflow from the Augusta Bay towards the open sea. This has been estimated to be 0.13 $kmol\ y^{-1}$ for the year 2012 and appears significantly lower than the 0.51 $kmol\ y^{-1}$ calculated by Salvagio Manta et al. (2016) for the same year. Our hypothesis to explain this discrepancy is that the previous study does not consider the dynamics of the $[Hg_T]$ at the inlets (the Hg_T outflow is calculated only on the basis of the mercury concentration measured in February 2012), and that the approach used in the previous paper does not take into account the dynamics of inflow and outflow of the water mass at the two inlets.

In this work, the annual recycled mercury flux (D) is calculated by subtraction using the mass balance equation (18), as well as it was done in previous works on the Augusta Bay (Sprovieri et al., 2011; Salvagio Manta et al., 2016). The model results for the recycled mercury flux are shown in Fig.7d. Here, values calculated by our model (2.50 $kmol\ y^{-1}$ for the year 2011 and 2.46 $kmol\ y^{-1}$ for the year 2012) are larger and probably more realistic than those estimated in Salvagio Manta et al. (2016) (0.84 $kmol\ y^{-1}$). Indeed, the former are obtained by considering the seasonal oscillations of all other mercury fluxes during the year, while the latter are calculated without considering the seasonal changes of mercury fluxes (Salvagio Manta et al., 2016).

In order to reproduce the effects induced by scavenging process on the mercury dynamics, our model calculates the annual sinking mercury flux, whose results are shown in Fig. 6d. Here, a significant gap between the recycled flux (2.50 $kmol\ y^{-1}$ for the year 2011) and the sinking flux (0.07 $kmol\ y^{-1}$ for the year 2011) is observed probably due to the underestimation of the amount of mercury captured by POM (see Eqs. (4)-(5)). More specifically, this behaviour could be caused by the underestimation of NPP, which is calculated by using a conversion equation calibrated for oceans (Baines et al., 1994) rather than for coastal zones.

On the contrary, very high values of the annual Hg_T accumulation rate in surface sediment layer (12.07 $kmol\ y^{-1}$ for the year 2011), respect to those of the annual recycled flux (2.50 $kmol\ y^{-1}$ for the year 2011), are obtained by our model. This result is caused by the high sedimentation rate (11.7 $mm\ y^{-1}$) estimated experimentally (Sprovieri, 2015; ICRAM, 2008) and used in our calculations for annual Hg_T accumulation rate (Covelli et al., 1999). However, the sedimentation rate could be overestimated due to sampling methods used. In fact, the results obtained by the sediment transport model indicate a low average sedimentation rate for the Augusta Bay.

4.2 Mercury in sediments

The spatio-temporal dynamics of $[Hg_T^{sed}]$ in the sediments of Augusta Bay and the mercury concentration of the two species $(Hg^{II}$ and $MeHg)$ dissolved in pore water have been obtained by solving Eqs. (20)-(26). All environmental parameters and variables used for the sediment compartment are reported in Tables S1-S2 of the Supplement.

In Fig. 8, the vertical profiles of mercury concentration in the sediments indicate that $[Hg_T^{sed}]$, $[Hg^{II}_{pore-water}]$ and $[MeHg_{pore-water}]$

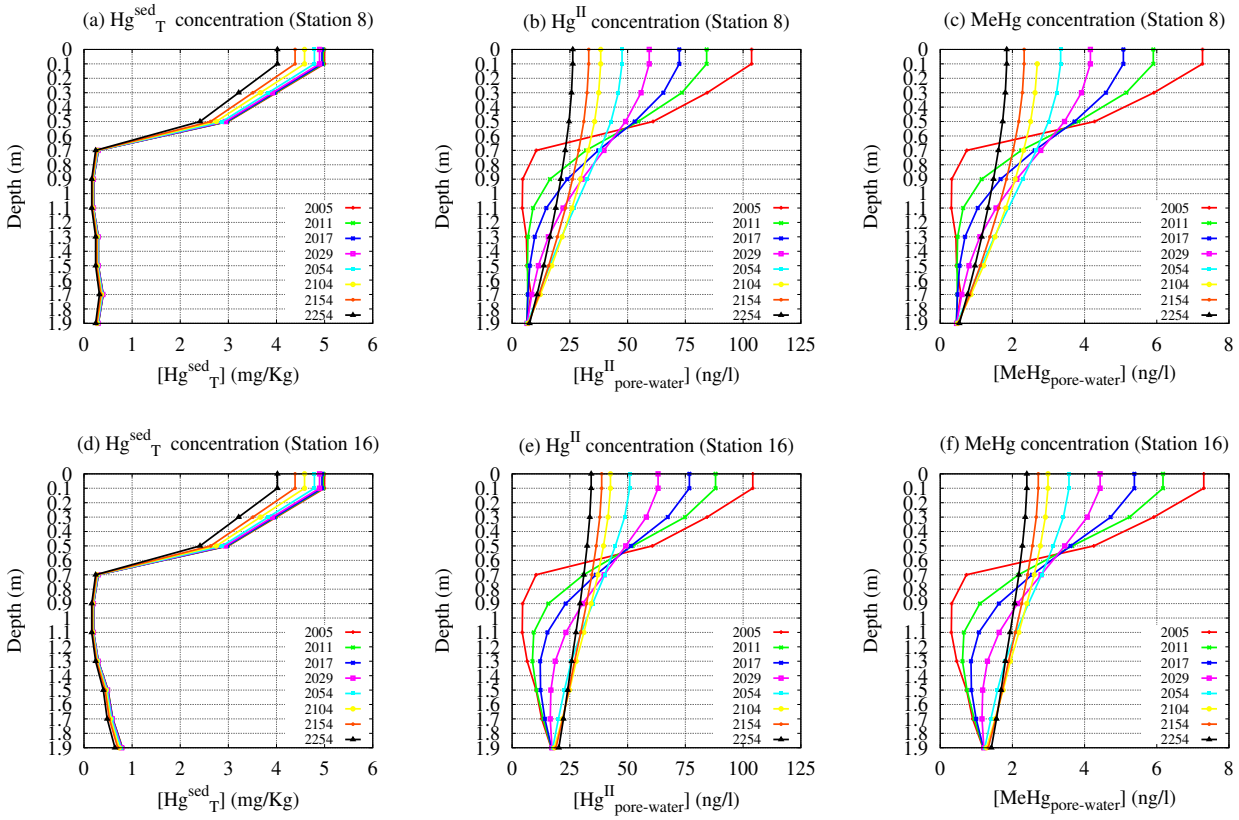

Figure 8. Dynamics of vertical profiles of $[Hg_T^{sed}]$ in sediments (panels a,d), $[Hg^{II}]$ and $[MeHg]$ in pore waters (panels b, c, e and f) at the stations 8 and 16 (sampling May 2011).

always reach their maximum value within the shallower surface layer of the sediments ($< 0.5\ m$ of depth). However, the shape of the vertical profiles for $[Hg^{II}_{pore-water}]$ and $[MeHg_{pore-water}]$ in pore water changes as a function of time. Also, the magnitude of the concentration peaks decreases over the whole 3D domain during the period studied. In particular, the pore water mercury concentration assumes a nearly-uniform distribution along the whole sediment column after several years of model simulation, even if the highest mercury concentrations are always observed in the shallowest layer of the sediments.

The highest $[Hg^{II}_{pore-water}]$ and $[MeHg_{pore-water}]$ in the sediment surface layer support the high benthic mercury fluxes measured even several years after the chlor-alkali plant closure. Moreover, the results of $[Hg^{II}_{pore-water}]$ and $[MeHg_{pore-water}]$

also indicate that the benthic mercury fluxes will remain elevated until the beginning of 23^{rd} century.

Finally, the comparison performed for the $[Hg_D^{sed}]$ in pore water indicates good agreement between the theoretical results and the experimental data (see Table S12 of the Supplement).

5 Discussion

In this work we introduced the innovative HR3DHG biogeochemical model, verified and validated, in all its modules, with the rich database acquired for the Augusta Bay. The model is an advection-diffusion-reaction model (Melaku Canu et al., 2015; Yakushev et al., 2017; Pakhomova et al., 2018; Valenti et al., 2017; Dutkiewicz et al., 2009) that reproduces the spatio-temporal dynamics of the mercury concentration in seawater. The advection-diffusion-reaction model was coupled with: (i) a diffusion-reaction model, which estimates the mercury concentration in the pore waters of the sediment compartment, (ii) the equation which reproduces the mechanism responsible for the desorption of the two mercury species from the solid to the liquid phase of the sediments. This "integrated" model, which allows to give a description of the mercury dynamics in highly polluted marine sites, introduces some novelties in the landscape of the mathematical modelling of spatio-temporal dynamics in a biogeochemical context.

This "integrated" model also estimates the total amount of mercury present in biological species which occupy the lowest trophic level of the food chain, i.e. phytoplankton populations. For this purpose, we incorporated the Phytoplankton MERLIN-Expo model (Pickhardt and Fischer, 2007; Radomyski and Ciffroy, 2015) to describe the mechanism of mercury uptake in phytoplankton cells. Moreover, we reproduced the spatio-temporal dynamics of phytoplankton communities in seawater using a Nutrient-Phytoplankton model (Dutkiewicz et al., 2009; Morozov et al., 2010; Valenti et al., 2012; Denaro et al., 2013a, c, b; Valenti et al., 2015, 2016a, b, c, 2017; Morozov et al., 2019). This "integrated" model, together with the Nutrient-Phytoplankton model and the Phytoplankton MERLIN-Expo model, constitutes a new global biogeochemical (HR3DHG) model describing the mercury dynamics and its effects on the lowest level of the trophic chain.

The HR3DHG model simultaneously provides a high-resolution spatio-temporal dynamics of $[Hg]$ in seawater and sediment, and Hg fluxes at the boundaries of the 3D domain. The former is useful to locate the most polluted areas within the investigated basin. The latter are necessary to obtain the annual mercury mass balance of the basin in the quasi-stationary condition and to predict the mercury outflow towards the open sea, even after a very long time.

For comparison, the different approach used in the WASP models did not allow to reproduce the dynamics of mercury concentration distribution at 3D high resolution in polluted sites characterized by elevated spatial heterogeneity. Similar criticalities came out from the study of HR-1D models (Soerensen et al., 2016; Pakhomova et al., 2018), in which the effects of horizontal velocity field on the mercury dynamics could not be taken into account. Moreover, both the mechanism of the desorption of the total mercury in sediments and the processes involved in dissolved mercury dynamics in pore water were not considered in the most part of advection-diffusion-reaction models, such as the BROM. In general, only few models (Rajar et al., 2007; Zagar et al., 2007; Canu and Rosati, 2017) were able to make forecasts about the mercury depletion time in the sediment compartment

of highly polluted sites, such as Augusta Bay.

Finally, the biogeochemical models introduced in previous works (Soerensen et al., 2016; Pakhomova et al., 2018) provided neither the NPP coming from the Nutrient-Phytoplankton model (Baines et al., 1994; Brunet et al., 2007; Zhang et al., 2014), nor the load of POM-relseased Hg_D obtained using the Phytoplankton MERLIN-Expo model (Pickhardt and Fischer, 2007; Radomyski and Ciffroy, 2015) (see Section 3.1).

All the aforementioned aspects are therefore an element of novelty in the context of 3D biogeochemical modelling. The HR3DHG model considers the effects of the seasonal changes of the environmental variables on the mercury outflows towards the atmosphere and the open sea, and this also is a new feature in biogeochemical model.

Application of the HR3DHG model to the case study of Augusta Bay provides crucial information for that environment, helping us to revise our view of the mercury dynamics in the highly contaminated coastal marine sites of the Mediterranean sea. Firstly, the mass transfer coefficients at the water-sediment interface are highly sensitive to the *layer thickness above the sediment* and their variation could cause significant changes of mercury benthic fluxes. Specifically, for each mercury species in sediments, a small decrease of this parameter causes a great increase of benthic fluxes, with a consequent strong enhancement of dissolved mercury concentration in seawater.

The model framework for the sediment compartment causes that the spatio-temporal dynamics of the benthic mercury flux strongly depends on the spatial distribution of the sediment porosity and of the initial total mercury concentration in the top-sediments, which were fixed using the experimental data.

Sensitivity analysis performed on the environmental parameters and variables used in the seawater compartment indicates that the spatio-temporal dynamics of $[Hg_T]$ and $[Hg_D]$ primarily depends on the velocity field of the marine currents obtained from the hydrodynamic model (Umgiesser, 2009; Umgiesser et al., 2014; Cucco et al., 2016a, b), even if the role played by the vertical and horizontal diffusivities (Pacanowski and Philander, 1981; Massel, 1999; Denman and Gargett, 1983) cannot be neglected. Specifically, the spatio-temporal behaviour of $[Hg_D]$ changed significantly when alternative velocity fields for the Augusta Bay were used in the biogeochemical module, confirming a feature already observed in previous models (Zagar et al., 2007). Conversely, limited changes in the spatial distribution of $[Hg_D]$ were observed when different values of vertical and horizontal diffusivities were set in our model.

The magnitude of the elemental mercury concentration is tightly connected with the values assigned to the rate constants of the photochemical redox reactions, while the role played by the other reaction rates appears negligible for this mercury species.

According to the available experimental data, the theoretical results obtained with the HR3DHG model suggest that the amount of mercury bound to the particulate matter is quite high in seawater compartment (about 47% of the Hg_T on average). In particular, Hg_D is about 35% of the Hg_T in the seawater compartment, while the amount of mercury dissolved in pore water is negligible with respect to the total amount in the sediments. Because of the exponential decay of $[Hg_T]$ in sediments, the concentration of the three mercury species dissolved in seawater decreases slowly as a function of time, whereas their concentration ratios remain approximately constant. Specifically, the mean concentrations of mercury are partitioned as 79.0% of Hg^{II}, 18.8% of elemental mercury and 2.2% of $MeHg$, namely values very similar to those observed experimentally in other contaminated sites (Zhang et al., 2014; Melaku Canu et al., 2015). The same ratio is observed for mercury which outflows from

the inlets of Augusta Bay to the open sea. Here, the theoretical results of the HR3DHG model show a progressive decrease in annual mercury outflow from the bay.

On the whole, the mercury dissolved in seawater derives from sediments through the benthic flux of Hg^{II} and $MeHg$. In particular, these two mercury species are released directly by the sediments, while the elemental mercury is generated by the redox reactions which involve the other two species. The elemental mercury concentration at the water surface contributes to the mercury evasion flux, even if only a small part of elemental mercury in the seawater is released in the atmosphere.

Notably, the theoretical results of the HR3DHG model demonstrate the pivotal role played by the recycling process in the mercury mass balance of the Augusta Bay. Estimates for annual recycled mercury flux indicate that the most part (94%) of the amount of mercury released by sediments remains within the Augusta basin, while the mercury outflows at the boundaries of basin are negligible with respect to the annual benthic mercury fluxes. More specifically, in the quasi-stationary condition, the model results (not shown) indicate that most of the recycled mercury returns to the sediments where is re-buried, and that the amount of mercury absorbed by the POM (0.008 $kmol\ y^{-1}$ for the year 2011), and recycled in seawater, is negligible. In this last respect, it is however important to underscore that even a reduced amount of $MeHg$ entering living phytoplankton cells can be very dangerous for the health of human beings due to the bio-accumulation processes which occur throughout the food chain (Williams et al., 2010; Tomasello et al., 2012; Lee and Fischer, 2017).

The dynamics of the particulate matter deposition-resuspension process (Neumeier et al., 2008; Ferrarin et al., 2008) does not significantly modify the spatial distribution of the Hg_T recycled at the surface layer of the sediments. Moreover, The theoretical results show that the recycled mercury flux in the Augusta Bay is only partially described by the scavenging process. In particular, an underestimation of the sinking flux for POM-bound mercury is observed when the NPP coming from the NP model is used in Eqs. (4)-(5). Probably, this behaviour is due to the $chl-a$ concentration conversion equation of Baines et al.(1994), which has been calibrated for oceans instead of coastal zones. For this reason, the NPP estimation would need further experimental and theoretical investigations. Moreover, a deeper knowledge of the scavenging process, which determines the particulate Hg dynamics, would be necessary, from a theoretical point of view, to obtain a better estimation of the Hg_T removed from the water column.

The theoretical results from the HR3DHG model show that, without specific and appropriate recovery actions, the mercury benthic flux could remain high for a very long time, representing a threat for this environment, for its ecosystems and for human health.

Furthermore, climate changes due to the increase in global temperature could significantly influence the dynamics of mercury, with undesirable increases in its concentration and consequent negative effects on the zoobenthos and benthic fishes. Finally, for its features, the HR3DHG model may represent a useful tool to explore and predict the effects of environmental changes on the mercury dynamics for several possible forthcoming scenarios.

6 Conclusions

A novel biogeochemical integrated model, HR3DHG, has been designed and implemented to reproduce the spatio-temporal dynamics of three species of mercury in the highly contaminated Augusta Bay. The model consistently reproduces the biogeochemical dynamics of mercury fluxes at the boundaries of the 3D domain, which is necessary for an accurate and reliable approximation of the annual mass balance for the whole basin. Direct comparison of model and experimental data suggests a good capacity of HR3DHG to capture the crucial processes dominating the dynamics of Hg species in the different marine compartments and at their interfaces, with reliable estimations of benthic fluxes and evasion towards the atmosphere. The model provides robust information on the recycling of the Hg species in a confined coastal area and can be considered as a reliable numerical tool to describe high-resolution variability of the most important biogeochemical variables driving Hg concentrations. Finally, model results for the Augusta Bay suggest a permanent and relevant long-term (at century scale) mercury benthic fluxes, associated with negative effects for the biota of the investigated marine ecosystem and with significant health risks. Finally, the HR3DHG model represents a promising tool to explore and predict the effects of climate changes on the mercury dynamics in the marine ecosystems.

Code and data availability. The experimental data used in this study are available and properly referenced along the paper or collected in the tables of the Supplement. The software code files are available at *http://biomatlab.iasi.cnr.it/models/hr3dhgv1.zip*.

Author contributions. GD devised the the HR3DHG model; GD, AB and ADG designed the software used to solve numerically the equations of the model; GD and MS jointly wrote the manuscript; DV and BS supported the HR3DHG model development; AB, DV, BS and ADG made the management of simulations; DSM and MB performed the Hg data collection; DSM developed the sampling strategy; DSM and MB performed the study of Hg biogeochemistry; MS investigated the Hg biogeochemical dynamics; AC investigated the hydrodynamics in Augusta Bay; AC performed the ocean modelling and generated the code of SHYFEM model; EQ performed the data statistics and mapping. All authors contributed to review the manuscript.

Competing interests. The authors declare that they have no conflict of interest.

Acknowledgements. The experimental data used in this study are available and properly referenced along the paper or collected in the tables of the Supplement. We acknowledge the financial support by Ministry of University, Research and Education of Italian Government, Project "Centro Internazionale di Studi Avanzati su Ambiente, ecosistema e Salute umana - CISAS".

References

Bagnato, E., Sprovieri, M., Barra, M., Bitetto, M., Bonsignore, M., Calabrese, S., Di Stefano, V., Oliveri, E., Parello, F., and Mazzola, S.: The sea-air exchange of mercury (Hg) in the marine boundary layer of the Augusta basin (southern Italy): Concentrations and evasion flux, Chemosphere, 93, 2024–2032, https://doi.org/10.1016/j.chemosphere.2013.07.025, 2013.

Baines, S. B., Pace, M. L., and Karl, D. M.: Why does the relationship between sinking flux and planktonic primary production differ between lakes and oceans?, Limnol. Oceanogr., 39(2), 213–226, https://doi.org/10.4319/lo.1994.39.2.0213, 1994.

Batrakova, N., Travnikov, O., and Rozovskaya, O.: Chemical and physical transformations of mercury in the ocean: a review, Ocean Sci., 10, 1047–1063, https://doi.org/https://doi.org/10.5194/os-10-1047-2014, 2014.

Bellucci, L. G., Giuliani, S., Romano, S., Albertazzi, S., Mugnai, C., and Frignani, M.: An integrated approach to the assessment of pollutant delivery chronologies to impacted areas: Hg in the Augusta Bay (Italy), Environ. Sci. Technol., 46, 2040–2046, https://doi.org/10.1021/es203054c, 2012.

Bianchi, F., Dardanoni, G., Linzalone, N., and Pierini, A.: Malformazioni congenite nei nati residenti nel Comune di Gela (Sicilia, Italia), Epidemiol. Prev., 30(1), 19–26, 2006.

Bonsignore, M., Manta, D. S., Oliveri, E., Sprovieri, M., Basilone, G., Bonanno, A., Falco, F., Traina, A., and Mazzola, S.: Mercury in fishes from Augusta Bay (southern Italy): risk assessment and health implication, Food Chem. Toxicol., 56, 184–194, https://doi.org/10.1016/j.fct.2013.02.025, 2013.

Bonsignore, M., Tamburrino, S., Oliveri, E., Marchetti, A., Durante, C., Berni, A., Quinci, E., and Sprovieri, M.: Tracing mercury pathways in Augusta Bay (southern Italy) by total concentration and isotope determination, Environ. Pollut., 205, 178–185, https://doi.org/10.1016/j.envpol.2015.05.033, 2015.

Bonsignore, M., Andolfi, N., Barra, M., Madeddu, M., Tisano, F., Ingallinella, V., Castorina, M., and Sprovieri, M.: Assessment of mercury exposure in human populations: a status report from Augusta Bay (southern Italy), Environ. Res. Spec. Issue Hum. Biomonitoring, 150, 592–599, https://doi.org/10.1016/j.envres.2016.01.016, 2016.

Brunet, C., Casotti, R., Vantrepotte, V., and Conversano, F.: Vertical variability and diel dynamics of picophytoplankton in the Strait of Sicily, Mediterranean Sea, in summer, Mar. Ecol. Prog. Ser., 346, 15–26, 2007.

Bryant, L. D., McGinnis, D. F., Lorrai, C., Brand, A., Little, J. C., and Wüest, A.: Evaluating oxygen fluxes using microprofiles from both sides of the sediment–water interface, Limnol. Oceanogr. Methods, 8, 610–627, https://doi.org/10.4319/lom.2010.8.610, 2010.

Budillon, F., Ferraro, L., Hopkins, T. S., Iorio, M., Lubritto, C., Sprovieri, M., Bellonia, A., Marzaioli, F., and Tonielli, R.: Effects of intense anthropogenic settlement of coastal areas on seabed and sedimentary systems: a case study from the Augusta Bay (southern Italy), Rend. Online Soc. Geol. Italy, 3, 142–143, 2008.

Burchard, H. and Petersen, O.: Models of turbulence in the marine environment. A comparative study of two-equation turbulence models, J. Mar. Syst., 21(1-4), 23–53, https://doi.org/10.1016/S0924-7963(99)00004-4, 1999.

Canu, D. and Rosati, G.: Long-term scenarios of mercury budgeting and exports for a Mediterranean hot spot (Marano-Grado Lagoon, Adriatic Sea), Estuar. Coast. Shelf Sci., 198, 518–528, https://doi.org/https://doi.org/10.1016/j.ecss.2016.12.005, 2017.

Ciffroy, P.: The River MERLIN-Expo model, Fun Project 4 - Seventh Framework Programme, 2015.

Cossa, D. and Coquery, M.: The Handbook of Environmental Chemistry, Vol. 5, Part K (2005): 177-208. The Mediterranean Mercury Anomaly, a Geochemical or a Biologocal Issue, Springer-Verlag Berlin Heidelberg, 2005.

Covelli, S., Faganeli, J., Horvat, M., and Bramati, A.: Porewater Distribution and Benthic Flux Measurements of Mercury and Methylmercury in the Gulf of Trieste (Northern Adriatic Sea), Estuar. Coast. Shelf Sci., 48, 415–428, https://doi.org/https://doi.org/10.1006/ecss.1999.0466, 1999.

Covelli, S., Faganeli, J., De Vittor, C., Predonzani, S., Acquavita, A., and Horvat, M.: Benthic fluxes of mercury species in a lagoon environment (Grado Lagoon, Northern Adriatic Sea, Italy), Appl. Geochem., 23, 529–546, https://doi.org/10.1016/j.apgeochem.2007.12.011, 2008.

Cucco, A., Quattrocchi, G., Olita, A., Fazioli, L., Ribotti, A., Sinerchia, M., Tedesco, C., and Sorgente, R.: Hydrodynamic modeling of coastal seas: the role of tidal dynamics in the Messina Strait, Western Mediterranean Sea, Nat. Hazard Earth Sys., 16, 1553–1569, https://doi.org/10.5194/nhess-16-1553-2016, 2016a.

Cucco, A., Quattrocchi, G., Satta, A., Antognarelli, F., De Biasio, F., Cadau, E., Umgiesser, G., and Zecchetto, S.: Predictability of wind-induced sea surface transport in coastal areas, J. Geophys. Res. Oceans, 121(8), 5847–5871, https://doi.org/https://doi.org/10.1002/2016JC011643, 2016b.

Cucco, A., Quattrocchi, G., and Zecchetto, S.: The role of temporal resolution in modeling the wind induced sea surface transport in coastal seas, J. Mar. Syst., 193, 46–58, https://doi.org/https://doi.org/10.1016/j.jmarsys.2019.01.004, 2019.

De Marchis, M., Freni, G., and Napoli, E.: Three-dimensional numerical simulations on wind- and tide-induced currents: The case of Augusta Harbour (Italy), Comput. Geosci., 72, 65–75, 2014.

Denaro, G., Valenti, D., La Cognata, A., Spagnolo, B., Bonanno, A., Basilone, G., Mazzola, S., Zgozi, S., Aronica, S., and Brunet, C.: Spatio-temporal behaviour of the deep chlorophyll maximum in Mediterranean Sea: Development of a stochastic model for picophytoplankton dynamics, Ecol. Complex., 13, 21–34, https://doi.org/10.1016/j.ecocom.2012.10.002, 2013a.

Denaro, G., Valenti, D., Spagnolo, B., Basilone, G., Mazzola, S., Zgozi, S., Aronica, S., and Bonanno, A.: Dynamics of two picophytoplankton groups in Mediterranean Sea: Analysis of the Deep Chlorophyll Maximum by a stochastic advection-reaction-diffusion model, PLoS ONE, 8(6), e66 765, https://doi.org/10.1371/journal.pone.0066765, 2013b.

Denaro, G., Valenti, D., Spagnolo, B., Bonanno, A., Basilone, G., Mazzola, S., Zgozi, S., and Aronica, S.: Stochastic dynamics of two picophytoplankton populations in a real marine ecosystem, Acta Phys. Pol. B, 44, 977–990, https://doi.org/10.5506/APhysPolB.44.977, 2013c.

Denman, K. L. and Gargett, A. E.: Time and space scales of vertical mixing and advection of phytoplankton in the upper ocean, Limnol. Oceanogr., 28, 801–815, https://doi.org/https://doi.org/10.4319/lo.1983.28.5.0801, 1983.

Driscoll, C. T., Mason, R. P., Chan, H. M., Jacob, D. J., and Pirrone, N.: Mercury as a Global Pollutant: Sources, Pathways, and Effects, Environ. Sci. Technol., 47, 4967–4983, https://doi.org/10.1021/es305071v, 2013.

Dutkiewicz, S., Follows, M. J., and Bragg, J. G.: Modeling the coupling of ocean ecology and biogeochemistry., Global Biogeochem. Cy., p. GB4017, https://doi.org/https://doi.org/10.1029/2008GB003405, 2009.

Ferrarin, C., Umgiesser, G., Cucco, A., Hsu, T. W., Roland, A., and Amos, C. L.: Development and validation of a finite element morphological model for shallow water basins, Coast. Eng., 55, 716–731, https://doi.org/10.1016/j.coastaleng.2008.02.016, 2008.

Ferrarin, C., Bajo, M., Bellafiore, D., Cucco, A., De Pascalis, F., and Ghezzo, M.: Toward homogenization of Mediterranean lagoons and their loss of hydrodiversity, Geophys. Res. Lett., 41(16), 5935–5941, https://doi.org/https://doi.org/10.1002/2014GL060843, 2014.

Fiasconaro, A., Valenti, D., and Spagnolo, B.: Nonmonotonic Behaviour of Spatiotemporal Pattern Formation in a Noisy Lotka-Volterra System, Acta Phys. Pol. B, 35, 1491–1500, 2004.

Han, S., Lehman, R. D., Choe, K. Y., and Gill, A.: Chemical and physical speciation of mercury in Offatts Bayou: A seasonally anoxic bayou in Galveston Bay, Limnol. Oceanogr., 52(4), 1380–1392, https://doi.org/https://doi.org/10.4319/lo.2007.52.4.1380, 2007.

Hines, M. E., Potrait, E. N., Covelli, S., Faganeli, J., Emili, A., Zizek, E., and Horvat, M.: Mercury methylation and demethylation in Hg-contaminated lagoon sediments (Marano and Grado Lagoon, Italy), Estuar. Coast. Shelf Sci., 113, 85–95, https://doi.org/10.1016/j.ecss.2011.12.021, 2012.

Horvat, M., Kotnik, J., Logar, M., Fajon, V., Zvoranic, T., and Pirrone, N.: Speciation of mercury in surface and deep-sea waters in the Mediterranean Sea, Atmospheric Environ., 37(1), S93–S108, https://doi.org/10.1016/S1352-2310(03)00249-8, 2003.

ICRAM: Progetto preliminare di bonifica dei fondali della rada di Augusta nel sito di interesse nazionale di Priolo e Elaborazione definitiva, BoI-Pr-SI-PR-Rada di Augusta-03.22, 2008.

La Barbera, A. and Spagnolo, B.: Spatio-Temporal Patterns in Population Dynamics, Physica A, 314, 120–124, https://doi.org/10.1016/S0378-4371(02)01173-1, 2002.

Lee, C. S. and Fischer, N. S.: Bioaccumulation of methylmercury in a marine copepod, Environ Toxicol Chem., 36(5), 1287–1293, https://doi.org/10.1002/etc.3660, 2017.

Lehnherr, I., St. Louis, V. L., Hintelmann, H., and Kirk, J. L.: Methylation of inorganic mercury in polar marine waters, Nat. Geosci., 4, 298–302, https://doi.org/https://doi.org/10.1038/ngeo1134, 2011.

Liu, G., Cai, J., and O'Driscoll, N.: Environmental Chemistry and Toxycology of Mercury, John Wiley and Sons, Inc., Hoboken, New Jersey, 2012.

Mason, R. P., Choi, A. L., Fitzgerald, W. F., Hammerschimidt, C. R., Lamborg, C. H., Soerensen, A. L., and Sunderland, E. M.: Mercury biogeochemical cycling in the ocean and policy implications, Environ. Res., 112, 101–117, https://doi.org/10.1016/j.envres.2012.03.013, 2012.

Massel, S. R.: Fluid Mechanics for Marine Ecologists, Springer-Verlag, Berlin Heidelberg, 1999.

Melaku Canu, D., Rosati, G., Solidoro, C., Heimbürger, L., and Acquavita, A.: A comprehensive assessment of the mercury budget in the Marano-Grado Lagoon (Adriatic Sea) using a combined observational modeling approach, Mar. Chem., 177, 742–752, https://doi.org/10.1016/j.marchem.2015.10.013, 2015.

Monperrus, M., Tessier, E., Amouroux, D., Leynaert, A., Huonnic, P., and Donard, O. F. X.: Mercury methylation, demethylation and reduction rates in coastal and marine surface waters of the Mediterranean Sea, Mar. Chem., 107, 49–63, https://doi.org/10.1016/j.marchem.2007.01.018, 2007a.

Monperrus, M., Tessier, E., Point, D., Vidimova, K., Amouroux, D., Guyoneaud, R., Leynaert, A., Grall, J., Chauvaud, L., Thouzeau, G., and Donard, O. F. X.: The biogeochemistry of mercury at the sediment-water interface in the Thau Lagoon. 2. Evaluation of mercury methylation potential in both surface sediment and the column, Estuar. Coast. Shelf Sci., 72, 485–486, https://doi.org/https://doi.org/10.1016/j.ecss.2006.11.014, 2007b.

Morozov, A., Arashkevich, E., Nikishina, A., and Solovyev, K.: Nutrient-rich plankton communities stabilized via predator-prey interactions: revisiting the role of vertical heterogeneity, Math. Med. Biol., 28(2), 185–215, https://doi.org/10.1093/imammb/dqq010, 2010.

Morozov, A., Denaro, G., Spagnolo, B., and Valenti, D.: Revisiting the role of top-down and bottom-up controls in stabilisation of nutrient-rich plankton communities, Commun. Nonlinear Sci. Numer. Simul., 79, 104 885, https://doi.org/https://doi.org/10.1016/j.cnsns.2019.104885, 2019.

Neumeier, U., Ferrarin, C., Amos, C. L., Umgiesser, G., and Li, M. Z.: Sedtrans05: An improved sediment-transport model for continental shelves and coastal waters with a new algorithm for cohesive sediments, Comput. Geosci., 34, 1223–1242, https://doi.org/10.1016/j.cageo.2008.02.007, 2008.

Ogrinc, N., Monperrus, M., Kotnik, J., Fajon, V., Vidimova, K., Amouroux, D., Kocman, D., Tessier, E., Zizek, S., and Horvat, M.: Distribution of mercury and methylmercury in deep-sea surficial sediments of the Mediterranean Sea, Mar. Chem., 107, 31–48, https://doi.org/https://doi.org/10.1016/j.marchem.2007.01.019, 2007.

Oliveri, E., Manta, D. S., Bonsignore, M., Cappello, S., Tranchida, G., Bagnato, E., Sabatino, N., Santisi, S., and Sprovieri, M.: Mobility of mercury in contaminated marine sediments: Biogeochemical pathways, Mar. Chem., 186, 1–10, https://doi.org/10.1016/j.marchem.2016.07.002, 2016.

Pacanowski, R. and Philander, S. G. H.: Parameterization of Vertical Mixing in Numerical Models of Tropical Oceans, J. Phys. Oceanogr., 11, 1443–1451, https://doi.org/10.1175/1520-0485(1981)011$<$ 1443 : $POVMIN$ $>$2.0.CO;2, 1981.

Pakhomova, S. V., Yakushev, E. V., Protsenko, E. A., Rigaud, S., Cossa, D., Knoery, J., Couture, R. M., Radakovitch, O., Yakubov, S. K., Krzeminska, D., and Newton, A.: Modeling the Influence of Eutrophication and Redox Conditions on Mercury Cycling at the Sediment-Water Interface in the Berre Lagoon, Front. Mar. Sci., 5, 291, https://doi.org/10.3389/fmars.2018.00291, 2018.

Pickhardt, P. C. and Fischer, N. S.: Accumulation of Inorganic and Methylmercury by Freshwater Phytoplankton in Two Contrasting Water Bodies, Environ. Sci. Technol., 41, 125–131, https://doi.org/10.1021/es060966w, 2007.

Qureshi, A., O'Driscoll, N. J., MacLeod, M., Neuhold, Y. M., and Hungerbuhler, K.: Photoreactions of mercury in surface ocean water: gross reaction kinetics and possible pathways, Environ. Sci. Technol., 44, 644–649, https://doi.org/10.1021/es9012728, 2010.

Radomyski, A. and Ciffroy, P.: The Phytoplankton MERLIN-Expo model, Fun Project 4 - Seventh Framework Programme, 2015.

Rajar, R., Cetina, M., Horvat, M., and Zagar, D.: Mass balance of mercury in the Mediterranean Sea, Mar. Chem., 107, 89–102, https://doi.org/https://doi.org/10.1016/j.marchem.2006.10.001, 2007.

Roache, P. J.: Fundamentals of Computational Fluid Dynamics, Hermosa Publishers, Albuquerque, New Mexico, 1998.

Rosati, G., Heimbürger, L. E., Melaku Canu, D., Lagane, C., Rijkenberg, M. J. A., Gerringa, L. J. A., Solidoro, C., Gencarelli, C. N., Hedgecock, I. M., De Baar, H. J. W., and Sonke, J. E.: Mercury in the Black Sea: New Insights From Measurements and Numerical Modeling, Global Biogeochem. Cy., 32, 529–550, https://doi.org/https://doi.org/10.1002/2017GB005700, 2018.

Salvagio Manta, D., Bonsignore, M., Oliveri, E., Barra, M., Tranchida, G., Giaramita, L., Mazzola, S., and Sprovieri, M.: Fluxes and the mass balance of mercury in Augusta Bay (Sicily, southern Italy), Estuar. Coast. Shelf Sci., 181, 134–143, https://doi.org/10.1016/j.ecss.2016.08.013, 2016.

Schulz, H. D. and Zabel, M.: Marine Geochemistry, Springer - Verlag Berlin Heidelberg, 2006.

Soerensen, A. L., Sunderland, E. M., Holmes, C. D., Jacob, D. J., Yantosca, R. M., Skov, H., Christensen, J. H., Strode, S. A., and Mason, R. P.: An improved global model for air-sea exchange of mercury: High concentrations over the north Atlantic, Environ. Sci. Technol., 44, 8574–8580, https://doi.org/10.1021/es102032g, 2010.

Soerensen, A. L., Schartup, A. T., Gustafsson, E., Gustafsson, B. G., Undeman, E., and Björn, E.: Eutrophication Increases Phytoplankton Methylmercury Concentrations in a Coastal Sea - A Baltic Sea Case Study, Environ. Sci. Technol., 50, 11 787–11 796, https://doi.org/10.1021/acs.est.6b02717, 2016.

Sørensen, P. B., Fauser, P., Carlsen, L., and Vikelsøe, J.: Theoretical evaluation of the sediment/water exchange description in generic compartment models (SimpleBox), NERI Technical Report No.360, 2001.

Sprovieri, M.: Inquinamento ambientale e salute umana, il caso studio della Rada di Augusta, CNR Edizioni, P. Aldo Moro, 7, I-00185 Roma, Italia, 2015.

Sprovieri, M., Oliveri, E., Di Leonardo, R., Romano, E., Ausili, A., Gabellini, M., Barra, M., Tranchida, G., Bellanca, A., Neri, R., Budillon, F., Saggiomo, R., Mazzola, S., and Saggiomo, V.: The key role played by the Augusta basin (southern Italy) in the mercury contamination of the Mediterranean Sea, J. Environ. Monit., 13, 1753–1760, https://doi.org/10.1039/C0EM00793E, 2011.

Strode, S., Jaeglè, L., and Emerson, S.: Vertical transport of anthropogenic mercury in the ocean, Global Biogeochem. Cy., 24, GB4014, https://doi.org/https://doi.org/10.1029/2009GB003728, 2010.

Sunderland, E. M., Gobas, F. A. P. C., Branfireum, B. A., and Heyes, A.: Environmental controls on the speciation and distribtuion of mercury in coastal sediments, Mar. Chem., 102, 111–123, https://doi.org/10.1016/j.marchem.2005.09.019, 2006.

Thi, N. N. P., Huisman, J., and Sommeijer, B. P.: Simulation of three-dimensional phytoplankton dynamics: competition in light-limited environments, J. Comput. Appl. Math., 174, 57–77, https://doi.org/10.1016/j.cam.2004.03.023, 2005.

Tomasello, B., Copat, C., Pulvirenti, V., Ferrito, V., Ferrante, M., Renis, M., Sciacca, S., and Tigano, C.: Biochemical and bioaccumulation approaches for investigating marine pollution using Mediterranean rainbow wrasse, Coris julis (Linneaus 1798), Ecotoxicol. Environ. Safe., 86, 168–175, https://doi.org/10.1016/j.ecoenv.2012.09.012, 2012.

Tveito, A. and Winther, R.: Introduction to Partial Differential Equations: A Computational Approach, Springer-Verlag, New York, 1998.

Umgiesser, G.: SHYFEM. Finite Element Model for Coastal Seas. User Manual, The SHYFEM Group, Georg Umgiesser, ISMAR-CNR, Venezia, Italy, 2009.

Umgiesser, G., Canu, D. M., Cucco, A., and Solidoro, C.: A finite element model for the Venice Lagoon. Development, set up, calibration and validation, J. Mar. Syst., 51, 123–145, https://doi.org/10.1016/j.jmarsys.2004.05.009, 2004.

Umgiesser, G., Ferrarin, C., Cucco, A., De Pascalis, F., Bellafiore, D., Ghezzo, M., and Bajo, M.: Comparative hydrodynamics of 10 Mediterranean lagoons by means of numerical modeling, J. Geophys. Res. Oceans, 119(4), 2212–2226, https://doi.org/https://doi.org/10.1002/2013JC009512, 2014.

Valenti, D., Fiasconaro, A., and Spagnolo, B.: Pattern formation and spatial correlation induced by the noise in two competing species, Acta Phys. Pol. B, 35, 1481–1489, 2004.

Valenti, D., Tranchina, L., Cosentino, C., Brai, M., Caruso, A., and Spagnolo, B.: Environmental Metal Pollution Considered as Noise: Effects on the Spatial Distribution of Benthic Foraminifera in two Coastal Marine Areas of Sicily (Southern Italy), Ecol. Model., 213, 449–462, https://doi.org/10.1016/j.ecolmodel.2008.01.023, 2008.

Valenti, D., Denaro, G., La Cognata, A., Spagnolo, B., Bonanno, A., Mazzola, S., Zgozi, S., and Aronica, S.: Picophytoplankton dynamics in noisy marine environment, Acta Phys. Pol. B, 43, 1227–1240, https://doi.org/10.5506/APhysPolB.43.1227, 2012.

Valenti, D., Denaro, G., Spagnolo, B., Conversano, F., and Brunet, C.: How diffusivity, thermocline and incident light intensity modulate the dynamics of deep chlorphyll maximum in Tyrrhenian Sea, PLoS ONE, 10(1), e0115 468, https://doi.org/https://doi.org/10.1371/journal.pone.0115468, 2015.

Valenti, D., Denaro, G., Conversano, F., Brunet, C., Bonanno, A., Basilone, G., Mazzola, S., and Spagnolo, B.: The role of noise on the steady state distributions of phytoplankton populations, J. Stat. Mech., p. 054044, https://doi.org/10.1088/1742-5468/2016/05/054044, 2016a.

Valenti, D., Denaro, G., Spagnolo, B., Mazzola, S., Basilone, G., Conversano, F., Brunet, C., and Bonanno, A.: Stochastic models for phytoplankton dynamics in Mediterranean Sea, Ecol. Complex., 27, 84–103, https://doi.org/10.1016/j.ecocom.2015.06.001, 2016b.

Valenti, D., Giuffrida, A., Denaro, G., Pizzolato, N., Curcio, L., Mazzola, S., Basilone, G., Bonanno, A., and Spagnolo, B.: Noise Induced Phenomena in the Dynamics of Two Competing Species, Math. Model. Nat. Phenom., 11(5), 158–174, https://doi.org/https://doi.org/10.1051/mmnp/201611510, 2016c.

Valenti, D., Denaro, G., Ferreri, R., Genovese, S., Aronica, S., Mazzola, S., Bonanno, A., Basilone, G., and Spagnolo, B.: Spatio-temporal dynamics of a planktonic system and chlorophyll distribution in a 2D spatial domain: matching model and data, Sci. Rep., 7, 220, https://doi.org/https://doi.org/10.1051/mmnp/201611510, 2017.

Williams, J. J., Dutton, J., Chen, C. Y., and Fischer, N. S.: Metal (As, Cd, Hg, and CH_3Hg) bioaccumulation from water and food by the benthic amphypod *Leptocheirus Plumulosus*, Environ. Toxicol. Chem., 29(8), 1755–1761, https://doi.org/10.1002/etc.207, 2010.

Yakushev, E. V., Protsenko, E. A., Bruggeman, J., Wallhead, P., Pakhomova, S. V., Yakubov, S. K., Bellerby, R. G. J., and Couture, R. M.: Bottom RedOx Model (BROM v.1.1): a coupled benthic-pelagic model for simulation of water and sediment biogeochemistry, Geosci. Model Dev., 10, 453–482, https://doi.org/10.5194/gmd-10-453-2017, 2017.

Zagar, D., Petkovsek, G., Rajar, R., Sirnik, N., Horvat, M., Voudouri, A., Kallos, G., and Cetina, M.: Modelling of mercury transport and transformations in the water compartment of the Mediterranean Sea, Mar. Chem., 107, 64–88, https://doi.org/https://doi.org/10.1016/j.marchem.2007.02.007, 2007.

Zagar, D., Sirnik, N., Cetina, M., Horvat, M., Kotnik, J., Ogrinc, N., Hedgecock, I. M., Cinnirella, S., De Simone, F., Gencarelli, C. N., and Pirrone, N.: Mercury in the Mediterranean. Part 2: processes and mass balance, Environ. Sci. Pollut. Res., 21, 4081–4094, https://doi.org/10.1007/s11356-013-2055-5, 2014.

Zhang, Y., Jaeglé, L., and Thompson, L.: Natural biogeochemical cycle of mercury in a global three-dimensional ocean tracer model, Global Biogeochem. Cy., 28, GB004 814, https://doi.org/10.1002/2014GB004814, 2014.

Zhu, S., Zhang, Z., and Zagar, D.: Mercury transport and fate models in aquatic systems: A review and synthesis, Sci. Total Environ., 639, 538–549, https://doi.org/10.1016/j.scitotenv.2018.04.397, 2018.

Supplement of "HR3DHG version 1: modelling the spatio-temporal dynamics of mercury in the Augusta Bay (southern Italy)"

Giovanni Denaro[1], Daniela Salvagio Manta[2], Alessandro Borri[3], Maria Bonsignore[4], Davide Valenti[1,5], Enza Quinci[4], Andrea Cucco[6], Bernardo Spagnolo[5,7,8], Mario Sprovieri[4], and Andrea De Gaetano[3]

[1]CNR-IRIB, Consiglio Nazionale delle Ricerche - Istituto per la Ricerca e l'Innovazione Biomedica, Via Ugo La Malfa 153, I-90146 Palermo, Italy
[2]CNR-IAS, National Research Council of Italy – Institute of Anthropic Impacts and Sustainability in marine environment, ex Complesso Roosevelt, Lungomare Cristoforo Colombo, 4521, Loc. Addaura, Palermo, Italy
[3]CNR-IASI Biomathematics Laboratory, Consiglio Nazionale delle Ricerche - Istituto di Analisi dei Sistemi ed Informatica "A. Ruberti", Via dei Taurini 19, I-00185 Rome, Italy
[4]CNR-IAS, National Research Council of Italy – Institute of Anthropic Impacts and Sustainability in marine environment, U.O.S di Capo Granitola, Via del Faro 3, I-91020 Campobello di Mazara (TP), Italy
[5]Dipartimento di Fisica e Chimica "Emilio Segrè", Università di Palermo, Group of Interdisciplinary Theoretical Physics and CNISM, Unità di Palermo, Viale delle Scienze, Ed. 18, I-90128 Palermo, Italy
[6]CNR-IAS, Consiglio Nazionale delle Ricerche - Istituto per lo studio degli impatti Antropici e Sostenibilità in ambiente marino, U.O.S. di Oristano, località Sa Mardini, I-09072 Torregrande (OR), Italy
[7]Radiophysics Department, National Research Lobachevsky State University of Nizhni Novgorod, 23 Gagarin Avenue, Nizhni Novgorod 603950, Russia
[8]Istituto Nazionale di Fisica Nucleare, Sezione di Catania, Via S. Sofia 64, I-90123 Catania, Italy

Correspondence: Alessandro Borri (alessandro.borri@iasi.cnr.it)

S1 The Advection-Diffusion-Reaction Model - Seawater Compartment

The spatio-temporal dynamics of the dissolved elemental mercury concentration (Hg^0) in the Augusta basin (Zhang et al., 2014; Melaku Canu et al., 2015; Whalin et al., 2007; Monperrus et al., 2007b; Bagnato et al., 2013) is described by the following partial differential equation (PDE):

$$\begin{aligned}\frac{\partial Hg^0}{\partial t} = & +\frac{\partial}{\partial x}\left[D_x\frac{\partial Hg^0}{\partial x}\right]-\frac{\partial}{\partial x}(v_x Hg^0)+\frac{\partial}{\partial y}\left[D_y\frac{\partial Hg^0}{\partial y}\right]-\frac{\partial}{\partial y}(v_y Hg^0)\\ & +\frac{\partial}{\partial z}\left[D_z\frac{\partial Hg^0}{\partial z}\right]-\frac{\partial}{\partial z}(v_z Hg^0)+k_{Ph-de}\cdot MeHg\\ & -(k_1+k_3)\cdot Hg^0+(k_2+k_4)\cdot Hg^{II}+S_L^0,\end{aligned} \tag{S1}$$

where

- v_x, v_y and v_z are the components of the velocity field $[m/h]$;
- D_x and D_y are the horizontal turbulent diffusivities $[m^2/h]$;
- D_z is the vertical turbulent diffusivity $[m^2/h]$;
- k_{Ph-de} is the rate constant for the photo-demethylation of methyl-mercury $[1/h]$;
- k_1 is the rate constant for the photo-oxidation of elemental mercury $[1/h]$;
- k_2 is the rate constant for the photo-reduction of inorganic mercury $[1/h]$;
- k_3 is the rate constant for the biological oxidation of elemental mercury $[1/h]$;
- k_4 is the rate constant for the biological reduction of inorganic mercury $[1/h]$;
- S_L^0 is the direct loads of elemental mercury $[ng\cdot l^{-1}\cdot h^{-1}]$.

The integration domain of the PDEs is constituted by a mesh of 10 and 18 elements regularly spaced of 454.6 m in both x- and y-direction and of a variable number of vertical layers of 5 m depth in the z-direction. The mesh covers the whole Augusta Harbour and part of the adjacent coastal area. A fixed time step of 300 sec has been chosen to satisfy the several stability conditions and constrains associated to the adopted numerical method (Tveito and Winther, 1998).

The PDEs parameters are obtained according to Lehnherr et al. (2011), Melaku Canu et al. (2015) and Zhang et al. (2014), while the components of the velocity field are reproduced for the year 2011 by using the hydrodynamic 3D SHYFEM model (Umgiesser et al., 2004; Umgiesser, 2009). The horizontal and vertical turbulent diffusivities (Pacanowski and Philander, 1981; Denman and Gargett, 1983; Peters et al., 1988; Massel, 1999; Katz et al., 1979; Thi et al., 2005) are calibrated in order to fit the experimental data both for total and dissolved mercury concentrations in seawater and for the mercury fluxes at the 3D domain boundaries.

The photo-demethylation rate constant for methyl-mercury is fixed according to Melaku Canu et al. (2015). In the Section 3.1 of main text, the photochemical and biological redox reaction rate constants of Hg^0 and Hg^{II} use the parameterizations

of Strode et al. (2007), with updates Soerensen at al. (2010). Specifically, the photochemical oxidation and photochemical reduction first-order rate constants (k_1 and k_2) are directly proportional to the short-wave radiation flux (RAD) at the sea surface attenuated by dissolved organic carbon (DOC) and pigments in the surface ocean (C_{pig}) (Zhang et al., 2014; Soerensen et al., 2010; Qureshi et al., 2010; Batrakova et al., 2014). Also, the biological oxidation and biological reduction first-order rate constants (k_3 and k_4) are directly proportional to the organic carbon remineralization rate (OCRR) of the microbial reactions. Therefore, the photochemical and biological first-order rate constants are calculated as follows:

$$k_1 = k_{photo-ox} \cdot RAD(z,t), \tag{S2}$$

$$k_2 = k_{photo-red} \cdot RAD(z,t), \tag{S3}$$

$$k_3 = k_{bio-ox} \cdot OCRR(x,y,z,t), \tag{S4}$$

$$k_4 = k_{bio-red} \cdot OCRR(x,y,z,t), \tag{S5}$$

where $k_{photo-ox}$ and $k_{photo-red}$ are two constants reported by Soerensen at al. (2010) and according to Qureshi et al. (2010), k_{bio-ox} and $k_{bio-red}$ are two constants estimated by Zhang et al. (2014) using the experimental findings of the Hg^0 concentration and net evasion flux in the oceans. The short-wave radiation flux at the water surface ($RAD(0,t)$) is set up by using the remote sensing data (see the NASA web site http://eosweb.larc.nasa.gov/sse/RETScreen/). The RAD is assumed to decrease exponentially with the depth z, according to the Lambert-Beer's law, and to vary as a function of time t due to the seasonal oscillations of the incident radiation flux $RAD(0,t)$. The organic carbon remineralization rate ($OCRR(x,y,z,t)$), is calculated within ($z < z_0$) and out ($z > z_0$) the euphotic zone as follows:

$$OCRR(x,y,z,t) = \frac{NPP(x,y,z,t)}{z_0} \cdot (1 - peratio(x,y,z,t)), \quad if \quad z < z_0 \tag{S6}$$

where NPP is the net primary production $[g\ \ C \cdot m^{-2} \cdot h^{-1}]$ from MODIS satellite data obtained by the NP model, z_0 is the depth of euphotic zone $[m]$, $peratio$ is the ratio of the particulate organic carbon concentration (POC) export to NPP out of the euphotic zone $[dimensionless]$, $F_{POC}(z)$ is the sinking flux of POC $[g\ \ \cdot m^{-2} \cdot h^{-1}]$. Since the bathymetry of the Augusta Bay indicates that the water column depth in the whole basin is less than the theoretical euphotic zone depth ($z_0 = 75\ m$) fixed by Zhang et al.(2014), in our model we use only the equation for $z < z_0$ (Zhang et al., 2014). Here, the NPP is calculated by using the conversion equation for $chl\ a$ concentration (Baines et al., 1994), as follows:

$$log(NPP(x,y,z,t)) = 2.09 + 0.81 \cdot log(chl\ a(x,y,z,t)), \tag{S7}$$

where $chl\ a$ is the chlorophyll concentration $[mg \cdot m^{-3}]$ obtained by the NP model (see Section S4).
On the other hand, the $peratio$ is obtained by using the following equation (Zhang et al., 2014):

$$peratio(x,y,z,t) = -0.0081 \cdot T + 0.0806 \ln chl\ a(x,y,z,t) + 0.426, \tag{S8}$$

where T is the surface atmospheric temperature $[C]$ coming from remote sensing.

S1.1 Dissolved elemental mercury concentration

S1.1.1 Boundary conditions at the water-atmosphere interface - Dissolved elemental mercury concentration

The mercury flux at the water-atmosphere interface (z=0) is obtained by both the River Model and Bagnato et al. (2013), as follows:

$$\left[D_z \frac{\partial Hg^0}{\partial z} - v_z Hg^0\right]\Big|_{z=0} = Wetdep_{Hg^0} - \phi_{GEM} = \\ = \frac{Hg_{gas-atm} \cdot Pr}{\Delta t} + MTC_{water-atm} \cdot \left(Hg_{gas-atm} - H \cdot Hg^0|_{z=0}\right), \tag{S9}$$

where

- $Wetdep_{Hg^0}$ is the surface wet deposition flux (dry+wet) of gaseous mercury concentration $[ng \cdot m^{-2} \cdot h^{-1}]$;
- ϕ_{GEM} is the surface evasion flux of elemental mercury concentration $[ng \cdot m^{-2} \cdot h^{-1}]$;
- $Hg_{gas-atm}$ is the gaseous mercury concentration in the atmosphere as a function of time $[ng/l]$;
- Pr is the amount of precipitation as a function of time $[m]$;
- Δt is the exposition time of the basin $[h]$;
- $MTC_{water-atm}$ is the gas phase overall mass transfer coefficient $[m/h]$;
- H is the Henry's law constant $[dimensionless]$.

The temporal behaviour of $Hg_{gas-atm}$ is reproduced for one year by using the experimental data collected by IAS-CNR in 2011, and reported in a previous work (Bagnato et al., 2013). The dynamics of precipitations is obtained by using the remote sensing data on the average monthly precipitations in Augusta Bay (see the NASA web site http://eosweb.larc.nasa.gov/sse/RETScreen/). The $MTC_{water-atm}$ is calculated according to the River model (Ciffroy, 2015) as follows:

$$MTC_{water-atm} = \frac{MTC_{water-atm,w} \cdot MTC_{water-atm,g}}{MTC_{water-atm,w} + H \cdot MTC_{water-atm,g}}. \tag{S10}$$

Here, the water film mass transfer coefficient ($MTC_{water-atm,w}$) and the gas film mass transfer coefficient ($MTC_{water-atm,g}$) are given by:

$$MTC_{water-atm,w} = 0.108 \cdot (u_{wind})^{1.64} \cdot \left(\frac{PM_{CO_2}}{PM_{molar}}\right)^{0.25}, \tag{S11}$$

$$MTC_{water-atm,g} = 864 \cdot (0.2 \cdot u_{wind} + 0.3) \cdot \left(\frac{PM_{H_2O}}{PM_{molar}}\right)^{0.3}, \tag{S12}$$

where

- u_{wind} is the wind speed $[m/s]$;

- PM_{CO_2} is the molar mass of carbon dioxide $[g/mol]$;
- PM_{molar} is the molar mass of elemental mercury $[g/mol]$;
- PM_{H_2O} is the molar mass of water $[g/mol]$.

The wind speed is obtained by averaging the values of annual mean wind speed of the last 15 years for the studied area (see the NASA web site http://eosweb.larc.nasa.gov).

The annual mercury evasion flux at the seawater-atmosphere interface (V) is obtained by integrating the ϕ_{GEM} for the whole horizontal surface of the basin, and for the whole year. The annual atmospheric deposition of the elemental mercury is calculated by integrating the ϕ_{dep} for the whole horizontal surface of the basin, and for the whole year.

S1.1.2 Boundary conditions (lateral fluxes) - Dissolved elemental mercury concentration

The lateral fluxes for all variables are set up equal to zero at the boundaries of Augusta basin (Valenti et al., 2017) except where inlets rivers and sewerage are localized. Moreover, we can neglect the elemental mercury flux at the water-sediment interface ($z = z_b$). Therefore, we fix the following fluxes at the basin boundaries:

$$\left[D_x \frac{\partial Hg^0}{\partial x} - v_x Hg^0\right] = \left[D_y \frac{\partial Hg^0}{\partial y} - v_y Hg^0\right] = \left[D_z \frac{\partial Hg^0}{\partial z} - v_z Hg^0\right]\Big|_{z=z_b} = 0. \tag{S13}$$

Since the direct Hg^0 loads from rivers and sewerage are assumed to be negligible for the whole basin, we set:

$$\left[D_x \frac{\partial Hg^0}{\partial x} - v_x Hg^0\right] = INPUT_{x_{point-source}} = \left(\frac{Q_{source}}{A_{source}}\right)\Big|_x \cdot Hg^0_{source} \simeq 0, \tag{S14}$$

$$\left[D_y \frac{\partial Hg^0}{\partial y} - v_y Hg^0\right] = INPUT_{y_{point-source}} = \left(\frac{Q_{source}}{A_{source}}\right)\Big|_y \cdot Hg^0_{source} \simeq 0, \tag{S15}$$

where

- Q_{source} is the average flow rate of water at the point source $[m^3/h]$;
- A_{source} is the longitudinal section of the point source $[m^2]$;
- Hg^0_{source} is the elemental mercury concentration of the point source $[\mu g/m^3]$;
- $INPUT_{x_{point-source}}$ and $INPUT_{y_{point-source}}$ are the fluxes of elemental mercury $[\mu g \cdot m^{-2} \cdot h^{-1}]$ along x-direction and y-direction, respectively, entering the basin from the point source.

The lateral fluxes at inlets (Scirocco and Levante) of the basin (Salvagio Manta et al., 2016) as a function of depth and time are given by:

$$\begin{aligned}\phi^0_{x_{inlet}}(z,t) &= \left[D_x \tfrac{\Delta Hg^0}{\Delta x} - v_{x_{inlet}}(z,t) \cdot Hg^0_{ext}(z)\right] = \\ &= \left[D_x \tfrac{\Delta Hg^0}{\Delta x} + v_{x_{inlet}}(z,t) \cdot Hg^0_{int}(z,t)\right],\end{aligned} \tag{S16}$$

$$\phi^0_{y_{inlet}}(z,t) = \left[D_y \frac{\Delta Hg^0}{\Delta y} - v_{y_{inlet}}(z,t) \cdot Hg^0_{ext}(z)\right] = \\ = \left[D_y \frac{\Delta Hg^0}{\Delta y} + v_{y_{inlet}}(z,t) \cdot Hg^0_{int}(z,t)\right], \tag{S17}$$

where

- $v_{x_{inlet}}(z,t)$ is the absolute value of the marine currents velocity at the inlet along the x-direction $[m/h]$;
- $v_{y_{inlet}}(z,t)$ is the absolute value of the marine currents velocity at the inlet along the y-direction $[m/h]$;
- $Hg^0_{int}(z,t)$ ($Hg^0_{ext}(z)$) is the internal (external) dissolved elemental mercury concentrations close to the inlet $[\mu g/m^3]$;
- ΔHg^0 is the difference between the internal and external dissolved elemental mercury concentrations at the inlet of basin $[\mu g/m^3]$;
- $\phi^0_{x_{inlet}}(z,t)$ and $\phi^0_{y_{inlet}}(z,t)$ are the horizontal fluxes at the inlet $[\mu g \cdot m^{-2} \cdot h^{-1}]$.

The advection terms of Eqs. (S16)-(S17) are negative when the marine current velocities cause the external seawater to enter into the Augusta Bay, while they are positive when the marine current velocities cause the internal seawater to come out the basin.

The same boundary conditions (lateral fluxes) are also valid for Hg^{II} , $MeHg$ and Hg_T. The annual net outflow of elemental mercury from basin to open sea is obtained by integrating Eqs. (S16)-(S17) for the whole lateral surface of the two inlets, and for the whole year. Similarly, the annual net outflows of Hg^{II} and $MeHg$ are calculated.

In order to perform the mass balance for the Augusta Bay, we calculate the annual net outflow of total mercury (O) from the basin towards the open sea by considering both the spatio-temporal behaviour of total mercury concentration reproduced by the advection-diffusion-reaction model, and the marine currents velocities at the inlets calculated by the SHYFEM model (see Section S3).

S1.2 Dissolved inorganic mercury concentration

The dynamics of the dissolved inorganic mercury concentration (Hg^{II}) within the 3-D domain of the Augusta basin (Han et al., 2007; Whalin et al., 2007; Monperrus et al., 2007b; Zhang et al., 2014; Batrakova et al., 2014; Melaku Canu et al., 2015; Salvagio Manta et al., 2016) is described by the following PDE:

$$\frac{\partial Hg^{II}}{\partial t} = \\ + \frac{\partial}{\partial x}\left[D_x \frac{\partial Hg^{II}}{\partial x}\right] - \frac{\partial}{\partial x}(v_x Hg^{II}) + \frac{\partial}{\partial y}\left[D_y \frac{\partial Hg^{II}}{\partial y}\right] - \frac{\partial}{\partial y}(v_y Hg^{II}) \\ + \frac{\partial}{\partial z}\left[D_z \frac{\partial Hg^{II}}{\partial z}\right] - \frac{\partial}{\partial z}(v_z Hg^{II}) + (k_1 + k_3) \cdot Hg^0 - (k_2 + k_4) \cdot Hg^{II} - k_{me} \cdot Hg^{II} + k_{deme} \cdot MeHg \\ + S^{II}_L + S^{II}_{DOM} - S^{II}_{SPM}, \tag{S18}$$

where

- k_{me} is the rate constant for the methylation of inorganic mercury $[1/h]$;

- k_{deme} is the rate constant for the biotic demethylation of methyl-mercury $[1/h]$;
- S_L^{II} is the direct loads of the inorganic mercury $[ng \cdot l^{-1} \cdot h^{-1}]$;
- S_{DOM}^{II} is the load of the dissolved inorganic mercury released by the particulate organic matter $[ng \cdot l^{-1} \cdot h^{-1}]$;
- S_{SPM}^{II} is the sinking flux of the SPM-bound inorganic mercury $[ng \cdot l^{-1} \cdot h^{-1}]$.

The integration domain of the PDE is constituted by a mesh of 10 and 18 elements regularly spaced of 454.6 m in both x- and y-direction and of a variable number of vertical layers of 5 m depth in the z-direction. The mesh covers the whole Augusta Harbour and part of the adjacent coastal area. A fixed time step of 300 sec has been chosen to satisfy the several stability conditions and constrains associated to the adopted numerical method (Tveito and Winther, 1998).

The rate constants for the methylation of inorganic mercury and the biotic demethylation of methyl-mercury are fixed according to Lehnherr et al. (2011). The other rate constants of Eq. (S18) are defined in the section 1 (Zhang et al., 2014; Strode et al., 2007; Soerensen et al., 2010; Qureshi et al., 2010; Batrakova et al., 2014; Baines et al., 1994). S_L^{II}, S_{SPM}^{II} and S_{DOM}^{II} are defined in the Section 3.1 of the main paper.

The load of dissolved inorganic mercury released by particulate organic matter (S_{DOM}^{II}) is given by:

$$S_{DOM}^{II} = \quad \lambda \cdot m \cdot b \cdot PHg^{II}, \tag{S19}$$

where

- PHg^{II} is the inorganic mercury mass accumulated in each cell of picoeukaryotes $[\mu g/cell]$;
- b is the cell concentration of picoeukaryotes $[cell/m^3]$;
- m is the mortality of picoeukaryotes community $[h^{-1}]$

All parameters and variables of Eq. (S19) are defined in the Phytoplankton model and NP model (see sections 4 and 5) except λ, which is the mercury recycling coefficient for picoeukaryotes (Ciffroy, 2015; Dutkiewicz et al., 2009; Morozov et al., 2010; Valenti et al., 2012; Denaro et al., 2013a, c, b; Valenti et al., 2015, 2016a, b, c, 2017).

The adsorption rate of the suspended particulate matter for the dissolved inorganic mercury (S_{SPM}^{II}) is obtained by Zhang et al. (2014), as follows:

$$S_{SPM}^{II} = \quad -\frac{\partial}{\partial z}\left[NPP \cdot (peratio) \cdot \left(\frac{z}{z_0}\right)^{-0.9} \cdot \left(\frac{k_D}{f_{org}}\right) \cdot Hg^{II}(z)\right], \tag{S20}$$

where

- NPP is the net primary production $[mol \;\; C \cdot m^{-2} \cdot h^{-1}]$;
- $peratio$ is the ratio of particulate organic carbon (POC) export to NPP out of the euphotic zone $[dimensionless]$;
- k_D is the water-SPM partition coefficient for dissolved mercury $[l/Kg]$;

- f_{org} is the organic fraction of suspended particulate matter in dissolved-phase $[dimensionless]$, which takes on a different value in each position (x,y) of the domain;
- z_0 is the depth of euphotic zone $[m]$.

The NPP is set up by using the remote sensing data reported in previous work (D'Ortenzio, 2003). The spatial distribution of f_{org} is reproduced by using the SPOM and SPM concentrations measured in the Augusta Bay during the oceanographic survey of October 2017. The partition coefficient k_D is calibrated in such a way to obtain the best fit with the experimental data for total and dissolved mercury concentrations in the seawater compartment. The $peratio$ is calculated by using the following equation (Zhang et al., 2014):

$$peratio = -0.0081 \cdot T + 0.0806 \ln Chl + 0.426, \tag{S21}$$

where T is the surface atmospheric temperature (C) and Chl is the surface chlorophyll concentration ($mg\ m^{-3}$). The former is obtained from remote sensing data. The latter is set on the basis of the values measured in Augusta basin during the oceanographic survey of May 2011.

The dissolved inorganic mercury concentration as a function of depth ($Hg^{II}(z)$) is obtained by solving Eq. (S18). Since the sinking flux of the SPM-bound inorganic mercury (S^{II}_{SPM}) has to vanish at $z = 0$ due to the condition of "cleaned" SPM entering through the seawater surface, in the Eq. (S20) we fix the dissolved inorganic mercury concentration equal to zero at the seawater-atmosphere interface ($Hg^{II}(0) = 0$).

The annual amount of inorganic mercury removed by the suspended particulate along the water column (scavenging process) is obtained by integrating Eq. (S20) on the whole 3D domain of the Augusta Bay.

S1.2.1 Boundary conditions at the water-atmosphere interface - Dissolved inorganic mercury concentration

The inorganic mercury flux at the water-atmosphere interface (z=0) is calculated by the River Model and Bagnato et al. (2013), as follows:

$$\left[D_z \frac{\partial Hg^{II}}{\partial z} - v_z Hg^{II}\right]\Big|_{z=0} = Wetdep_{Hg^{II}} + Drydep_{Hg^{II}} = \frac{Hg^{II}_{atm} \cdot Pr}{\Delta t} + Drydep_{Hg^{II}}, \tag{S22}$$

where

- $Wetdep_{Hg^{II}}$ is the surface wet deposition flux of inorganic mercury $[ng \cdot m^{-2} \cdot h^{-1}]$;
- $Drydep_{Hg^{II}}$ is the surface dry deposition flux of inorganic mercury $[ng \cdot m^{-2} \cdot h^{-1}]$;
- Hg^{II}_{atm} is the inorganic mercury concentration in atmosphere as a function of time $[ng/m^3]$;
- Pr is the amount of precipitation as a function of time $[m]$;
- Δt is the exposition time of the basin $[h]$.

The time behaviour of the inorganic mercury concentration in atmosphere (Hg^{II}_{atm}) is reproduced for one year by using the experimental data collected reported in a previous work (Bagnato et al., 2013). The dynamics of precipitations is obtained by using the remote sensing data on the average monthly precipitations in Augusta Bay (see the NASA web site http://eosweb.larc.nasa.gov). The $Drydep_{Hg^{II}}$ is set equal to that estimated by Rajar et al. (2007) for the whole Mediterranean basin (Rajar et al., 2007).

The annual atmospheric deposition of the inorganic mercury is calculated by integrating Eq. (S22) for the whole horizontal surface of the basin and for the whole year. The annual total atmospheric mercury deposition (AD) is equal to the sum of the amounts of inorganic and elemental mercury deposited on the surface of the Augusta basin in one year.

S1.2.2 Boundary conditions at the water-sediment interface - Dissolved inorganic mercury concentration

The inorganic mercury flux at the water-sediment interface ($z = z_b$) is calculated as a function of time in each position (x,y) of the domain (River Merlin-Expo model, 2015):

$$\left[D_z \frac{\partial Hg^{II}}{\partial z} - v_z Hg^{II}\right]\Big|_{z=z_b} = MTC^{II}_{sed-water} \cdot \left(Hg^{II}_{pore-water} - Hg^{II}|_{z=z_b}\right), \tag{S23}$$

where

- $MTC^{II}_{sed-water}$ is the mass transfer coefficient for the inorganic mercury at the water-sediment interface $[m/h]$, which takes on a different value in each position (x,y) of the domain;
- $Hg^{II}_{pore-water}$ is the inorganic mercury concentration in the pore water of the shallowest layer of the sediment $[\mu g/m^3]$;
- $Hg^{II}|_{z=z_b}$ is the dissolved inorganic mercury concentration in the deepest layer of the seawater $[\mu g/m^3]$;
- z_b is the depth of the water column $[m]$ in each position (x,y).

The annual benthic flux of inorganic mercury ($B_{Hg^{II}}$) is obtained by integrating Eq. (S23) for the whole horizontal surface of the basin, and for the whole year.

The mass transfer coefficient for the inorganic mercury at the water-sediment interface ($MTC^{II}_{sed-water}$) (Ciffroy, 2015) is calculated as follows:

$$MTC^{II}_{sed-water} = \frac{D_{w-in} \cdot \varphi^{4/3}_{sed}}{\delta^{II}_{sed} + \delta_w \cdot \varphi^{4/3}_{sed}}, \tag{S24}$$

where

- D_{w-in} is the molecular diffusion coefficient for the inorganic mercury $[m^2/h]$;
- φ_{sed} is the porosity of the sediment $[dimensionless]$;
- δ^{II}_{sed} is the boundary layer thickness above the sediment for the inorganic mercury $[m]$;
- δ_w is the boundary layer thickness below sediment $[m]$.

The molecular diffusion coefficient is that reported by Schulz and Zabel (2006), while the porosity of the sediment is calculated using the values of specific weight and humidity reported in the study of ICRAM (2008). The *boundary layer thickness below the sediment* is obtained by the marine currents velocities at the seawater-sediment interface, according to previous works (Ciffroy, 2015; Sørensen et al., 2001). Finally, the *boundary layer thickness above the sediment for the inorganic mercury* is calibrated on the basis of benthic mercury fluxes measured close to the seabed during the oceanographic surveys of September 2011 and June 2012 (Salvagio Manta et al., 2016).

Unlike the mass transfer coefficient for the inorganic mercury at the water-sediment interface ($MTC^{II}_{sed-water}$), the mass transfer coefficient for the inorganic mercury within the sediment is estimated by considering an alternative mechanism for the mercury diffusion in the pore water, in accordance with recent works (Schulz and Zabel, 2006; Ogrinc et al., 2007). Initially we calculate the molecular diffusion coefficient for the inorganic mercury in the pore water of the sediment (D^{in}_{sed}) as follows (Boudreau, 1996; Ogrinc et al., 2007):

$$D^{in}_{sed} = \varphi_{sed} \cdot \frac{D_{w-in}}{\theta^2} = \frac{\varphi_{sed} \cdot D_{w-in}}{1 - ln(\varphi^2_{sed})}, \tag{S25}$$

where θ is the tortuosity of the sediment $[dimensionless]$, which is estimated from porosity using the equation by Boudreau (1996).

According to Oliveri et al. (2016), we calculate the inorganic mercury concentration in the pore water and the total mercury concentration in the sediment as a function of time, by using the following differential equations:

$$\begin{aligned} \frac{dHg^{II}_{pore-water}}{dt} &= +K_{demeth} \cdot MeHg_{pore-water} - K_{meth} \cdot Hg^{II}_{pore-water} + \frac{\partial}{\partial x}\left[D^{in}_{sed} \cdot \frac{\partial Hg^{II}_{pore-water}}{\partial x}\right] \\ &+ \frac{\partial}{\partial y}\left[D^{in}_{sed} \cdot \frac{\partial Hg^{II}_{pore-water}}{\partial y}\right] + \frac{\partial}{\partial z}\left[D^{in}_{sed} \cdot \frac{\partial Hg^{II}_{pore-water}}{\partial z}\right] - \frac{(1-f_{MeHg})}{K^{II}_d} \cdot \frac{dHg^{sed}_T}{dt} \\ \frac{dHg^{sed}_T}{dt} &= -\alpha \cdot Hg^{sed}_T \Rightarrow Hg^{sed}_T(t) = Hg^{sed}_T(0) \cdot exp(-\alpha \cdot t), \;\; with \;\; \alpha > 0, \end{aligned} \tag{S26}$$

where

- K_{demeth} is the rate constant for the de-methylation of methyl-mercury in the pore water of the sediment $[1/h]$;
- K_{meth} is the rate constant for the methylation of inorganic mercury in the pore water of the sediment $[1/h]$;
- $MeHg_{pore-water}$ is the methyl-mercury concentration in the pore water of the sediment $[\mu g/m^3]$;
- α is the de-adsorption rate (constant) for the total mercury concentration in the sediment $[1/h]$;
- f_{MeHg} is the fraction of methyl-mercury in the sediment $[dimensionless]$;
- K^{II}_d is the sediment-pore water distribution coefficient for the inorganic mercury $[l/Kg]$.

The rate constants of the first equation, except α, have been estimated for the Gulf of Trieste by Melaku Canu et al. (2015), while the fraction of methyl-mercury in the sediment has been measured during the oceanographic survey of October 2017. The sediment-pore water distribution coefficient for the inorganic mercury is calibrated, according to previous works (Melaku Canu

et al., 2015; Liu et al., 2012; Oliveri et al., 2016), in such a way to better reproduce the real inorganic mercury concentration measured in the pore water. Finally, the de-adsorption rate for the total mercury concentration and the sediment-pore water distribution coefficient for the inorganic mercury have been calibrated on the basis of the mercury concentration measured experimentally in the samples of pore water collected in May 2011 (Oliveri et al., 2016).

S1.2.3 Initial conditions for the inorganic mercury concentration in pore water

In general, the inorganic mercury concentration in pore water is estimated by the total mercury concentration (Hg_T^{sed}) and the sediment-pore water distribution coefficient (K_d^{II}) (Cossa and Coquery, 2005; Sunderland et al., 2006; Hines et al., 2012; Monperrus et al., 2007a). On this basis, we fix the initial condition (t=0) for the inorganic mercury concentration in pore water using the following equation:

$$Hg_{pore-water}^{II}(0) = (1 - f_{MeHg}) \cdot \frac{Hg_T^{sed}(0)}{K_d^{II}}, \tag{S27}$$

where $Hg_T^{sed}(0)$ is the total mercury concentration in the sediment at $t = 0$ (initial condition) $[mg/Kg]$, with different values in each position (x,y,z) of the domain. This is estimated in the 3D domain of the Augusta Bay by interpolating the experimental data collected by ICRAM during the oceanographic survey performed in the period 2005-2006 (ICRAM, 2008).

S1.2.4 Initial conditions for the total mercury concentration, specific weight and humidity in the sediments. Interpolation methods

The spatial distribution of total mercury, specific weight and percentage of the humidity of the sediments of the Augusta Bay were estimated within the whole study area in order to simulate mercury flux at the sediment/water interface and between sediment layers. The vertical profiles of these variables were interpolated through Inverse Distance Weighting (IDW) on transects of points of a mesh 18×10 with 454.6 m of distance between the nodes, able to cover the entire investigated area. The values corresponding to the nodes at depth 10 cm, 30 cm, 50 cm, 90 cm, 110 cm, 130 cm, 150 cm, 170 cm and 190 cm were extracted and included as input data in the mathematical model.

S1.2.5 Boundary conditions (lateral fluxes) - Dissolved inorganic mercury concentration

The Augusta basin can be considered as closed except for the inlets, rivers and sewerage (Valenti et al., 2017). Therefore, we fix the following lateral fluxes at the boundaries of the domain:

$$\left[D_x \frac{\partial Hg^{II}}{\partial x} - v_x Hg^{II}\right] = \left[D_y \frac{\partial Hg^{II}}{\partial y} - v_y Hg^{II}\right] = 0. \tag{S28}$$

For all points of basin where rivers and sewerage are localized, we set:

$$\left[D_x \frac{\partial Hg^{II}}{\partial x} - v_x Hg^{II}\right] = INPUT_{x_{point-source}} = \left(\frac{Q_{source}}{A_{source}}\right)\Big|_x \cdot Hg_{source}^{II} \simeq 0, \tag{S29}$$

$$\left[D_y \frac{\partial Hg^{II}}{\partial y} - v_y Hg^{II}\right] = INPUT_{y_{point-source}} = \left(\frac{Q_{source}}{A_{source}}\right)\Big|_y \cdot Hg_{source}^{II} \simeq 0, \tag{S30}$$

where

- Q_{source} is the average flow rate of water for the point source $[m^3/h]$;
- A_{source} is the longitudinal section of the point source $[m^2]$;
- Hg^{II}_{source} is the mercury concentration of the point source $[\mu g/m^3]$;
- $INPUT_{x_{point-source}}$ and $INPUT_{y_{point-source}}$ are the fluxes of inorganic mercury $[\mu g \cdot m^{-2} \cdot h^{-1}]$ along x-direction and y-direction, respectively, entering the basin from the point source.

The lateral fluxes of inorganic mercury concentration at inlets (Scirocco and Levante) of the basin (Salvagio Manta et al., 2016) as a function of depth and time are given by:

$$\phi^{II}_{x_{inlet}}(z,t) = \left[D_x \frac{\Delta Hg^{II}}{\Delta x} - v_{x_{inlet}}(z,t) \cdot Hg^{II}_{ext}(z)\right] = \\ = \left[D_x \frac{\Delta Hg^{II}}{\Delta x} + v_{x_{inlet}}(z,t) \cdot Hg^{II}_{int}(z,t)\right], \tag{S31}$$

$$\phi^{II}_{y_{inlet}}(z,t) = \left[D_y \frac{\Delta Hg^{II}}{\Delta y} - v_{y_{inlet}}(z,t) \cdot Hg^{II}_{ext}(z)\right] = \\ = \left[D_y \frac{\Delta Hg^{II}}{\Delta y} + v_{y_{inlet}}(z,t) \cdot Hg^{II}_{int}(z,t)\right], \tag{S32}$$

where

- $v_{x_{inlet}}(z,t)$ is the absolute value of the marine currents velocity at the inlet along the x-direction $[m/h]$;
- $v_{y_{inlet}}(z,t)$ is the absolute value of the marine currents velocity at the inlet along the y-direction $[m/h]$;
- $Hg^{II}_{int}(z)$ ($Hg^{II}_{ext}(z)$) is the internal (external) dissolved inorganic mercury concentrations close to the inlet $[\mu g/m^3]$;
- ΔHg^{II} is the difference between the internal and external dissolved inorganic mercury concentrations at the inlet of basin $[\mu g/m^3]$;
- $\phi^{II}_{x_{inlet}}(z,t)$ and $\phi^{II}_{y_{inlet}}(z,t)$ are the horizontal fluxes of inorganic mercury concentration at the inlet $[\mu g \cdot m^{-2} \cdot h^{-1}]$.

The advection terms of Eqs. (S31)-(S32) are negative when the marine current velocities cause the external seawater to enter the Augusta Bay, while they are positive when the marine current velocities cause the internal seawater to come out from the basin. The annual net outflow of inorganic mercury from basin to open sea is obtained by integrating Eqs. (S31)-(S32) for the whole lateral surface of the two inlets and for the whole year.

S1.3 Dissolved methyl-mercury concentration

On the basis of the overall equation for the mass conservation of the state variables in dissolved phase (Han et al., 2007; Whalin et al., 2007; Monperrus et al., 2007b; Zhang et al., 2014; Batrakova et al., 2014; Melaku Canu et al., 2015; Salvagio Manta

et al., 2016), the dynamics of dissolved methyl-mercury concentration ($MeHg$) within the 3-D domain of Augusta basin is described by the following PDE:

$$\begin{aligned}\frac{\partial MeHg}{\partial t} = & +\frac{\partial}{\partial x}\left[D_x\frac{\partial MeHg}{\partial x}\right]-\frac{\partial}{\partial x}(v_x MeHg)+\frac{\partial}{\partial y}\left[D_y\frac{\partial MeHg}{\partial y}\right]-\frac{\partial}{\partial y}(v_y MeHg)\\ & +\frac{\partial}{\partial z}\left[D_z\frac{\partial MeHg}{\partial z}\right]-\frac{\partial}{\partial z}(v_z MeHg)-k_{Ph-de}\cdot MeHg+k_{me}\cdot Hg^{II}\\ & +S_L^{MM}+S_{DOM}^{MM}-S_{SPM}^{MM},\end{aligned} \tag{S33}$$

where

- S_L^{MM} is the direct loads of methyl-mercury $[ng\cdot l^{-1}\cdot h^{-1}]$;
- S_{DOM}^{MM} is the load of dissolved methyl-mercury released by particulate organic matter $[ng\cdot l^{-1}\cdot h^{-1}]$;
- S_{SPM}^{MM} is the adsorption rate of suspended particulate matter for dissolved methyl-mercury $[ng\cdot l^{-1}\cdot h^{-1}]$.

The integration domain of the PDE is constituted by a mesh of 10 and 18 elements regularly spaced of 454.6 m in both x- and y-direction and of a variable number of vertical layers of 5 m depth in the z-direction. The mesh covers the whole Augusta Harbour and part of the adjacent coastal area. A fixed time step of 300 sec has been chosen to satisfy the several stability conditions and constrains associated to the adopted numerical method (Tveito and Winther, 1998).

The rate constants for the methylation of inorganic mercury and the biotic demethylation of methyl-mercury are fixed according to Lehnherr et al. (2011). The other rate constants of Eq. (S33) are defined in the section 1 (Zhang et al., 2014; Strode et al., 2007; Soerensen et al., 2010; Qureshi et al., 2010; Batrakova et al., 2014; Baines et al., 1994).

The load of dissolved methyl-mercury released by the particulate organic matter (S_{DOM}^{MM}) is given by:

$$S_{DOM}^{MM} = \lambda\cdot m\cdot b\cdot PMeHg, \tag{S34}$$

where

- $PMeHg$ is the methyl-mercury mass accumulated in each cell of picoeukaryotes $[\mu g/cell]$;
- b is the cell concentration of picoeukaryotes $[cell/m^3]$;
- m is the mortality of picoeukaryotes community $[h^{-1}]$.

All parameters and variables of Eq. (S34) are defined in the Phytoplankton model and NP model (see sections 4 and 5) except λ, which is the mercury recycling coefficient for picoeukaryotes (Ciffroy, 2015; Dutkiewicz et al., 2009; Morozov et al., 2010; Valenti et al., 2012; Denaro et al., 2013a, c, b; Valenti et al., 2015, 2016a, b, c, 2017).

The adsorption rate of the suspended particulate matter for the dissolved organic mercury (S_{SPM}^{MM}) is obtained in agrement with Zhang et al. (2014), as follows:

$$S_{SPM}^{MM} = -\frac{\partial}{\partial z}\left[NPP\cdot(peratio)\cdot\left(\frac{z}{z_0}\right)^{-0.9}\cdot\left(\frac{k_D}{f_{org}}\right)\cdot MeHg(z)\right], \tag{S35}$$

where

- NPP is the net primary production $[mol\ \ C \cdot m^{-2} \cdot h^{-1}]$;
- $peratio$ is the ratio of particulate organic carbon (POC) export to NPP out of the euphotic zone $[dimensionless]$;
- k_D is the water-SPM partition coefficient for the dissolved mercury $[l/Kg]$;
- z_0 is the depth of the euphotic zone $[m]$.

The NPP is set by using the remote sensing data reported in a previous work (D'Ortenzio, 2003). The spatial distribution of f_{org} is reproduced by using the SPOM and SPM concentrations measured in the Augusta Bay during the oceanographic survey of October 2017. The partition coefficient k_D is calibrated in such a way to obtain the best fit between theoretical results and experimental data for total and dissolved mercury concentrations in the seawater compartment. The $peratio$ is calculated by using Eq. (S21) (see section 1.2).

The dissolved methyl-mercury concentration as a function of depth ($MeHg(z)$) is obtained by solving Eq. (S33). Since the adsorption rate of the SPM for the dissolved methyl-mercury (S^{II}_{SPM}) has to vanish at $z = 0$ because of the condition of "cleaned" SPM entering at seawater surface, in the Eq. (S35) we fix the dissolved methyl-mercury concentration equal to zero at the seawater-atmosphere interface ($MeHg(0) = 0$).

The annual amount of methyl-mercury removed by the suspended particulate along the water column (scavenging process) is obtained by integrating Eq. (S35) on the whole 3D domain of the Augusta Bay, as well as for the inorganic mercury. The annual total mercury flux recycled for scavenging (S) is equal to the sum of the amounts of inorganic mercury and methyl-mercury adsorbed by the SPM along the water column in one year.

S1.3.1 Boundary conditions at the water-atmosphere interface - Dissolved methyl-mercury concentration

According to Mason et al. (2012), the methyl-mercury flux at the water-atmosphere interface (z=0) is estimated to be 0.5 % of total Hg deposition flux ($\simeq 0.5\%$ of Hg^{II} deposition flux). Therefore, in our model we set:

$$\left[D_z \frac{\partial MeHg}{\partial z} - v_z MeHg\right]\Big|_{z=0} = Wetdep_{MeHg} + Drydep_{MeHg} = 0.005 \cdot \left[D_z \frac{\partial Hg^{II}}{\partial z} - v_z Hg^{II}\right]\Big|_{z=0}, \tag{S36}$$

where

- $Wetdep_{MeHg}$ is the surface wet deposition flux of methyl-mercury $[ng \cdot m^{-2} \cdot h^{-1}]$;
- $Drydep_{MeHg}$ is the surface dry deposition flux of contaminated particles $[ng \cdot m^{-2} \cdot h^{-1}]$;

The methyl-mercury concentration in atmosphere ($MeHg_{atm}$) is assumed to be equal to zero for the whole year, according to Driscoll et al.(2013). The dynamics of precipitations is obtained by using the remote sensing data on the average monthly precipitations in Augusta Bay (see the NASA web site http://eosweb.larc.nasa.gov).

The annual atmospheric deposition of the methyl-mercury is set equal to zero since the methyl-mercury concentration in atmosphere ($MeHg_{atm}$) is assumed negligible.

The annual atmospheric deposition of the methyl-mercury is calculated by integrating Eq. (S36) for the whole horizontal

surface of the basin and for the whole year. The annual total atmospheric mercury deposition (AD) is equal to the sum of the amounts of elemental, inorganic and methyl mercury deposited on the surface of the Augusta basin in one year.

S1.3.2 Boundary conditions at the water-sediment interface - Dissolved methyl-mercury concentration

The methyl-mercury flux at the water-sediment interface ($z = z_b$) is calculated as a function of time in each position (x,y) of the domain (River Merlin-Expo model, 2015) (Covelli et al., 2008; Ciffroy, 2015):

$$\left[D_z \frac{\partial MeHg}{\partial z} - v_z MeHg\right]\Big|_{z=z_b} = MTC^{MM}_{sed-water} \cdot (MeHg_{pore-water} - MeHg|_{z=z_b}), \tag{S37}$$

where

- $MTC^{MM}_{sed-water}$ is the mass transfer coefficient for the methyl-mercury at the water-sediment interface $[m/h]$, which takes on a different value in each position (x,y) of the domain;
- $MeHg_{pore-water}$ is the methyl-mercury concentration in the pore water of the shallowest layer of the sediment $[\mu g/m^3]$;
- $MeHg|_{z=z_b}$ is the dissolved methyl-mercury concentration in the deepest layer of seawater $[\mu g/m^3]$;
- z_b is the depth of the water column $[m]$ in each position (x,y).

The annual benthic flux of methyl-mercury (B_{MeHg}) is obtained by integrating Eq. (S37) for the whole horizontal surface of the basin and for the whole year. The annual mercury benthic flux (B) is equal to the sum of the amounts of inorganic mercury and methyl-mercury released from the sediments of the Augusta Bay in one year.

The mass transfer coefficient for the methyl-mercury at the water-sediment interface ($MTC^{MM}_{sed-water}$) (Ciffroy, 2015) is calculated as follows:

$$MTC^{MM}_{sed-water} = \frac{D_{w-or} \cdot \varphi_{sed}^{4/3}}{\delta^{MM}_{sed} + \delta_w \cdot \varphi_{sed}^{4/3}}, \tag{S38}$$

where

- D_{w-or} is the molecular diffusion coefficient for the methyl-mercury $[m^2/h]$;
- φ_{sed} is the porosity of the sediment $[dimensionless]$;
- δ^{MM}_{sed} is the boundary layer thickness above the sediment for the methyl-mercury $[m]$;
- δ_w is the boundary layer thickness below the sediment $[m]$.

The molecular diffusion coefficient is that reported by Schulz and Zabel (2006), while the porosity of the sediment is calculated by using the values of specific weight and humidity reported in the study of ICRAM (2008). The *boundary layer thickness below the sediment* is obtained by the marine currents velocities at the seawater-sediment interface, according to the previous

works (Ciffroy, 2015; Sørensen et al., 2001). Finally, Here, the *boundary layer thickness above the sediment for the methyl-mercury* is calibrated on the basis the methyl-mercury concentration measured close to the seabed during the oceanographic surveys of October 2017.

The molecular diffusion coefficient for methyl-mercury is calculated similarly to that for inorganic mercury (see Eq. (S25) of Section 1.2.2). Unlike the mass transfer coefficient for the methyl-mercury at the water-sediment interface ($MTC^{MM}_{sed-water}$), the mass transfer coefficient for the methyl-mercury in sediment is estimated by considering an alternative mechanism for the mercury diffusion in the pore water, in agreement with recent works (Schulz and Zabel, 2006; Ogrinc et al., 2007). Therefore, initially we calculate the molecular diffusion coefficient for the methyl-mercury in the pore water of the sediment (D^{or}_{sed}) as follows (Boudreau, 1996; Ogrinc et al., 2007):

$$D^{or}_{sed} = \varphi_{sed} \cdot \frac{D_{w-or}}{\theta^2} = \frac{\varphi_{sed} \cdot D_{w-or}}{1 - ln(\varphi^2_{sed})}, \tag{S39}$$

where θ is the tortuosity of the sediment $[dimensionless]$, which is estimated from porosity using the equation by Boudreau (1996).

Than, according to Oliveri et al. (2016), we calculate the methyl-mercury concentration in the pore water and the total mercury concentration in the sediment as a function of time, by considering the molecular diffusion within the sediment, as follows:

$$\begin{aligned} \frac{dMeHg_{pore-water}}{dt} &= -K_{demeth} \cdot MeHg_{pore-water} + K_{meth} \cdot Hg^{II}_{pore-water} + \frac{\partial}{\partial x}\left[D^{or}_{sed} \cdot \frac{\partial MeHg_{pore-water}}{\partial x}\right] \\ &+ \frac{\partial}{\partial y}\left[D^{or}_{sed} \cdot \frac{\partial MeHg_{pore-water}}{\partial y}\right] + \frac{\partial}{\partial z}\left[D^{or}_{sed} \cdot \frac{\partial MeHg_{pore-water}}{\partial z}\right] - \frac{f_{MeHg}}{K^{MM}_d} \cdot \frac{dHg^{sed}_T}{dt} \\ \frac{dHg^{sed}_T}{dt} &= -\alpha \cdot Hg^{sed}_T \Rightarrow Hg^{sed}_T(t) = Hg^{sed}_T(0) \cdot exp(-\alpha \cdot t), \;\; with \;\; \alpha > 0, \end{aligned} \tag{S40}$$

where

- K_{demeth} is the rate constant for the de-methylation of methyl-mercury in the pore water of the sediment $[1/h]$;
- K_{meth} is the rate constant for the methylation of inorganic mercury in the pore water of the sediment $[1/h]$;
- $Hg^{II}_{pore-water}$ is the inorganic mercury concentration in the pore water of the sediment $[\mu g/m^3]$;
- α is the de-adsorption rate (constant) for the total mercury concentration in the sediment $[1/h]$;
- f_{MeHg} is the fraction of the methyl-mercury in the sediment $[dimensionless]$;
- K^{MM}_d is the sediment - pore water distribution coefficient for methyl-mercury $[l/Kg]$.

The rates of the first equation, except α, have been estimated for the Gulf of Trieste by Melaku Canu et al. (2015), while the fraction of the methyl-mercury in the sediment has been measured during the oceanographic survey of October 2017.

Here, the rate constants, the de-adsorption rate and the fraction of the methyl-mercury are the same of Eq. (S26) (see Section 1.2.2), while the sediment-pore water distribution coefficient for the methyl-mercury is fixed equal to the square root of the distribution coefficient for the inorganic mercury, according to Liu et al. (2012). Finally, the sediment-pore water distribution coefficient for the methyl-mercury is calibrated on the basis of the mercury concentration measured experimentally in the samples of the pore water collected in May 2011 (Oliveri et al., 2016).

S1.3.3 Initial conditions for methyl-mercury concentration in the pore water

In general, the methyl-mercury concentration in the pore water is estimated by the total mercury concentration (Hg_T^{sed}) and the sediment-pore water distribution coefficient (K_d^{MM}) (Cossa and Coquery, 2005; Sunderland et al., 2006; Hines et al., 2012; Monperrus et al., 2007a). On this basis, we fix the initial condition (t=0) for the methyl-mercury concentration in the pore water by using the following equation:

$$MeHg_{pore-water}(0) = f_{MeHg} \cdot \frac{Hg_T^{sed}(0)}{K_d^{MM}}. \tag{S41}$$

where $Hg_T^{sed}(0)$ is the total mercury concentration in the sediment at t=0 (initial condition) $[mg/Kg]$, which takes on a different value in each position (x,y,z) of the domain. This is estimated in the 3D domain of the Augusta Bay by interpolating the experimental data collected by ICRAM during the oceanographic survey performed in the period 2005-2006 (ICRAM, 2008) (see section 1.2.2.2).

S1.3.4 Boundary conditions (lateral fluxes) - Dissolved methyl-mercury concentration

The Augusta basin can be considered as closed except for the inlets, rivers and sewerage (Valenti et al., 2017). Therefore, we fix the following lateral fluxes at boundaries of the domain:

$$\left[D_x \frac{\partial MeHg}{\partial x} - v_x MeHg\right] = \left[D_y \frac{\partial MeHg}{\partial y} - v_y MeHg\right] = 0, \tag{S42}$$

For all points of the basin where rivers and sewerage are localized, we set:

$$\left[D_x \frac{\partial MeHg}{\partial x} - v_x MeHg\right] = INPUT_{x_{point-source}} = \left(\frac{Q_{source}}{A_{source}}\right)\Big|_x \cdot MeHg_{source} \simeq 0, \tag{S43}$$

$$\left[D_y \frac{\partial MeHg}{\partial y} - v_y MeHg\right] = INPUT_{y_{point-source}} = \left(\frac{Q_{source}}{A_{source}}\right)\Big|_y \cdot MeHg_{source} \simeq 0, \tag{S44}$$

where

- Q_{source} is the average flow rate of water at the point source $[m^3/h]$;
- A_{source} is the longitudinal section of the point source $[m^2]$;
- $MeHg_{source}$ is the methyl-mercury concentration of the point source $[\mu g/m^3]$;
- $INPUT_{x_{point-source}}$ and $INPUT_{y_{point-source}}$ are the fluxes of mercury $[\mu g \cdot m^{-2} \cdot h^{-1}]$ along x-direction and y-direction, respectively, entering the basin from the point source.

The lateral fluxes of the methyl-mercury concentration at the inlets (Scirocco and Levante) of the basin (Salvagio Manta et al., 2016) as a function of depth and time are given by:

$$\begin{aligned} \phi_{x_{inlet}}^{MM}(z,t) &= \left[D_x \frac{\Delta MeHg}{\Delta x} - v_{x_{inlet}}(z,t) \cdot MeHg_{ext}(z)\right] = \\ &= \left[D_x \frac{\Delta MeHg}{\Delta x} + v_{x_{inlet}}(z,t) \cdot MeHg_{int}(z,t)\right]), \end{aligned} \tag{S45}$$

$$\phi^{MM}_{y_{inlet}}(z,t) = \left[D_y \frac{\Delta MeHg}{\Delta y} - v_{y_{inlet}}(z,t) \cdot MeHg_{ext}(z)\right] = \\ = \left[D_y \frac{\Delta MeHg}{\Delta y} + v_{y_{inlet}}(z,t) \cdot MeHg_{int}(z,t)\right]), \tag{S46}$$

where

- $v_{x_{inlet}}(z,t)$ is the absolute value of the marine currents velocity at the inlet along the x-direction $[m/h]$;
- $v_{y_{inlet}}(z,t)$ is the absolute value of the marine currents velocity at the inlet along the y-direction $[m/h]$;
- $MeHg_{int}(z,t)$ ($MeHg_{ext}(z)$) is the internal (external) dissolved methyl-mercury concentrations close to the inlet $[\mu g/m^3]$;
- $\Delta MeHg$ is the difference between the internal and external dissolved methyl-mercury concentrations at the inlet of the basin $[\mu g/m^3]$;
- $\phi^{MM}_{x_{inlet}}(z,t)$ and $\phi^{MM}_{y_{inlet}}(z,t)$ are the horizontal fluxes of methyl-mercury concentration at the inlet $[\mu g \cdot m^{-2} \cdot h^{-1}]$.

The advection terms of Eqs. (S45)-(S46) are negative when the marine current velocities cause the external seawater to enter the Augusta Bay, while they are positive when the marine current velocities cause the internal seawater to come out from the basin. The annual net outflow of methyl-mercury from basin to open sea is obtained by integrating Eqs. (S45)-(S46) for the whole lateral surface of the two inlets and for the whole year.

In the same way, we obtain the annual net outflow of total mercury (O) from the basin towards the open sea by considering both the spatio-temporal behaviour of total mercury concentration reproduced by the advection-diffusion-reaction model, and the marine currents velocities at the inlets calculated by the SHYFEM model (see section 3).

S2 SPM concentration

The dynamics of the suspended particulate matter (SPM) concentration takes into account the physical processes investigated in the River model (Ciffroy, 2015; Melaku Canu et al., 2015; Neumeier et al., 2008; Ferrarin et al., 2008). The effects on the SPM dynamics are described by the following PDE:

$$\frac{\partial SPM}{\partial t} = + \frac{\partial}{\partial x}\left[D_x \frac{\partial SPM}{\partial x}\right] - \frac{\partial}{\partial x}(v_x \cdot SPM) + \frac{\partial}{\partial y}\left[D_y \frac{\partial SPM}{\partial y}\right] - \frac{\partial}{\partial y}(v_y \cdot SPM) \\ + \frac{\partial}{\partial z}\left[D_z \frac{\partial SPM}{\partial z}\right] - \frac{\partial}{\partial z}(v_z \cdot SPM) - \frac{\partial}{\partial z}(w_s \cdot SPM) + S_L^{SPM}, \tag{S47}$$

where

- w_s is the settling velocity of particles $[m/h]$;
- S_L^{SPM} is the direct loads of suspended particulate matter $[\mu g/m^3]$.

Since the direct loads of SPM (Ciffroy, 2015; Melaku Canu et al., 2015) for the Augusta basin were unknown, the SPM concentration dynamics could not be reproduced correctly. Therefore,

In this work, we reproduced the spatial distribution of SPM and POM concentration at the steady state by interpolating the experimental data observed in recent samplings (October 2017) performed in the site investigated. From a mathematical point of view, the stationarity condition for the SPM concentration is described as follows:

$$\frac{\partial SPM}{\partial t} = 0. \tag{S48}$$

Moreover, we recall that the boundary conditions are not taken into account when the steady state condition is set.

Specifically, the SPM and POM values obtained in the sampling stations at the surface and bottom layers were linearly interpolated on the z-direction, in such a way to get different values for each vertical layer. Then, for each batimetry, on the x-y plane, the SPM value of each node of the grid has been determined as the weighted sum of the station values, with weight coefficients set as the inverse square distances of node centroids from the stations.

In general, the used setting is acceptable because the net flux of particles, due to the settling and the resuspension processes, is negligible according to a preliminary analysis performed by IAS-CNR (Oristano).

The experimental SPM and POM concentrations were used to reproduce the spatial distribution of the fraction of suspended particulate matter as organic carbon (f_{oc}), which was necessary to obtain the sinking fluxes of Hg^{II} and $MeHg$ (Zhang et al., 2014). Afterwards, the SPM concentrations were used to calculate the $[Hg_T]$ in seawater (see Section 3.1).

S2.1 SPM, SPIM and POM concentration

According to Zhang et al. (2014) and Rosati et al. (2018), the suspended particulate matter was defined as follows:

$$SPM = SPIM + POM, \tag{S49}$$

where

- $SPIM$ is the Suspended Particulate Inorganic Matter concentration $[ng/l]$;
- POM is the Suspended Particulate Organic Matter concentration $[ng/l]$.

Specifically, the particulate organic matter (POM) in dissolved-phase and the suspended particulate inorganic matter (SPIM) were given by:

$$POM = f_{org} \cdot SPM, \tag{S50}$$

$$SPIM = (1 - f_{org}) \cdot SPM, \tag{S51}$$

where

- f_{org} is the organic fraction of suspended particulate matter $[dimensionless]$.

Since we assumed that 52% of organic matter was carbon (Strode et al., 2010), the fraction of suspended particulate matter as organic carbon was calculated by using the following equation:

$$f_{oc} = 0.52 \cdot f_{org} = 0.52 \cdot \frac{POM}{SPM} \tag{S52}$$

S3 The 3D hydrodynamic model

A three-dimensional, finite element hydrodynamic model, SHYFEM (Umgiesser et al., 2004) was adopted to reproduce the tide and wind induced water circulation, and the sediment transport processes in Augusta Harbour and adjacent coastal area. The model resolves, for each layer, the vertically integrated shallow water equations in their formulation with water levels and transport terms. It was applied with success to reproduce the main hydrodynamics in gulfs, harbours, lagoons and coastal seas (Cucco et al., 2012; Umgiesser et al., 2014; Ferrarin et al., 2014; Cucco et al., 2016a; Farina et al., 2018). The model uses finite elements for horizontal spatial discretizations, z-layers for vertical discretizations and a semi-implicit algorithm for integration in time. It accounts for barotropic, baroclinic and atmospheric pressure gradients as well as wind drag and bottom friction, non-linear advection and vertical turbulent processes. The solved equation system reads as:

$$\begin{gathered}
\frac{\partial U_l}{\partial t} + Adv_l^x - fV_l = gh_l \frac{\partial \zeta}{\partial x} - \frac{gh_l}{\rho_0}\frac{\partial}{\partial x}\int_{-H_l}^{\zeta} \rho' dz + \frac{h_l}{\rho_0}\frac{\partial p_a}{\partial x} + \frac{1}{\rho_0}\left(\tau_x^{top(l)} - \tau_x^{bot(l)}\right) + A_H\left(\frac{\partial^2 U_l}{\partial x^2} + \frac{\partial^2 U_l}{\partial y^2}\right), \\
\frac{\partial V_l}{\partial t} + Adv_l^y - fU_l = gh_l \frac{\partial \zeta}{\partial y} - \frac{gh_l}{\rho_0}\frac{\partial}{\partial y}\int_{-H_l}^{\zeta} \rho' dz + \frac{h_l}{\rho_0}\frac{\partial p_a}{\partial y} + \frac{1}{\rho_0}\left(\tau_y^{top(l)} - \tau_y^{bot(l)}\right) + A_H\left(\frac{\partial^2 V_l}{\partial x^2} + \frac{\partial^2 V_l}{\partial y^2}\right), \\
\frac{\partial \zeta}{\partial t} + \sum_l \frac{\partial U_l}{\partial x} + \sum_l \frac{\partial V_l}{\partial y},
\end{gathered} \tag{S53}$$

where l indicates the vertical layer, (U_l, V_l) the horizontal transport components in x- and y- directions for each layer l, Adv_l^x and Adv_l^y the advective terms for each layer l, p_a the atmospheric pressure, g the gravitational constant, f the Coriolis parameter, ζ the water level, ρ_0 the standard water density, ρ' the water density, h_l the layer thickness, H_l the depth of the bottom of the layer l, $\tau_x^{top(l)}$ and $\tau_x^{bot(l)}$ the stress terms in the x-direction at the top and bottom of each layer l, $\tau_y^{top(l)}$ and $\tau_y^{bot(l)}$ the stress terms in the y-direction at the top and bottom of each layer l, A_h the horizontal eddy viscosity. For the computation of the vertical diffusivities and viscosities, the General Ocean Turbulence Model (GOTM), described in Burchard and Petersen (1999), was used. Wind and bottom friction terms, corresponding to the boundary conditions of the stress terms (τ_x,τ_y), are defined as:

$$\begin{aligned}
\tau_x^{surface} &= C_D \rho_a w_x \sqrt{w_x^2 + w_y^2}, \\
\tau_x^{bottom} &= C_B \rho_0 u_L \sqrt{u_L^2 + v_L^2}, \\
\tau_y^{surface} &= C_D \rho_a w_y \sqrt{w_x^2 + w_y^2}, \\
\tau_y^{bottom} &= C_B \rho_0 v_L \sqrt{u_L^2 + v_L^2},
\end{aligned} \tag{S54}$$

where C_D is the wind drag coefficient, C_B the bottom friction coefficient, ρ_a the air density, (w_x, w_y) the wind velocity components and (u_L, v_L) the bottom velocity components.

The hydrodynamic model is coupled with a sediment transport module that simulates the erosion, deposition and resuspension of both cohesive and non-cohesive sediments at the sea-bottom induced by the currents.

Specifically, as a first step, the sediment transport model computes the bed shear stress at the bottom boundary layer induced by the marine currents, to reproduce the re-suspension and the bed-load processes. Afterwards, the model calculates the suspended sediment concentration carried for advection and diffusion in the seawater. By this way, the rate of erosion and deposition are obtained for each nodes of the hydrodynamic finite element mesh.

The reader can refer to Umgiesser et al. (2004) and to Ferrarin et al. (2008) for a detailed description of the hydrodynamic and sediment transport model equations and the adopted numerical methods and parameterization.

S3.1 Hydrodynamic model and simulations setup

The model domain was defined between the 15.05^o E and 15.55^o E and between the 36.95^o N and 37.35^o N, including the Augusta Harbuor, the surrounding coastal areas and part of the Western Ionian Sea.

A finite element mesh composed by 21379 nodes and 40486 triangular elements with a spatial resolution varying between 20 meters for the inner harbour and few km for the far field was used for the horizontal discretization. The vertical direction was defined by 22 z-levels with layer depths ranging between 5 m and 200 m, by following an ad-hoc step distribution. The model temporal integration was set as variable in time and limited to a Courant number equal to 0.5, with time steps generally around 20 seconds.

The data used to reproduce the model bathymetry were obtained integrating the large-scale GEBCO dataset (http://www.gebco.net) with data obtained from the digitalization of the nautical charts describing the Augusta Harbour and surrounding coastal areas. In Fig.S6, the bathymetry and part of the finite element mesh reproducing the Augusta Bay and surrounding areas are shown.

The model was applied to reproduce the tide and wind induced water circulation, and the sediment transport during a ten years period between January 2007 and December 2017.

Baroclinic density gradients were neglected, being the interested coastal area not influenced by intense river inflows. The density vertical distribution was set as homogeneous and the GOTM (Burchard and Petersen, 1999) was used to reproduce the momentum transfer between each layers without any constrain related to the buoyancy variability along the vertical. The use of un-stratified model setup is generally acceptable if the interested domain is not affected by estuarine processes (Spydell et al., 2015; Cucco et al., 2016b). Therefore, wind and tide were set as the only external forcings promoting the water circulation in the harbour and surrounding coastal area. A similar approach was followed in several studies aimed at investigating the water circulation in bays, lagoons and harbours of the Mediterranean Sea, typically characterized by an extended shelf area and by the absence of intense fresh water inputs.

The wind data produced by the high-resolution non-hydrostatic meteorological prediction system SKIRON (Kallos and Pytharoulis, 2005) were used as model inputs. In particular, hourly fields of wind speeds and directions, obtained for the whole 10 years period and for the interested area with a spatial resolution of 0.008^o, were considered as model surface forcings. In addition, water elevation data were imposed along the model open boundary, corresponding to the open sea mesh border, following a Dirichlet condition. Adopted water level data consisted in hourly time series of tidal elevation. These data were obtained, for

the whole considered period, from the global tidal model OTIS (http://volkov.oce.orst.edu/tides/otis.html). Common values of the main model parameters C_D and C_B (see Eq. (S54)) were imposed (Cucco et al., 2019) and a 10 years simulation run was carried out to reproduce the wind and tide induced water circulation inside the harbour at different vertical levels.

The sediments grain size variability at the sea bottom was reproduced using experimental data acquired during two previous samplings (May 2011 and June 2012). The grain sizes vary between 600 μm and 50 μm indicating a sea bottom constituted by sands, silt and very fine silt.

The model results consisted both in hourly fields of the horizontal components of the current velocities computed at the surface level, between 0 and 5 m, and at deeper layers, between 5 and 10 m, 10 and 20 m, and 20 and 30 m, and hourly datasets of eroded and deposed volumes of sediments for each nodes of the finite element mesh along the whole simulation run. These data were subsequently processed to be used as input data for the biogeochemical model. As first step, a three-hours time averaged velocity field was derived from a time average procedure by using the SHYFEM model output produced at hourly frequency. Afterwards, the dataset of three hourly velocity field was used as input data for the second step of re-processing. In particular, an interpolation procedure based on the Laplacian method was applied to regrid the SHYFEM model outputs (obtained on an unstructured mesh) on the biogeochemical model computational grid. In Fig.S7, a snapshot of the horizontal components of the current velocities, obtained for the four selected vertical layers, are shown along with the points constituting the biogeochemical model computational regular mesh.

The results obtained from the interpolation procedure consist in three hourly sequences of the horizontal components of the current speed and of the eroded/deposed volumes of sediments. These values, calculated for a period of one year (from January 2011 to December 2011) at each point of the biogeochemical model grid, were used as input data to simulate the transport of the pollutants in the Augusta Bay.

S3.2 Hydrodynamic model validation

In shallow waters the hydrodynamic is mainly driven and influenced by several elements, including bathymetry, tidal oscillations, wind fields or density gradient. The latter contribution assumes a significant impact only when large freshwater inflow or thermal differences occur in the region (Van Rijn, 2011). In the Augusta bay, due to the seasonal and discontinuous riverine discharges, the contribution of freshwater inputs to spatial density gradients generation is negligible. Furthermore, the homogeneous and shallow bathymetry and the relatively small extent of the bay led to suppose that the spatial variability of the water temperature is not significant and therefore not strongly influencing the water circulation. This hypothesis is confirmed by Lisi et al. (2009), which suggests that the water circulation in the Augusta bay is influenced mainly by tides and wind and the harbour can be investigated as a lagoon (Lisi et al., 2009). In De Marchis et al. (2014) a modelling study of the water circulation of the Augusta bay was performed. A high resolution hydrodynamic model was applied to the harbour area and the wind and tide induced three-dimensional water circulation was investigated with success. The absence of available experimental data on water currents or tidal elevation led to compare SHYFEM model results with the numerical results obtained by De Marchis et al. (2014).

In order to make the two numerical applications comparable, SHYFEM was applied to reproduce the wind and tide induced

water circulation during the same investigated period and adopting the same atmospheric forcing of De Marchis et al. (2014). Specifically, a graph digitizing software was applied to extract the wind speed components to be used as SHYFEM model forcing whereas the tidal data obtained from OTIS tidal model for the reference period was used as model open boundary conditions.

A simulation run was then performed using the same parameter setup of the previous 10 years simulation run with the exception of the model vertical discretization which was slightly modified setting the first layers depths to 0.5 m. A spin up time of about 2 months was used to reduce the impact of the initial state conditioning and the three-dimensional water circulation was reproduced between the 10^{th} and the 16^{th} of October 2006. In Fig.S8 the model results for the surface (upper panels) and deeper layer water circulation (lower panels) are reported for the same time instants of Fig.10 and 11 of De Marchis et al. (2014) which correspond to the 13^{th} October 2006 at 16:00 and the 14^{th} October 2006 at 15:00. For both the time instants the wind speed is quite low, around 2.5 m/s and the wind directions are from Northwest in left panels and from Northeast in the right panels. The computed surface currents (upper panels of Fig.S8) follow the wind directions slightly bending rightward due to the Coriolis force. In the left panel, the surface flow varies between few cm/s along the bay perimeter up to around 10 to 12 cm/s in correspondence of the eastern mouth. In the right panel the surface current speed is quite homogeneous within the bay with values around 10 cm/s and peaks of 13 cm/s computed in the south central part of the harbour. The obtained flow patterns are quite similar to the ones reported in De Marchis et al. (2014), which, in the first case, reported a south-eastward surface flow with current speeds increasing toward the eastern bay inlet up to 12-13 cm/s (see panel C of Fig.10 in De Marchis et al. (2014)) and, in the second case, a south-westward surface flow mainly homogeneous and slightly increasing up to 13-14 cm/s in the southern part of the bay (see panel C of Fig.11 in De Marchis et al. (2014)). The same analogy is found for deeper layer flow fields computed for both the time instants, see lower panels of Fig.S8. In particular, in the left bottom panel, the sub-surface flow is varying in intensities, with peak speeds up to 3-4 cm/s in the central part of the bay, and in directions, from northward to north-eastward. In the right bottom panel, the current field is mainly directed north-westward and the speed is varying similarly to previous case. Comparing the obtained results with ones from previous application (see panels F of Fig.10 and 11 in De Marchis et al. (2014)), even the deeper layers current flows are similarly reproduced by the two numerical applications.

This analysis compensates the absence of experimental data to be used as reference for quantitative model results evaluation. The small differences between the flow patterns obtained from the two applications can arise from many aspects including the different adopted numerical models and methods and the different vertical discretizations of the model domain. Furthermore, the analysed time period, early October, allow to strength the hypothesis of Lisi et al. (2009) about the lagoon-type water circulation in the Augusta bay. In fact, in De Marchis et al. (2014), not only the baroclinic contribution was neglected but also the thermal stratification effects on the water circulation was not considered. Therefore, the success in modelling the bay hydrodynamic during early October and with relatively low wind speeds, when, in the southern Mediterranean areas the summer stratification still exist, indicates that, for this study case, the use of an un-stratified model approach can be acceptable.

S4 The advection-diffusion-reaction model for the picoeukaryotes community

Our study includes the analysis of the abundance of picoeukaryotes community (i.e. phytoplanktonic eukaryotes with size less than 3 μm), which represents the set of most representative populations of the Augusta Bay. In particular, we investigate the dynamics of the primary production of phytoplankton biomass by using an advection-diffusion-reaction model (Dutkiewicz et al., 2009; Morozov et al., 2010; Valenti et al., 2012; Denaro et al., 2013a, c, b; Valenti et al., 2015, 2016a, b, c, 2017), in which the effects of the growth limiting factors, i.e. light intensity and nutrient concentration, are taken into account. By solving the equations of the model, we get the steady spatial distribution of picoeukaryotes abundance, expressed in cells per unit volume and indicated by $b(x,y,z,t)$. Moreover, the spatial distributions of the phosphate concentration $R(x,y,z,t)$ and light intensity $I(x,y,z,t)$ are obtained.

The dynamics of the picoeukaryotes abundance is modeled by considering three processes (Valenti et al., 2012; Denaro et al., 2013a, c, b; Valenti et al., 2015, 2016a, b, c, 2017): i) net growth (reaction term); ii) passive movement (advection terms); iii) movement due to turbulence (diffusion terms).

The reaction term describes the nonlinear interactions between the net growth of picoeukaryotes abundance and the two limiting resources, i.e. light intensity and nutrient concentration. In particular, the net phytoplankton growth rate ($G(x,y,z,t)$) represents the balance between the gross production rate per capita and the mortality (Valenti et al., 2012; Denaro et al., 2013a, c, b; Valenti et al., 2015, 2016a, 2017). The former is given by $\min\{f_I(I), f_R(R)\}$, where $f_I(I)$ and $f_R(R)$ are obtained by the Michaelis-Menten formulas for light intensity and phosphate concentration (Valenti et al., 2012; Denaro et al., 2013a, c, b; Valenti et al., 2015, 2016a, 2017). The latter is described by the specific loss rate (m), in which we consider three processes: respiration, death, and grazing.

The advection terms allow to describe the effects on the spatial distribution of picoeukaryotes abundance induced both by the sinking velocity (w_z) along the z-direction, typical of the planktonic population investigated, and by the velocity field of marine currents reproduced by the SHYFEM model. The diffusion terms reproduce the effects of the turbulence on the spatial distribution of the picoeukaryotes community through the horizontal ($D_x = D_y$) and the vertical (D_v) turbulent diffusivities, whose values are the same used previously for mercury concentrations.

The equation for the dynamics of phosphate concentration $R(x,y,z,t)$ includes two reaction terms, which describe two different processes: i) the phosphate increase due to the recycling of the dead phytoplankton; ii) the phosphate decrease due to the uptake of the picoeukaryotes community. Moreover, also in this case, the effects of the local transport and turbulence, responsible for the mixing of nutrients in the 3D domain, are considered by inserting in the differential equation for the phosphate concentration three advection terms and three diffusion terms, respectively.

Finally, the light intensity $I(z,t)$ is assumed to decrease exponentially with the depth z, according to the Lambert-Beer's law (Valenti et al., 2012; Denaro et al., 2013a, c, b; Valenti et al., 2015, 2016a, 2017), and to vary as a function of time t due to the seasonal oscillations of the incident light intensity, $I_{in}(t)$.

Therefore, the model for picoeukaryotes community is defined by the following equations:

$$\begin{aligned}\frac{\partial b}{\partial t} = & +\frac{\partial}{\partial x}\left[D_x\frac{\partial b}{\partial x}\right]-\frac{\partial}{\partial x}(v_x b)+\frac{\partial}{\partial y}\left[D_y\frac{\partial b}{\partial y}\right]-\frac{\partial}{\partial y}(v_y b)+\frac{\partial}{\partial z}\left[D_z\frac{\partial b}{\partial z}\right]-\frac{\partial}{\partial z}(v_z b)-\frac{\partial}{\partial z}(w_z b)\\ & +b\cdot min\left(f_I(I),f_R(R)\right)-mb,\end{aligned} \tag{S55}$$

$$\begin{aligned}\frac{\partial R}{\partial t} = & +\frac{\partial}{\partial x}\left[D_x\frac{\partial R}{\partial x}\right]-\frac{\partial}{\partial x}(v_x R)+\frac{\partial}{\partial y}\left[D_y\frac{\partial R}{\partial y}\right]-\frac{\partial}{\partial y}(v_y R)+\frac{\partial}{\partial z}\left[D_z\frac{\partial R}{\partial z}\right]-\frac{\partial}{\partial z}(v_z R)+\sum_i \varepsilon\cdot m\cdot\frac{b}{Y}\\ & -\frac{b}{Y}\cdot min\left(f_I(I),f_R(R)\right),\end{aligned} \tag{S56}$$

$$I(z,t)=I_{in}(t)\exp\left\{-\int_0^z\left[a_{bg}+a\cdot chl\,a\right]dZ\right\}. \tag{S57}$$

Here, m and w_z are the mortality and the sinking velocity of eukaryotes population, respectively; ε is the nutrient recycling coefficient for the picoeukaryotes community; $1/Y$ is the nutrient cell content of picoeukaryotes; a_{bg} is the background turbidity; a is the average absorption coefficient for the picoeukaryotes community; $chl\,a$ is the *chlorophyll-a* concentration corresponding to the abundance of picoeukaryotes.

The half-saturation constants for growth of picoeukaryotes, used in the the Michaelis-Menten formulas, depend on the environmental conditions of investigated site. Since the *chlorophyll-a* concentrations, measured in the Augusta Bay, are those typical of oligotrophic waters of the Mediterranean Sea, the half-saturation constants are set equal to values previously obtained in the Southern Sicily by Valenti et al. (2017) adopting an accurate calibration procedure. All other parameters are set in accordance with the methods described in previous works (Hickman et al., 2010; Raven et al., 2005; Veldhuis et al., 2005; Timmermans et al., 2005), while the temporal behaviour of incident light intensity, $I_{in}(t)$, is obtained for the Augusta Bay by using the remote sensing data. Finally, the *chlorophyll-a* concentration, $chl\,a$, is calculated by the theoretical results for the picoeukaryotes abundance by using the conversion curve obtained by Brunet et al. (2007).

The NP model is completed by a set of equations, which describe the nutrient and phytoplankton fluxes at the boundaries of Augusta Bay. Here, we set the following conditions for the picoeukaryotes abundance and the phosphate concentration: no biomass can enter or leave the area investigated except through the inlets; no nutrient flux is present through the water surface; the phosphate concentration at the deepest layer of the water column is fixed equal to the value measured previously close to Augusta Bay; no nutrient flux is present through the lateral surfaces except at the inlets; the picoeukaryotes abundance and the phosphate concentration are set constant out of the Augusta Bay (Mediterranean Sea); the lateral fluxes for picoeukaryotes abundance and phosphate concentration at the inlets depend on the behaviour of horizontal velocities. The boundary conditions for the picoeukaryotes abundance and the phosphate concentration are defined by the following equations:

$$\left[D_z\frac{\partial b}{\partial z}-(w_z+v_z)b_i\right]\Big|_{z=0}=\left[D_z\frac{\partial b}{\partial z}-(w_z+v_z)b\right]\Big|_{z=z_b}=0, \tag{S58}$$

$$\left[D_x\frac{\partial b}{\partial x}-v_x b\right]=\left[D_y\frac{\partial b}{\partial y}-v_y b\right]=0,\quad b(x_{inlet},y_{inlet},z)=b_{ext}, \tag{S59}$$

$$\left.\frac{\partial R}{\partial z}\right|_{z=0} = 0, \quad R(x,y,z_b) = R_{in}(x,y,z_b), \tag{S60}$$

$$\left[D_x \frac{\partial R}{\partial x} - v_x R\right] = \left[D_y \frac{\partial R}{\partial y} - v_y R\right] = 0, \quad R(x_{inlet}, y_{inlet}, z) = R_{ext}, \tag{S61}$$

where z_b is the depth of the water column in each position (x,y); b_{ext} is the average picoeukaryotes abundance in the Mediterranean Sea; $R_{in}(x,y,z_b)$ is the phosphate concentration kept constant at the deepest layer of the water column; R_{ext} is the average phosphate concentration in the Mediterranean Sea.

Eqs. (S55)-(S61) describe the three-dimensional advection-diffusion-reaction model used to reproduce the spatio-temporal behaviour of the picoeukaryotes abundance, the phosphate concentration and the light intensity in the seawater compartment of the Augusta Bay. The theoretical results obtained by this model are used to calculate the sinking fluxes of the SPM-bound mercury and the loads of dissolved mercury released by POM.

S5 The Phytoplankton MERLIN-Expo model for the mercury contents in picoeukaryotes

The dynamics of the mercury content in picoeukaryotes is analyzed in the Augusta Bay by using the Phytoplankton MERLIN-Expo model (Radomyski and Ciffroy, 2015). Specifically, we investigate the behaviour of the most abundant two mercury species within the phytoplankton cells, i.e. inorganic mercury and methyl-mercury. By solving the equations of the model, we obtain the dynamics of the amount of inorganic mercury and methyl-mercury present in each picoeukaryote cell, indicated by $PHg^{II}(x,y,z,t)$ and $PMeHg(x,y,z,t)$, respectively.

The dynamics of the content of inorganic mercury and methyl-mercury in each picoeukaryote cell is modeled by considering three processes (Radomyski and Ciffroy, 2015): i) mercury absorption through the cell wall; ii) mercury elimination (excretion) through the cell wall; iii) mercury elimination via dilution. The first process is described by the uptake rate constant for the mercury, which is obtained by the water layer diffusion resistance, the lipid permeation resistance and the mercury concentration in the seawater. The second process is described by the elimination rate constant for the mercury, which depends on the water layer diffusion resistance, the lipid permeation resistance and the water-dissolved organic carbon partition coefficient. The third process is described by the growth rate constant for picoeukaryotes, which is obtained by the phytoplankton growth rate and the phytoplankton weight.

Thus, the Phytoplankton Merlin-Expo model (Radomyski and Ciffroy, 2015) for the two mercury species embedded at the picoeukaryotes cells is defined by the following equations:

$$\frac{dPHg^{II}}{dt} = W_{phy} \cdot k_{phy,up,inor} \cdot Hg^{II} - PHg^{II} \cdot (k_{phy,exc,inor} + k_{phy,gro}), \tag{S62}$$

$$\frac{dPMeHg}{dt} = W_{phy} \cdot k_{phy,up,meth} \cdot MeHg - PMeHg \cdot (k_{phy,exc,meth} + k_{phy,gro}), \tag{S63}$$

where W_{phy} is the phytoplankton cell weight, $k_{phy,up,inor}$ is the inorganic mercury uptake rate constant, $k_{phy,up,meth}$ is the methyl-mercury uptake rate constant, $k_{phy,exc,inor}$ is the elimination rate constant for the inorganic mercury, $k_{phy,exc,meth}$ is the elimination rate constant for the methyl-mercury; $k_{phy,gro}$ is the growth rate constant. According to the Phytoplankton Merlin-Expo model (Radomyski and Ciffroy, 2015), the rates of Eqs. (S62)-(S63) are calculated as follows:

$$k_{phy,up,inor} = \frac{W_{phy}^{-k}}{\rho_{water} + \rho_{lipid} \cdot (Hg^{II})^{b_{lipid}}}, \tag{S64}$$

$$k_{phy,up,meth} = \frac{W_{phy}^{-k}}{\rho_{water} + \rho_{lipid} \cdot (MeHg)^{b_{lipid}}}, \tag{S65}$$

$$k_{phy,exc,inor} = \frac{W_{phy}^{-k}}{\rho_{water} + \rho_{lipid}} \cdot \frac{1}{p_{carbonphy} \cdot 10^{log_{10}K_d^{II}}}, \tag{S66}$$

$$k_{phy,exc,meth} = \frac{W_{phy}^{-k}}{\rho_{water} + \rho_{lipid}} \cdot \frac{1}{p_{carbonphy} \cdot 10^{log_{10}K_d^{MM}}}, \tag{S67}$$

$$k_{phy,gro} = a_{growth} \cdot V_{cell}^{-b_{growth}}, \tag{S68}$$

where W_{phy} and V_{cell} are the phytoplankton weight and the phytoplankton cell volume of the picoeukaryotes, respectively; k is the allometric rate exponent of the phytoplankton; ρ_{lipid} and ρ_{water} are the lipid layer permeation resistance and the water layer diffusion resistance for the uptake of chemicals from water, respectively; b_{lipid} is the lipid permeation resistance exponent; Hg^{II} and $MeHg$ are the inorganic mercury concentration and the methyl-mercury concentration in the seawater, respectively; $p_{carbonphy}$ is the organic carbon fraction of phytoplankton; $log_{10}K_d^{II}$ and $log_{10}K_d^{MM}$ are the water-dissolved organic carbon partition coefficients for the inorganic mercury and the methyl-mercury, respectively; a_{growth} and b_{growth} are the intercept and the slope of the phytoplankton growth rate, respectively. The picoeukaryote weight, W_{phy}, and the phytoplankton cell volume, V_{cell}, are estimated by using the experimental findings reported in previous works (Radomyski and Ciffroy, 2015; Pickhardt and Fischer, 2007; Strickland, 1960). The mercury concentrations, Hg^{II} and $MeHg$, in the seawater are obtained by the advection-diffusion-reaction model (see section 1). All other parameters are set at the same values given in "The Phytoplankton Merlin-Expo model" (Radomyski and Ciffroy, 2015; Hendricks, 2007; Hauck et al., 2011; Allison and Allison, 2005).

As initial conditions, we fix that the mercury contents in each picoeukaryote cell depend on both the dissolved mercury concentrations in marine environment and the volume concentration factors estimated for specific chemicals (inorganic mercury and methyl-mercury) and phytoplankton species (picoeukaryotes) (Pickhardt and Fischer, 2007). In particular, the inorganic mercury content and the methyl-mercury content at the initial time ($t = 0$) are given by:

$$PHg^{II}(0) = W_{phy} \cdot VCF^{II} \cdot Hg^{II}(0), \qquad PMeHg(0) = W_{phy} \cdot VCF^{MM} \cdot MeHg(0) \tag{S69}$$

where VCF^{II} and VCF^{MM} are the volume concentration factors for the inorganic mercury and the methyl-mercury, respectively, in picoeukaryotes; $Hg^{II}(0)$ and $MeHg(0)$ are the inorganic mercury concentration and the methyl-mercury concentration at the initial time $t = 0$.

Eqs. (S62)-(S68) constitute the Phytoplankton MERLIN-Expo model used to reproduce the dynamics of the mercury contents within the picoeukaryotes cells, which populate the Augusta Bay. The theoretical results obtained by this model are used to calculate the loads of dissolved mercury released by the particulate organic matter.

References

Allison, J. D. and Allison, T. L.: Partition coefficients for metals in surface water, soil, and waste, U.S. Environmental Protection Agency, Washington, DC, 2005.

Bagnato, E., Sprovieri, M., Barra, M., Bitetto, M., Bonsignore, M., Calabrese, S., Di Stefano, V., Oliveri, E., Parello, F., and Mazzola, S.: The sea-air exchange of mercury (Hg) in the marine boundary layer of the Augusta basin (southern Italy): Concentrations and evasion flux, Chemosphere, 93, 2024–2032, https://doi.org/10.1016/j.chemosphere.2013.07.025, 2013.

Baines, S. B., Pace, M. L., and Karl, D. M.: Why does the relationship between sinking flux and planktonic primary production differ between lakes and oceans?, Limnol. Oceanogr., 39(2), 213–226, https://doi.org/10.4319/lo.1994.39.2.0213, 1994.

Batrakova, N., Travnikov, O., and Rozovskaya, O.: Chemical and physical transformations of mercury in the ocean: a review, Ocean Sci., 10, 1047–1063, https://doi.org/https://doi.org/10.5194/os-10-1047-2014, 2014.

Boudreau, B. P.: The diffusive tortuosity of fine-grained unlithified sediments, Geochim. Cosmochim. Acta, 60, 3139–3142, https://doi.org/https://doi.org/10.1016/0016-7037(96)00158-5, 1996.

Burchard, H. and Petersen, O.: Models of turbulence in the marine environment. A comparative study of two-equation turbulence models, J. Mar. Syst., 21(1-4), 23–53, https://doi.org/10.1016/S0924-7963(99)00004-4, 1999.

Ciffroy, P.: The River MERLIN-Expo model, Fun Project 4 - Seventh Framework Programme, 2015.

Cossa, D. and Coquery, M.: The Handbook of Environmental Chemistry, Vol. 5, Part K (2005): 177-208. The Mediterranean Mercury Anomaly, a Geochemical or a Biologocal Issue, Springer-Verlag Berlin Heidelberg, 2005.

Covelli, S., Faganeli, J., De Vittor, C., Predonzani, S., Acquavita, A., and Horvat, M.: Benthic fluxes of mercury species in a lagoon environment (Grado Lagoon, Northern Adriatic Sea, Italy), Appl. Geochem., 23, 529–546, https://doi.org/10.1016/j.apgeochem.2007.12.011, 2008.

Cucco, A., Sinerchia, M., Lefrançois, C., Magni, P., Ghezzo, M., Umgiesser, G., Perilli, A., and Domenici, P.: A metabolic scope based model of fish response to environmental changes, Ecol. Model., 237-238, 132–141, https://doi.org/10.1016/j.ecolmodel.2012.04.019, 2012.

Cucco, A., Quattrocchi, G., Olita, A., Fazioli, L., Ribotti, A., Sinerchia, M., Tedesco, C., and Sorgente, R.: Hydrodynamic modeling of coastal seas: the role of tidal dynamics in the Messina Strait, Western Mediterranean Sea, Nat. Hazard Earth Sys., 16, 1553–1569, https://doi.org/10.5194/nhess-16-1553-2016, 2016a.

Cucco, A., Quattrocchi, G., Satta, A., Antognarelli, F., De Biasio, F., Cadau, E., Umgiesser, G., and Zecchetto, S.: Predictability of wind-induced sea surface transport in coastal areas, J. Geophys. Res. Oceans, 121(8), 5847–5871, https://doi.org/https://doi.org/10.1002/2016JC011643, 2016b.

Cucco, A., Quattrocchi, G., and Zecchetto, S.: The role of temporal resolution in modeling the wind induced sea surface transport in coastal seas, J. Mar. Syst., 193, 46–58, https://doi.org/https://doi.org/10.1016/j.jmarsys.2019.01.004, 2019.

Denaro, G., Valenti, D., La Cognata, A., Spagnolo, B., Bonanno, A., Basilone, G., Mazzola, S., Zgozi, S., Aronica, S., and Brunet, C.: Spatio-temporal behaviour of the deep chlorophyll maximum in Mediterranean Sea: Development of a stochastic model for picophytoplankton dynamics, Ecol. Complex., 13, 21–34, https://doi.org/10.1016/j.ecocom.2012.10.002, 2013a.

Denaro, G., Valenti, D., Spagnolo, B., Basilone, G., Mazzola, S., Zgozi, S., Aronica, S., and Bonanno, A.: Dynamics of two picophytoplankton groups in Mediterranean Sea: Analysis of the Deep Chlorophyll Maximum by a stochastic advection-reaction-diffusion model, PLoS ONE, 8(6), e66 765, https://doi.org/10.1371/journal.pone.0066765, 2013b.

Denaro, G., Valenti, D., Spagnolo, B., Bonanno, A., Basilone, G., Mazzola, S., Zgozi, S., and Aronica, S.: Stochastic dynamics of two picophytoplankton populations in a real marine ecosystem, Acta Phys. Pol. B, 44, 977–990, https://doi.org/10.5506/APhysPolB.44.977, 2013c.

Denman, K. L. and Gargett, A. E.: Time and space scales of vertical mixing and advection of phytoplankton in the upper ocean, Limnol. Oceanogr., 28, 801–815, https://doi.org/https://doi.org/10.4319/lo.1983.28.5.0801, 1983.

D'Ortenzio, F.: Space and time occurrence of algal blooms in the Mediterranean: their significance for the trophic regime of the basin, PhD Thesis, Open University of London, UK, 2003.

Dutkiewicz, S., Follows, M. J., and Bragg, J. G.: Modeling the coupling of ocean ecology and biogeochemistry., Global Biogeochem. Cy., p. GB4017, https://doi.org/https://doi.org/10.1029/2008GB003405, 2009.

Farina, S., Quattrocchi, G., Guala, I., and Cucco, A.: Hydrodynamic patterns favouring sea urchin recruitment in coastal areas: A Mediterranean study case, Mar. Environ. Res., 139, 182–192, https://doi.org/10.1016/j.marenvres.2018.05.013, 2018.

Ferrarin, C., Umgiesser, G., Cucco, A., Hsu, T. W., Roland, A., and Amos, C. L.: Development and validation of a finite element morphological model for shallow water basins, Coast. Eng., 55, 716–731, https://doi.org/10.1016/j.coastaleng.2008.02.016, 2008.

Ferrarin, C., Bajo, M., Bellafiore, D., Cucco, A., De Pascalis, F., and Ghezzo, M.: Toward homogenization of Mediterranean lagoons and their loss of hydrodiversity, Geophys. Res. Lett., 41(16), 5935–5941, https://doi.org/https://doi.org/10.1002/2014GL060843, 2014.

Han, S., Lehman, R. D., Choe, K. Y., and Gill, A.: Chemical and physical speciation of mercury in Offatts Bayou: A seasonally anoxic bayou in Galveston Bay, Limnol. Oceanogr., 52(4), 1380–1392, https://doi.org/https://doi.org/10.4319/lo.2007.52.4.1380, 2007.

Hauck, A. J., Hendricks, H. W. M., Huijbregts, M. A. J., Ragas, A. M. J., Van der Meent, D., and Hendricks, A. J.: Parameter uncertainty in modeling bioaccumulation factors of fish, Environ. Toxicol. Chem., 30(2), 403–412, https://doi.org/10.1002/etc.393, 2011.

Hendricks, A. J.: The power of size: A meta-analysis reveals consistency of allometric regressions, Ecol. Model., 205, 196–208, https://doi.org/10.1016/j.ecolmodel.2007.02.029, 2007.

Hickman, A., Dutkiewicz, S., Williams, R., and Follows, M.: Modelling the effects of chromatic adaptation on phytoplankton community structure in the oligotrophic ocean, Mar. Ecol. Prog. Ser., 406, 1–17, 2010.

Hines, M. E., Potrait, E. N., Covelli, S., Faganeli, J., Emili, A., Zizek, E., and Horvat, M.: Mercury methylation and demethylation in Hg-contaminated lagoon sediments (Marano and Grado Lagoon, Italy), Estuar. Coast. Shelf Sci., 113, 85–95, https://doi.org/10.1016/j.ecss.2011.12.021, 2012.

ICRAM: Progetto preliminare di bonifica dei fondali della rada di Augusta nel sito di interesse nazionale di Priolo e Elaborazione definitiva, BoI-Pr-SI-PR-Rada di Augusta-03.22, 2008.

Kallos, G. and Pytharoulis, I.: Short-term predictions (weather forecasting purposes), Encyclopedia of Hydrological Sciences, edited by M. G. Anderson, pp. 2791-2811, John Wiley, London, U.K., 2005.

Katz, E. J., Bruce, J. G., and Petrie, B. D.: Salt and mass flux in the Atlantic Equatorial Undercurrent, Deep-Sea Res., 26, 139–160, 1979.

Lisi, I., Taramelli, A., Di Risio, M., Cappucci, S., and Gabellini, M.: Flushing efficiency of Augusta harbour (Italy), J. Coast. Res., 56, 841–845, 2009.

Liu, G., Cai, J., and O'Driscoll, N.: Environmental Chemistry and Toxycology of Mercury, John Wiley and Sons, Inc., Hoboken, New Jersey, 2012.

Massel, S. R.: Fluid Mechanics for Marine Ecologists, Springer-Verlag, Berlin Heidelberg, 1999.

Melaku Canu, D., Rosati, G., Solidoro, C., Heimbürger, L., and Acquavita, A.: A comprehensive assessment of the mercury budget in the Marano-Grado Lagoon (Adriatic Sea) using a combined observational modeling approach, Mar. Chem., 177, 742–752, https://doi.org/10.1016/j.marchem.2015.10.013, 2015.

Monperrus, M., Tessier, E., Amouroux, D., Leynaert, A., Huonnic, P., and Donard, O. F. X.: Mercury methylation, demethylation and reduction rates in coastal and marine surface waters of the Mediterranean Sea, Mar. Chem., 107, 49–63, https://doi.org/10.1016/j.marchem.2007.01.018, 2007a.

Monperrus, M., Tessier, E., Point, D., Vidimova, K., Amouroux, D., Guyoneaud, R., Leynaert, A., Grall, J., Chauvaud, L., Thouzeau, G., and Donard, O. F. X.: The biogeochemistry of mercury at the sediment-water interface in the Thau Lagoon. 2. Evaluation of mercury methylation potential in both surface sediment and the column, Estuar. Coast. Shelf Sci., 72, 485–486, https://doi.org/https://doi.org/10.1016/j.ecss.2006.11.014, 2007b.

Morozov, A., Arashkevich, E., Nikishina, A., and Solovyev, K.: Nutrient-rich plankton communities stabilized via predator-prey interactions: revisiting the role of vertical heterogeneity, Math. Med. Biol., 28(2), 185–215, https://doi.org/10.1093/imammb/dqq010, 2010.

Neumeier, U., Ferrarin, C., Amos, C. L., Umgiesser, G., and Li, M. Z.: Sedtrans05: An improved sediment-transport model for continental shelves and coastal waters with a new algorithm for cohesive sediments, Comput. Geosci., 34, 1223–1242, https://doi.org/10.1016/j.cageo.2008.02.007, 2008.

Ogrinc, N., Monperrus, M., Kotnik, J., Fajon, V., Vidimova, K., Amouroux, D., Kocman, D., Tessier, E., Zizek, S., and Horvat, M.: Distribution of mercury and methylmercury in deep-sea surficial sediments of the Mediterranean Sea, Mar. Chem., 107, 31–48, https://doi.org/https://doi.org/10.1016/j.marchem.2007.01.019, 2007.

Oliveri, E., Manta, D. S., Bonsignore, M., Cappello, S., Tranchida, G., Bagnato, E., Sabatino, N., Santisi, S., and Sprovieri, M.: Mobility of mercury in contaminated marine sediments: Biogeochemical pathways, Mar. Chem., 186, 1–10, https://doi.org/10.1016/j.marchem.2016.07.002, 2016.

Pacanowski, R. and Philander, S. G. H.: Parameterization of Vertical Mixing in Numerical Models of Tropical Oceans, J. Phys. Oceanogr., 11, 1443–1451, https://doi.org/10.1175/1520-0485(1981)011$<$1443:$POVMIN$$>$2.0.CO;2, 1981.

Peters, H., Gregg, M. C., and Toole, J. M.: On the Parameterization of Equatorial Turbulence, J. Geophys. Res., 93, 1199–1218, https://doi.org/https://doi.org/10.1029/JC093iC02p01199, 1988.

Pickhardt, P. C. and Fischer, N. S.: Accumulation of Inorganic and Methylmercury by Freshwater Phytoplankton in Two Contrasting Water Bodies, Environ. Sci. Technol., 41, 125–131, https://doi.org/10.1021/es060966w, 2007.

Qureshi, A., O'Driscoll, N. J., MacLeod, M., Neuhold, Y. M., and Hungerbuhler, K.: Photoreactions of mercury in surface ocean water: gross reaction kinetics and possible pathways, Environ. Sci. Technol., 44, 644–649, https://doi.org/10.1021/es9012728, 2010.

Radomyski, A. and Ciffroy, P.: The Phytoplankton MERLIN-Expo model, Fun Project 4 - Seventh Framework Programme, 2015.

Rajar, R., Cetina, M., Horvat, M., and Zagar, D.: Mass balance of mercury in the Mediterranean Sea, Mar. Chem., 107, 89–102, https://doi.org/https://doi.org/10.1016/j.marchem.2006.10.001, 2007.

Raven, J. A., Finkel, Z. V., and Irwin, A. J.: Picophytoplankton: bottom-up an top-down controls on ecology and evolution, J. Geophys. Res., 55, 209–215, 2005.

Salvagio Manta, D., Bonsignore, M., Oliveri, E., Barra, M., Tranchida, G., Giaramita, L., Mazzola, S., and Sprovieri, M.: Fluxes and the mass balance of mercury in Augusta Bay (Sicily, southern Italy), Estuar. Coast. Shelf Sci., 181, 134–143, https://doi.org/10.1016/j.ecss.2016.08.013, 2016.

Schulz, H. D. and Zabel, M.: Marine Geochemistry, Springer - Verlag Berlin Heidelberg, 2006.

Soerensen, A. L., Sunderland, E. M., Holmes, C. D., Jacob, D. J., Yantosca, R. M., Skov, H., Christensen, J. H., Strode, S. A., and Mason, R. P.: An improved global model for air-sea exchange of mercury: High concentrations over the north Atlantic, Environ. Sci. Technol., 44, 8574–8580, https://doi.org/10.1021/es102032g, 2010.

Sørensen, P. B., Fauser, P., Carlsen, L., and Vikelsøe, J.: Theoretical evaluation of the sediment/water exchange description in generic compartment models (SimpleBox), NERI Technical Report No.360, 2001.

Spydell, M. S., Feddersen, F., Olabarrieta, M., Chen, J., Guza, R. T., Raubenheimer, B., and Elgar, S.: Observed and modeled drifters at a tidal inlet, J. Geophys. Res. Oceans, 120, 4825–4844, https://doi.org/10.1002/2014JC010541, 2015.

Strickland, J. D. H.: Measuring the Production of Marine Phytoplankton, Fisheries Research Board of Canada (Bulletin), 1960.

Strode, S., Jaeglè, L., and Emerson, S.: Vertical transport of anthropogenic mercury in the ocean, Global Biogeochem. Cy., 24, GB4014, https://doi.org/https://doi.org/10.1029/2009GB003728, 2010.

Strode, S. A., Jaegle, L., Selin, N., Jacob, D. J., Park, R., Yantosca, R. M., Mason, R. P., and Slemr, F.: Air-sea exchange in the global mercury cycle, Global Biogeochem. Cy., 21, GB1017, https://doi.org/https://doi.org/10.1029/2006GB002766, 2007.

Sunderland, E. M., Gobas, F. A. P. C., Branfireum, B. A., and Heyes, A.: Environmental controls on the speciation and distribtuion of mercury in coastal sediments, Mar. Chem., 102, 111–123, https://doi.org/10.1016/j.marchem.2005.09.019, 2006.

Thi, N. N. P., Huisman, J., and Sommeijer, B. P.: Simulation of three-dimensional phytoplankton dynamics: competition in light-limited environments, J. Comput. Appl. Math., 174, 57–77, https://doi.org/10.1016/j.cam.2004.03.023, 2005.

Timmermans, K. R., van der Wagt, B., Veldhuis, M. J. W., Maatman, A., and de Baar, H. J. W.: Physiological responses of three species of marine pico-phytoplankton to ammonium, phospahte, iron and light limitation, J. Sea Res., 53, 109–120, 2005.

Tveito, A. and Winther, R.: Introduction to Partial Differential Equations: A Computational Approach, Springer-Verlag, New York, 1998.

Umgiesser, G.: SHYFEM. Finite Element Model for Coastal Seas. User Manual, The SHYFEM Group, Georg Umgiesser, ISMAR-CNR, Venezia, Italy, 2009.

Umgiesser, G., Canu, D. M., Cucco, A., and Solidoro, C.: A finite element model for the Venice Lagoon. Development, set up, calibration and validation, J. Mar. Syst., 51, 123–145, https://doi.org/10.1016/j.jmarsys.2004.05.009, 2004.

Umgiesser, G., Ferrarin, C., Cucco, A., De Pascalis, F., Bellafiore, D., Ghezzo, M., and Bajo, M.: Comparative hydrodynamics of 10 Mediterranean lagoons by means of numerical modeling, J. Geophys. Res. Oceans, 119(4), 2212–2226, https://doi.org/https://doi.org/10.1002/2013JC009512, 2014.

Valenti, D., Denaro, G., La Cognata, A., Spagnolo, B., Bonanno, A., Mazzola, S., Zgozi, S., and Aronica, S.: Picophytoplankton dynamics in noisy marine environment, Acta Phys. Pol. B, 43, 1227–1240, https://doi.org/10.5506/APhysPolB.43.1227, 2012.

Valenti, D., Denaro, G., Spagnolo, B., Conversano, F., and Brunet, C.: How diffusivity, thermocline and incident light intensity modulate the dynamics of deep chlorphyll maximum in Tyrrhenian Sea, PLoS ONE, 10(1), e0115 468, https://doi.org/https://doi.org/10.1371/journal.pone.0115468, 2015.

Valenti, D., Denaro, G., Conversano, F., Brunet, C., Bonanno, A., Basilone, G., Mazzola, S., and Spagnolo, B.: The role of noise on the steady state distributions of phytoplankton populations, J. Stat. Mech., p. 054044, https://doi.org/10.1088/1742-5468/2016/05/054044, 2016a.

Valenti, D., Denaro, G., Spagnolo, B., Mazzola, S., Basilone, G., Conversano, F., Brunet, C., and Bonanno, A.: Stochastic models for phytoplankton dynamics in Mediterranean Sea, Ecol. Complex., 27, 84–103, https://doi.org/10.1016/j.ecocom.2015.06.001, 2016b.

Valenti, D., Giuffrida, A., Denaro, G., Pizzolato, N., Curcio, L., Mazzola, S., Basilone, G., Bonanno, A., and Spagnolo, B.: Noise Induced Phenomena in the Dynamics of Two Competing Species, Math. Model. Nat. Phenom., 11(5), 158–174, https://doi.org/https://doi.org/10.1051/mmnp/201611510, 2016c.

Valenti, D., Denaro, G., Ferreri, R., Genovese, S., Aronica, S., Mazzola, S., Bonanno, A., Basilone, G., and Spagnolo, B.: Spatio-temporal dynamics of a planktonic system and chlorophyll distribution in a 2D spatial domain: matching model and data, Sci. Rep., 7, 220, https://doi.org/https://doi.org/10.1051/mmnp/201611510, 2017.

Van Rijn, L. C.: Principles of Fluid Flow and Surface Waves in Rivers, Estuaries, Seas and Oceans, Aqua Publications, 2011.

Veldhuis, M. J. W., Timmermans, K. R., Croot, P., and Van Der Wagt, B.: Picophytoplankton; a comparative study of their biochemical composition and photosynthetic properties, J. Sea Res., 53, 7–24, 2005.

Whalin, L., Kim, E., and Mason, R.: Factors influencing the oxidation, reduction, methylation and demethylation of mercury species in coastal waters, Mar. Chem., 107, 278–294, https://doi.org/10.1016/j.marchem.2007.04.002, 2007.

Zhang, Y., Jaeglé, L., and Thompson, L.: Natural biogeochemical cycle of mercury in a global three-dimensional ocean tracer model, Global Biogeochem. Cy., 28, GB004 814, https://doi.org/10.1002/2014GB004814, 2014.

SUPPLEMENTARY FIGURES AND TABLES

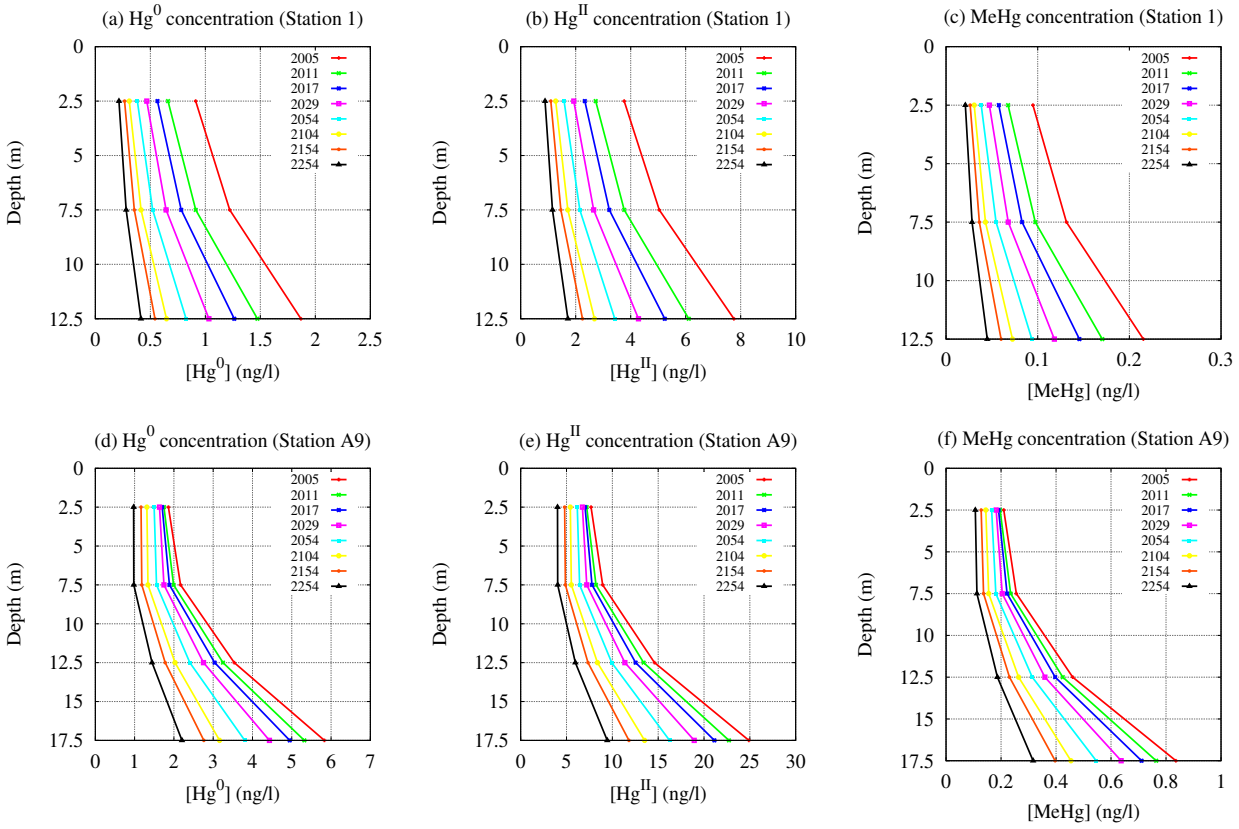

Figure S1. Spatio-temporal evolution of the three mercury species in seawater. Vertical profiles of $[Hg^0]$ (panels a,d), $[Hg^{II}]$ (panels b,e) and $[MeHg]$ (panels c,f) are shown for the sites closest to station 1 (sampling May 2011) and station $A9$ (sampling October 2017).

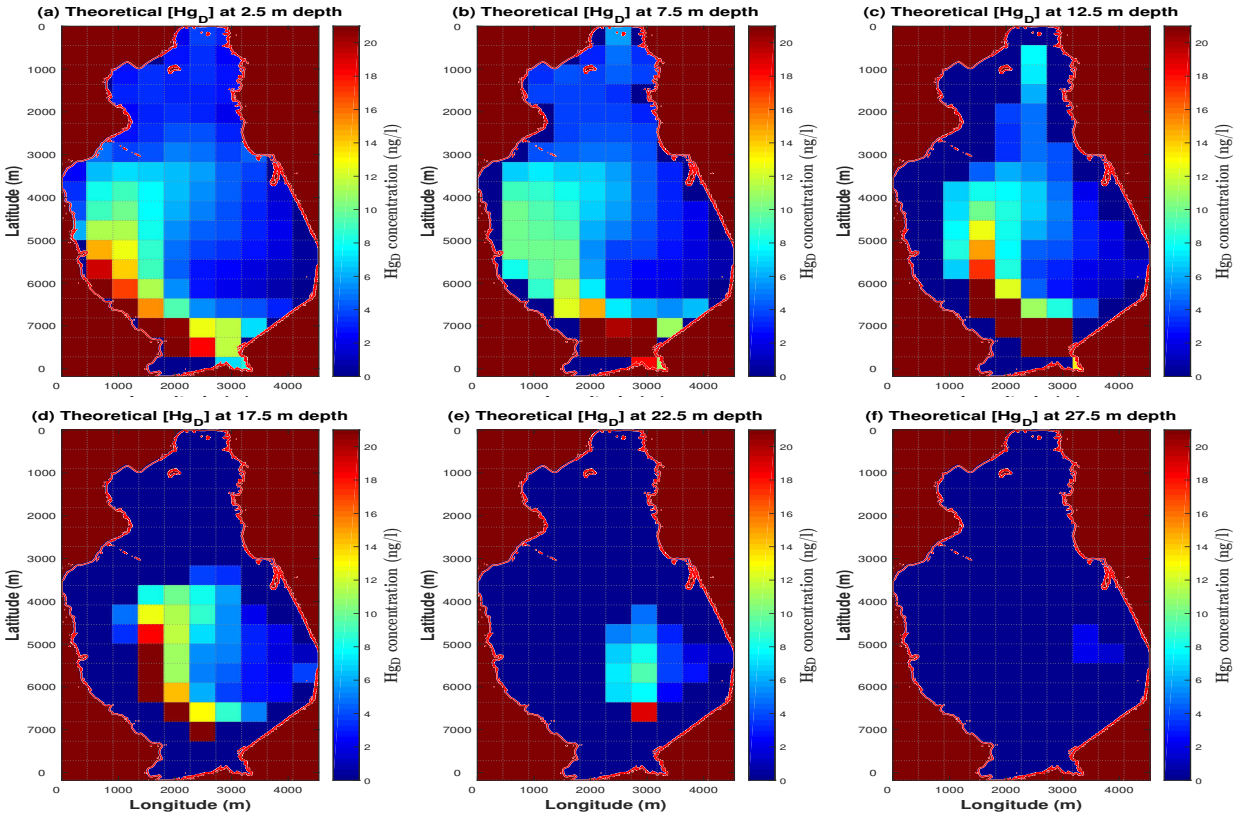

Figure S2. Theoretical distributions of the dissolved mercury concentration obtained by the model for the six different depths of the seawater compartment. The maps reproduce the spatial behaviour of the dissolved mercury concentration at the depths 2.5 m (panel a), 7.5 m (panel b), 12.5 m (panel c), 17.5 m (panel d), 22.5 m (panel e) and 27.5 m (panel f) during the sampling period of May 2011.

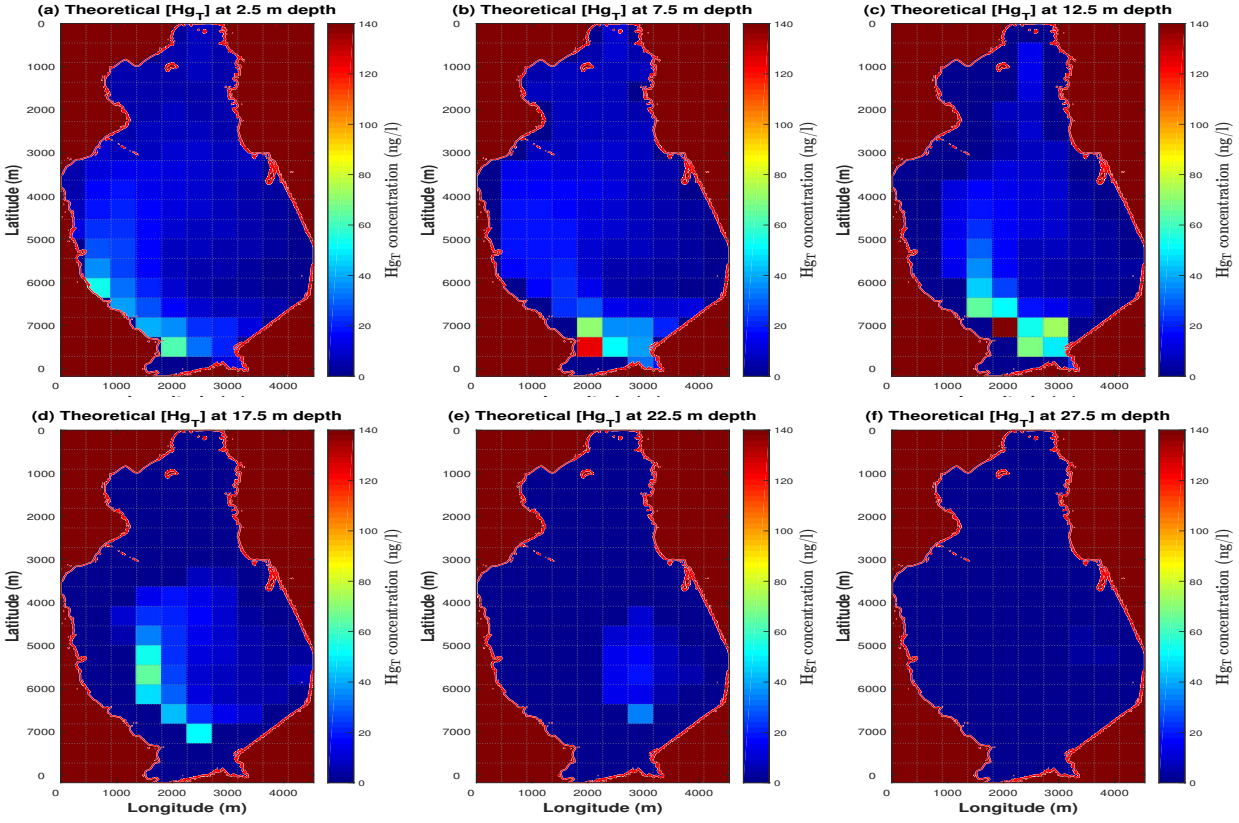

Figure S3. Theoretical distributions of the total mercury concentration obtained by the model for the six different depths of the seawater compartment. The maps reproduce the spatial behaviour of the total mercury concentration at the depths 2.5 m (panel a), 7.5 m (panel b), 12.5 m (panel c), 17.5 m (panel d), 22.5 m (panel e) and 27.5 m (panel f) during the sampling period of May 2011.

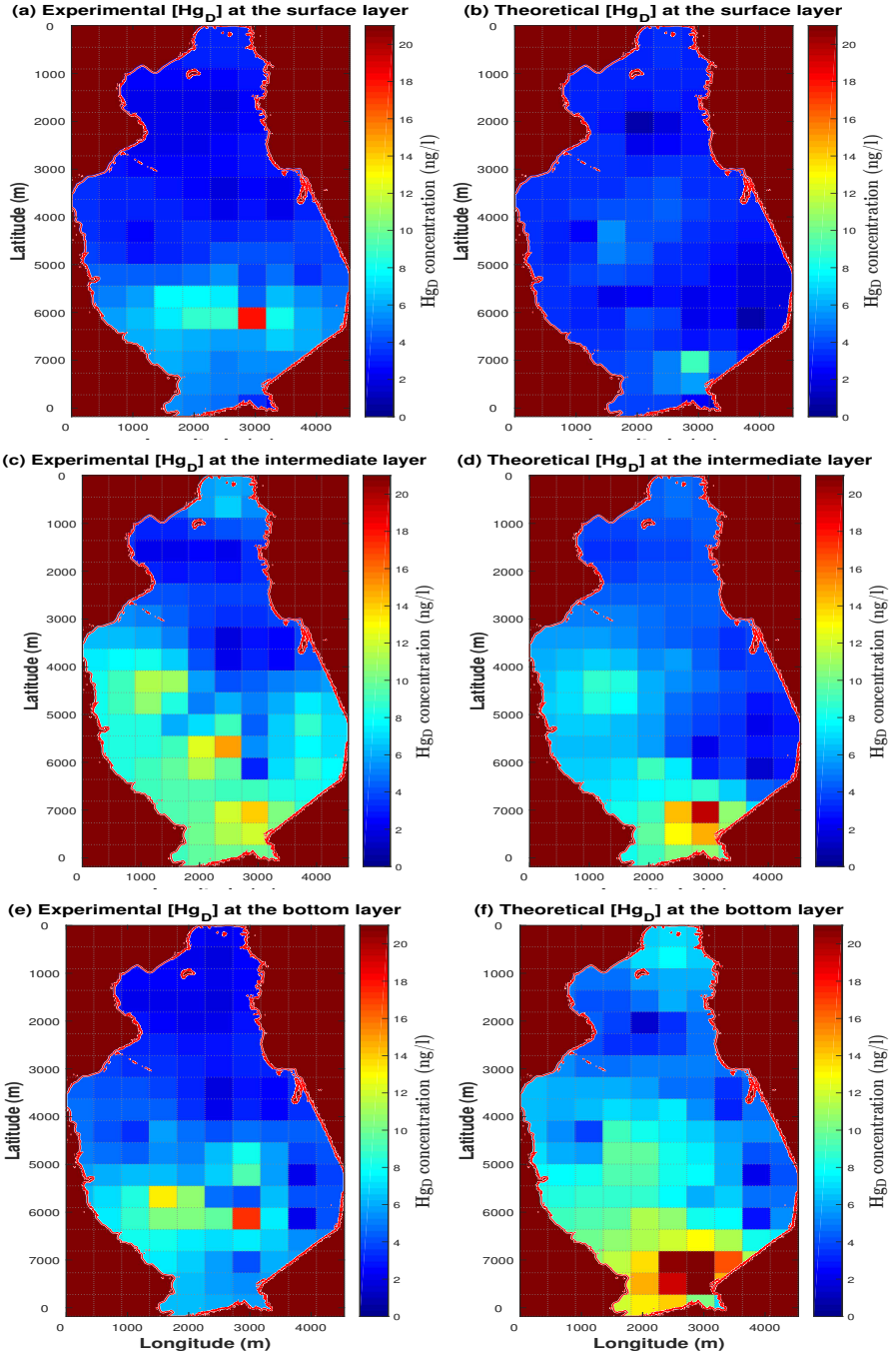

Figure S4. Comparison between the experimental data and the theoretical results for the dissolved mercury concentration. The maps reproduce the spatial distributions of the dissolved mercury concentration at surface layer (panels a, b), intermediate layer (panels c,d) and bottom layer (panels e,f) of the water column during the sampling period of May 2011. The spatial distributions are obtained by interpolating the experimental data collected in the Augusta Bay, and the theoretical results calculated by the model.

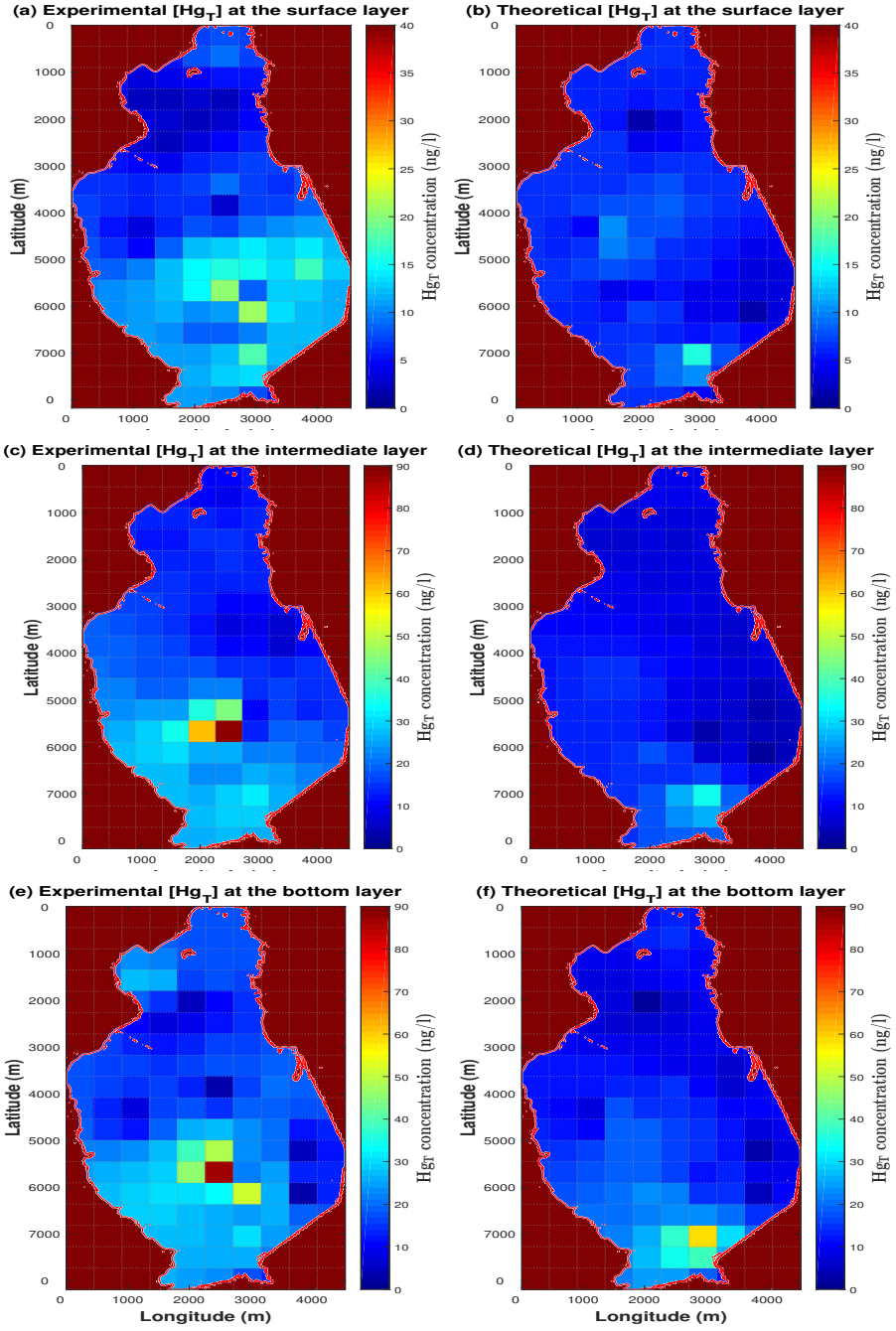

Figure S5. Comparison between the experimental data and the theoretical results for the total mercury concentration. The maps reproduce the spatial distributions of the total mercury concentration at surface layer (panels a, b), intermediate layer (panels c,d) and bottom layer (panels e,f) of the water column during the sampling period of May 2011. The spatial distributions are obtained by interpolating the experimental data collected in the Augusta Bay, and the theoretical results calculated by the model.

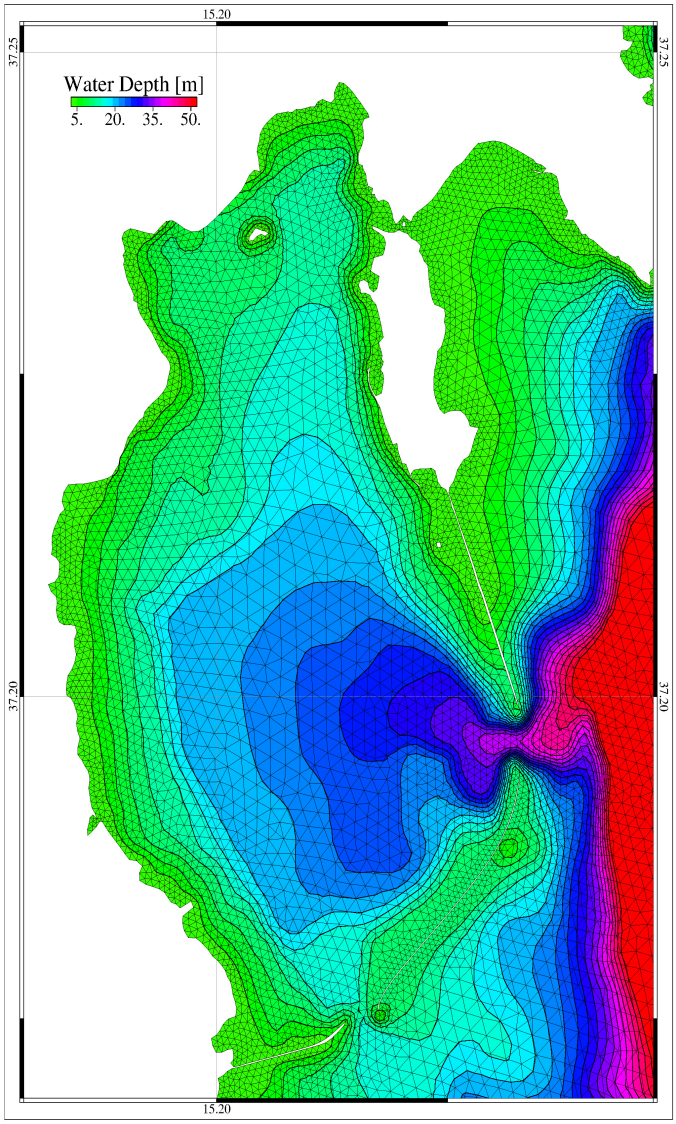

Figure S6. Zoom of the finite element mesh and bathymetry for the Augusta Bay and surrounding coastal area.

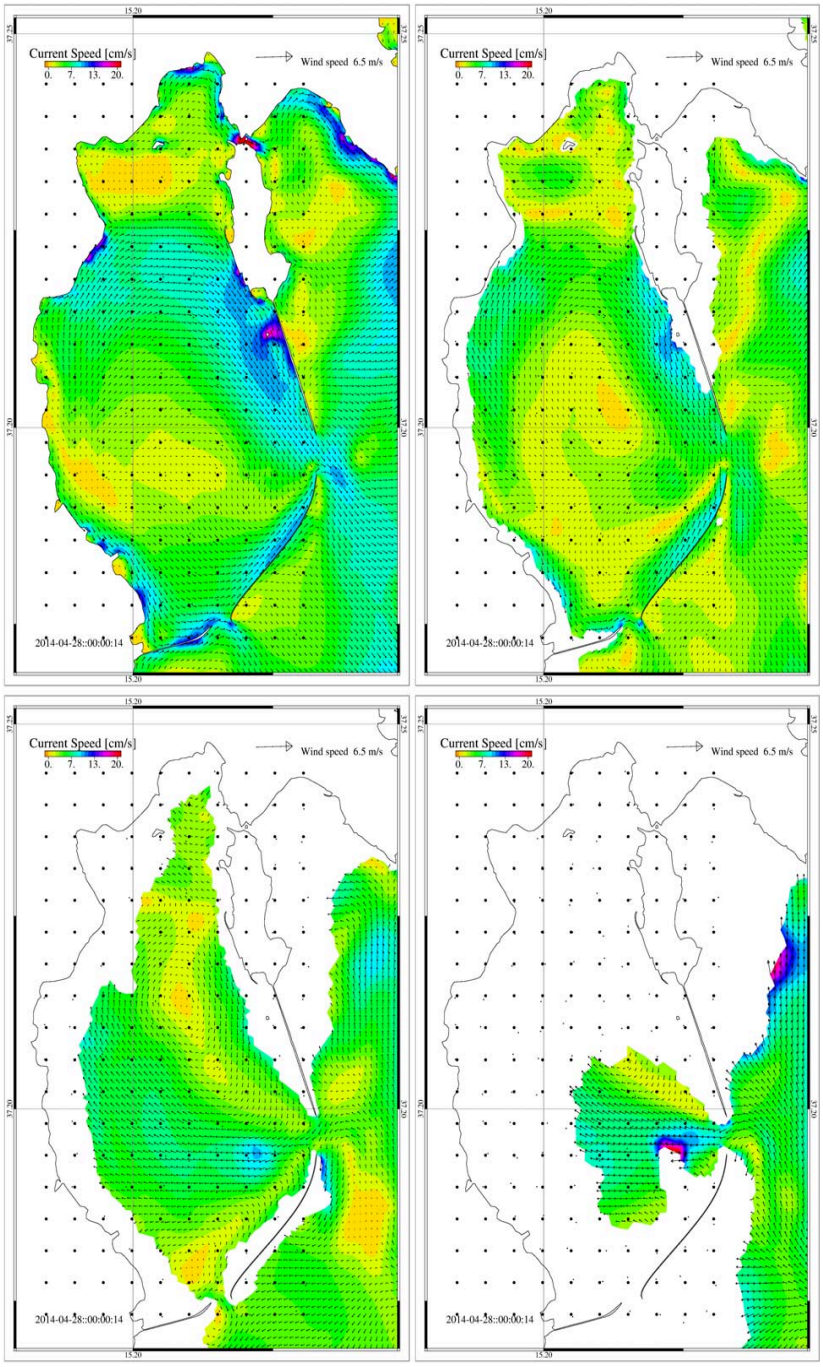

Figure S7. Velocity fields of marine currents computed by SHYFEM at different vertical levels in the Augusta harbour area. Black dots indicate the mesh points of the biogeochemical model domain. From left to right, the maps reproduce results obtained for the layers between 0-5 m, 5-10 m, 10-20 m e 20-30 m, respectively.

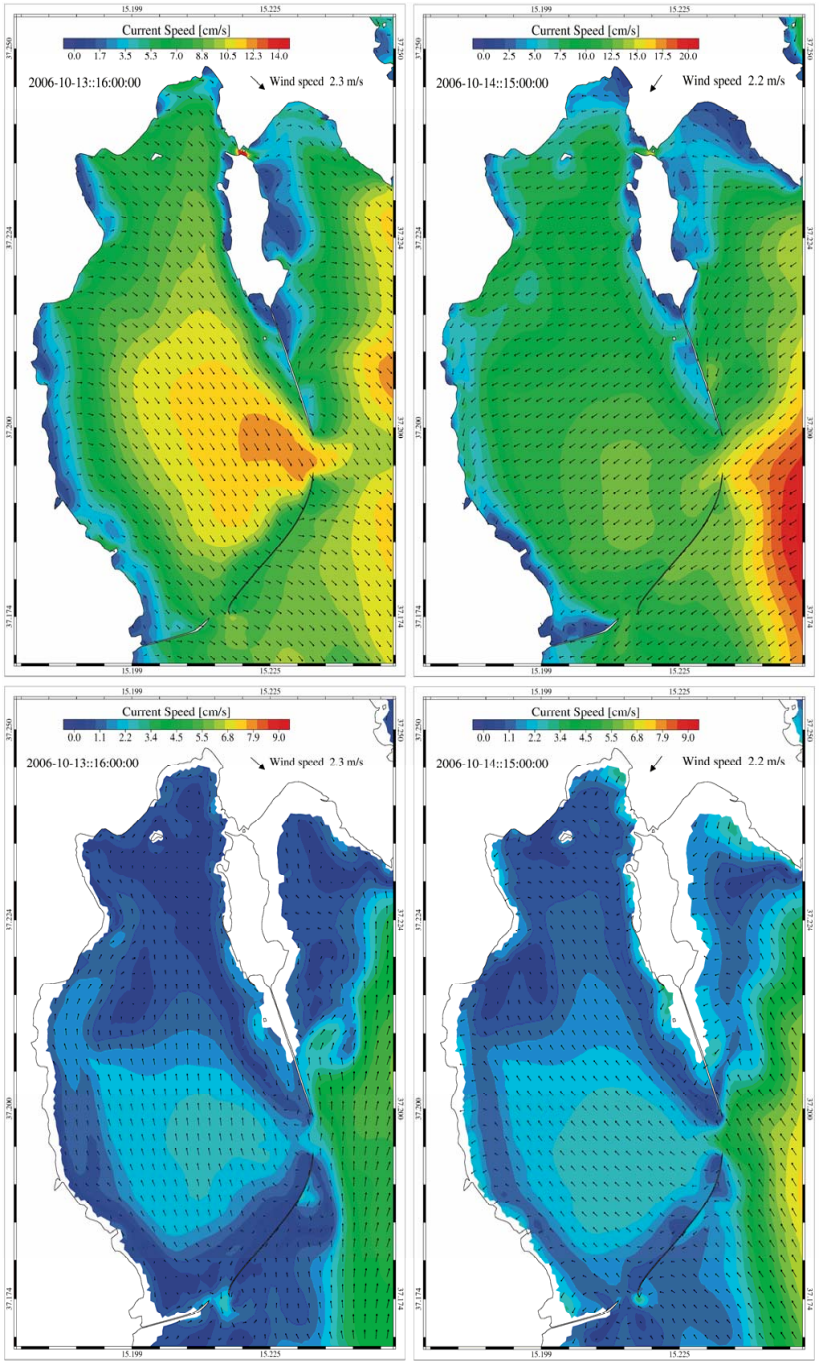

Figure S8. Current velocities at sea surface (upper panels) and deeper layers (bottom panels) computed at 16:00 of 13^{th} October 2006 (left panels) and at 15:00 of 14^{th} October 2006.

Symbol	Interpretation	Unit	Value	Reference
D_x	Horizontal turbulent diffusivity along x-axis	$m^2\ h^{-1}$	3600.0	Massel (1999)
D_y	Horizontal turbulent diffusivity along y-axis	$m^2\ h^{-1}$	3600.0	Massel (1999)
D_z	Vertical turbulent diffusivity along z-axis	$m^2\ h^{-1}$	1.2	Denman at al. (1983)
v_z	Vertical component of velocity field	$m\ h^{-1}$	0.0	Experimental data
k_D	Water-SPM partition coefficient for inorganic mercury	$l\ Kg^{-1}$	$10^{4.7}$	Experimental data
k_{Ph-de}	Rate constant for the photo-demethylation of methyl-mercury	h^{-1}	0.00216	Monperrus et al. (2007)
k_{deme}	Rate constant for the biotic demethylation of methyl-mercury	h^{-1}	0.014940	Lehnherr et al. (2011)
k_{me}	Rate constant for the methylation of inorganic mercury	h^{-1}	0.000272	Lehnherr et al. (2011)
v_{silt}	Silt settling velocity	$m\ h^{-1}$	0.208	Rosati et al. (2018)
k_{Dsilt}^{II}	Partition coefficient of Hg^{II} to silt	$l\ Kg^{-1}$	3000	Rosati et al. (2018)
k_{Dsilt}^{MM}	Partition coefficient of $MeHg$ to silt	$l\ Kg^{-1}$	1000	Rosati et al. (2018)
H	Henry's law constant	dimensionless	0.479	Experimental data
u_{wind}	Annual average wind speed	$m\ s^{-1}$	3.83	NASA website
PM_{CO_2}	Molar mass of carbon dioxide	$g\ mol^{-1}$	44.01	Periodic table of the elements
PM_{Hg^0}	Molar mass of elemental mercury	$g\ mol^{-1}$	200.59	Periodic table of the elements
PM_{H_2O}	Molar mass of water	$g\ mol^{-1}$	18.02	Periodic table of the elements
λ	Mercury recycling coefficient for picoeukaryotes population	dimensionless	0.52	Valenti et al. (2017)
D_{w-in}	Molecular diffusion coefficient for inorganic mercury	$m^2\ h^{-1}$	$2.534 \cdot 10^{-6}$	Schulz and Zabel (2006)
D_{w-or}	Molecular diffusion coefficient for methyl-mercury	$m^2\ h^{-1}$	$2.534 \cdot 10^{-6}$	Schulz and Zabel (2006)
δ_{sed}^{II}	Boundary layer thickness above sediment for inorganic mercury	m	0.00009	Calibration procedure
δ_{sed}^{MM}	Boundary layer thickness above sediment for methyl-mercury	m	0.00030	Calibration procedure
δ_w	Boundary layer thickness below sediment	m	0.0001	Sørensen et al. (2001)
K_{demeth}	Rate constant for the de-methylation of methyl-mercury in the pore water of the sediment	h^{-1}	0.007177	Hines et al. (2012)
K_{meth}	Rate constant for the methylation of inorganic mercury in the pore water of the sediment	h^{-1}	0.000503	Hines et al. (2012)
k_{MeHg}	Average fraction of methyl-mercury in the sediment	dimensionless	0.004	Experimental data
K_d^{II}	Sediment - pore water distribution coefficient for inorganic mercury	$l\ Kg^{-1}$	$10^{5.00}$	Liu et al. (2012)
K_d^{MM}	Sediment - pore water distribution coefficient for methyl-mercury	$l\ Kg^{-1}$	$10^{2.50}$	Liu et al. (2012)
α	De-adsorption rate for the total mercury concentration in the sediment	h^{-1}	$1.0 \cdot 10^{-7}$	Calibration procedure
dep	SPM deposition rate at the seawater-sediment interface	$mm\ y^{-1}$	11.7	Sprovieri et al.(2015)
ρ_{sed}	Surface sediment density	$g\ cm^{-3}$	2.6	Ogrinc et al.(2007)
$DepHg_{dry}^{II}$	Atmospheric dry deposition of Hg^{II}	$ng\ m^{-2}\ h^{-1}$	0.456	Rajar et al.(2007)
Hg_D^{bou}	Dissolved mercury concentration at the domain boundaries (Ionian sea)	$ng\ l^{-1}$	0.26	Horvat et al. (2003)
Hg_T^{bou}	Total mercury concentration at the domain boundaries (Ionian sea)	$ng\ l^{-1}$	0.31	Horvat et al. (2003)
L_{Lev}	Levante inlet width	m	400.0	Salvagio Manta et al. (2016)
L_{Sci}	Scirocco inlet width	m	300.0	Salvagio Manta et al. (2016)
Q_{source}	Average flow rate of water for point source	$m^3\ h^{-1}$	0.0	Field observations
Hg_{source}^0	Elemental mercury concentration of point source	$ng\ l^{-1}$	0.0	Field observations
Hg_{source}^{II}	Inorganic mercury concentration of point source	$ng\ l^{-1}$	0.0	Field observations
$MeHg_{source}$	Methyl-mercury concentration of point source	$ng\ l^{-1}$	0.0	Field observations
S_L^{II}	Direct loads of inorganic mercury	$ng\ l^{-1}\ h^{-1}$	0.0	Field observations
S_L^{MM}	Direct loads of methyl-mercury	$ng\ l^{-1}\ h^{-1}$	0.0	Field observations

Table S1: Environmental parameters used in the bio-geochemical model.

Symbol	Interpretation	Unit	Range	Periodicity	Reference
v_x	Horizontal velocity along x-axis	m h^{-1}	$0.0 - 0.5$	Three-hourly	Umgiesser (2009)
v_y	Horizontal velocity along y-axis	m h^{-1}	$0.0 - 0.5$	Three-hourly	Umgiesser (2009)
f_{org}	Organic fraction of suspended particulate matter in dissolved-phase	dimensionless	$0.004 - 0.010$	Constant	Experimental data
k_1	Rate constant for the photo-oxidation of elemental mercury	h^{-1}	$1.79 - 7.23$	Daily	Zhang et al. (2014)
k_2	Rate constant for the photo-reduction of inorganic mercury	h^{-1}	$0.43 - 1.75$	Daily	Zhang et al. (2014)
k_3	Rate constant for the biological oxidation of elemental mercury	h^{-1}	$0.00045 - 0.04830$	Three-hourly	Zhang et al. (2014)
k_4	Rate constant for the biological reduction of inorganic mercury	h^{-1}	$0.00028 - 0.02967$	Three-hourly	Zhang et al. (2014)
NPP	Net primary production	g C m^{-2} h^{-1}	$0.000386 - 0.007728$	Three-hourly	Baines et al.(1994)
T_{atm}	Surface atmospheric temperature	^{o}C	$11.52 - 29.83$	Daily	NASA website
$Hg_{gas-atm}$	Gaseous mercury concentration in atmosphere	ng m^{-3}	$1.50 - 2.10$	Daily	Bagnato et al. (2013)
Hg^{II}_{atm}	Inorganic mercury concentration in atmosphere	ng l^{-1}	$21.0 - 32.0$	Daily	Bagnato et al. (2013)
Pr	Daily amount of precipitation	mm	$0.41 - 3.33$	Monthly	NASA website
φ_{sed}	Porosity of the sediment	dimensionless	$0.18 - 0.56$	Constant	Experimental data
TOC_{sed}	Total organic carbon at the sediment surface	percent dry weight	$0.210 - 4.780$	Constant	Experimental data
Hg^{sed}_T	Initial total mercury concentration in sediment	mg Kg^{-1}	$0.005 - 300.000$	Constant	Sprovieri et al. (2011)
SPM	Suspended particulate matter conc. in seawater	mg l^{-1}	$18.4 - 31.0$	Constant	Experimental data
R_{in}	Nutrient concentration at the domain boundaries	mmol phos. m^{-3}	$0.010 - 0.100$	Constant	Experimental data
I_{in}	Incident light intensity at the water surface	$\mu mol\ ph.$ m^{-2} s^{-1}	$301.37 - 1524.30$	Daily	NASA website
$chla_{cell}$	Chl-a cellular content of picoeukaryotes	fg chl-a $cell^{-1}$	$10.00 - 660.00$	Constant	Brunet et al. (2007)
z_b	Depth of the water column	m	$0 - 30$	Constant	Sprovieri et al. (2015)

Table S2: Environmental variables used in the bio-geochemical model.

Symbol	Interpretation	Unit	Value	Reference
V_{cell}	Picoeukaryotes cell volume	μm^3 cell^{-1}	14.00	Experimental data
W_{phy}	Picoeukaryotes cell weight	μg cell^{-1}	0.000014	Strickland (1960)
VFC_{II}	Volume concentration factor for inorganic mercury	l Kg^{-1}	27500	Pickhardt and Fischer (2007)
VFC_{MM}	Volume concentration factor for methyl-mercury	l Kg^{-1}	800000	Pickhardt and Fischer (2007)
a_{growth}	Intercept of phytoplankton growth rate	dimensionless	0.22	Ciffroy (2015)
b_{growth}	Slope of phytoplankton growth rate	dimensionless	0.15	Ciffroy (2015)
k	Allometric rate exponent	dimensionless	0.25	Hendricks at al. (2007)
$p_{carbonphy}$	Organic carbon fraction of phytoplankton	dimensionless	0.29	Ciffroy (2015)
ρ_{lipid}	Lipid-layer permeation resistance	d	32.0	Hauck at al. (2011)
ρ_{water}	Water-layer diffusion resistance	d	0.0068	Hauck at al. (2011)
b_{lipid}	Lipid permeation resistance exponent	dimensionless	0.41	Hendricks at al. (2001)
$log_{10}K_d^{II}$	Water-Dissolved Organic Carbon partition coefficient for inorganic mercury	dimensionless	5.4	Allison and Allison (2005)
$log_{10}K_d^{MM}$	Water-Dissolved Organic Carbon partition coefficient for methyl-mercury	dimensionless	5.0	Allison and Allison (2005)
a_{bg}	Background turbidity	m^{-1}	0.060	Valenti et al. (2017)
a_1	Average absorption coefficient of picoeukaryotes	m^2 mg chl-a $^{-1}$	0.012	Hickman et al. (2010)
a_2	Average absorption coefficient of phytoplankton $> 3\mu m$	m^2 mg chl-a $^{-1}$	0.020	Hickman et al. (2010)
w	Sinking velocity of picoeukaryotes	m h^{-1}	0.000098	Valenti et al. (2017)
r	Maximum specific growth rate of picoeukaryotes	h^{-1}	0.096	Raven et al. (2005)
m_b	Specific loss rate of picoeukaryotes	h^{-1}	0.010	Veldhuis et al. (2005)
K_I	Half-saturation constant of light-limited growth of picoeukaryotes	μmol photons m^{-2} s^{-1}	67.50	Valenti et al. (2017)
K_R	Half-saturation constant of nutrient-limited growth of picoeukaryotes	mmol phosphorus m^{-3}	0.200	Valenti et al. (2017)
$1/Y$	Nutrient content of picoeukaryotes	mmol phosphorus cell^{-1}	2.00×10^{-12}	Timmermans et al. (2005)
ε	Nutrient recycling coefficient of picoeukaryotes	dimensionless	0.52	Valenti et al. (2017)

Table S3: Biological parameters used in the Phytoplankton model for mercury adsorption and Nutrient-Phytoplankton model.

	Experimental data		*Theoretical results*	
Station	*Latitude*	*Longitude*	*Latitude*	*Longitude*
1	37.23987	15.20895	37.23949	15.21003
2	37.23107	15.20865	37.23121	15.21003
3	37.23105	15.19742	37.23121	15.19981
4	37.22255	15.19837	37.22294	15.19981
5	37.21415	15.20992	37.21466	15.21003
6	37.21238	15.21960	37.21052	15.22024
7	37.20963	15.20972	37.21052	15.21003
10	37.20445	15.19772	37.20638	15.19981
11	37.20015	15.20268	37.20224	15.20492
12	37.19935	15.21425	37.19810	15.21514
13	37.19905	15.22560	37.19810	15.22535
15	37.19495	15.21528	37.193964	15.21514
17	37.19493	15.20853	37.19396	15.21003
20	37.18938	15.20723	37.18983	15.20492
21	37.18813	15.20765	37.18983	15.21003
23	37.19075	15.21442	37.18983	15.21514
24	37.19057	15.22560	37.18983	15.22535
25	37.18117	15.21388	37.18155	15.21514
26	37.17183	15.21913	37.17327	15.22024
27	37.19678	15.23880	37.19810	15.23046
$ST1$	37.19352	15.21455	37.19396	15.21514
$ST2$	37.21569	15.19763	37.21466	15.19981
$ST3$	37.17957	15.20695	37.18155	15.20492
$ST5$	37.20951	15.20962	37.21052	15.21003
$ST6$	37.19470	15.21552	37.19396	15.21514
$ST7$	37.18814	15.20757	37.18983	15.21003
$A3$	37.22650	15.20633	37.22708	15.20492
$A7$	37.20467	15.19467	37.20638	15.19470
$A9$	37.19333	15.20233	37.19396	15.19981
$A11$	37.18333	15.21350	37.18155	15.21514

Table S4: Latitude and longitude of all sampling sites considered in the analysis of experimental data and theoretical results.

Stat.	*Period*	*Depth* $[m]$	Hg^0 $[ng/l]$	Hg^{II} $[ng/l]$	$MeHg$ $[ng/l]$	Hg_D $[ng/l]$	Hg^0/Hg_D	Hg^{II}/Hg_D	$MeHg/Hg_D$
1	23 − 26/05/11	2.50	0.661	2.727	0.068	3.456	0.191	0.789	0.020
1	23 − 26/05/11	7.50	0.912	3.763	0.097	4.774	0.191	0.788	0.021
1	23 − 26/05/11	12.50	1.473	6.113	0.171	7.757	0.190	0.788	0.022
2	23 − 26/05/11	2.50	0.590	2.434	0.061	3.085	0.191	0.789	0.020
2	23 − 26/05/11	7.50	0.689	2.840	0.072	3.601	0.191	0.789	0.020
2	23 − 26/05/11	12.50	1.181	4.909	0.138	6.228	0.190	0.788	0.022
3	23 − 26/05/11	2.50	0.630	2.600	0.061	3.291	0.191	0.790	0.019
3	23 − 26/05/11	7.50	0.751	3.110	0.076	3.937	0.191	0.790	0.019
4	23 − 26/05/11	2.50	0.662	2.733	0.063	3.458	0.192	0.790	0.018
4	23 − 26/05/11	7.50	0.733	3.033	0.075	3.841	0.190	0.790	0.020
5	23 − 26/05/11	2.50	0.764	3.152	0.072	3.988	0.192	0.790	0.018
5	23 − 26/05/11	7.50	0.813	3.357	0.079	4.249	0.191	0.790	0.019
5	23 − 26/05/11	12.50	0.910	3.792	0.103	4.805	0.189	0.789	0.022
6	23 − 26/05/11	2.50	0.653	2.696	0.063	3.412	0.191	0.790	0.019
6	23 − 26/05/11	7.50	0.590	2.436	0.057	3.083	0.191	0.790	0.019
6	23 − 26/05/11	12.50	0.430	1.791	0.046	2.267	0.190	0.790	0.020
10	23 − 26/05/11	2.50	1.486	6.132	0.151	7.769	0.191	0.789	0.020
10	23 − 26/05/11	7.50	1.941	8.009	0.219	10.169	0.191	0.788	0.021
10	23 − 26/05/11	17.50	2.396	9.896	0.291	12.583	0.190	0.787	0.023
11	23 − 26/05/11	2.50	1.014	4.183	0.098	5.295	0.191	0.790	0.019
11	23 − 26/05/11	7.50	1.173	4.838	0.118	6.129	0.192	0.789	0.019
11	23 − 26/05/11	17.50	2.186	9.081	0.272	11.539	0.189	0.787	0.024
12	23 − 26/05/11	2.50	0.663	2.738	0.060	3.461	0.192	0.791	0.017
12	23 − 26/05/11	12.50	0.769	3.173	0.076	4.018	0.191	0.790	0.019
12	23 − 26/05/11	22.50	1.495	6.374	0.198	8.069	0.185	0.790	0.025
13	23 − 26/05/11	2.50	0.343	1.414	0.031	1.788	0.192	0.791	0.017
13	23 − 26/05/11	17.50	0.369	1.523	0.038	1.930	0.191	0.789	0.020
13	23 − 26/05/11	27.50	0.291	1.209	0.034	1.534	0.190	0.788	0.022
17	23 − 26/05/11	2.50	0.531	2.192	0.049	2.772	0.192	0.790	0.018
17	23 − 26/05/11	12.50	0.704	2.903	0.074	3.681	0.191	0.789	0.020
17	23 − 26/05/11	22.50	1.365	5.685	0.176	7.226	0.189	0.787	0.024
20	23 − 26/05/11	2.50	1.023	4.222	0.109	5.354	0.191	0.789	0.020
20	23 − 26/05/11	12.50	2.342	9.675	0.286	12.303	0.190	0.786	0.023
20	23 − 26/05/11	17.50	2.676	11.161	0.352	14.189	0.189	0.786	0.025
23	23 − 26/05/11	2.50	0.378	1.561	0.037	1.976	0.191	0.790	0.019
23	23 − 26/05/11	12.50	0.524	2.161	0.057	2.742	0.191	0.788	0.021
23	23 − 26/05/11	22.50	1.392	6.024	0.199	7.615	0.183	0.791	0.026
24	23 − 26/05/11	2.50	0.164	0.676	0.016	0.856	0.192	0.790	0.019
24	23 − 26/05/11	7.50	0.218	0.898	0.023	1.139	0.191	0.788	0.020
24	23 − 26/05/11	17.50	0.474	2.039	0.064	2.577	0.184	0.791	0.025
25	23 − 26/05/11	2.50	2.205	9.096	0.254	11.555	0.191	0.787	0.022
25	23 − 26/05/11	7.50	3.900	16.088	0.483	20.471	0.190	0.786	0.024
25	23 − 26/05/11	12.50	7.804	32.755	1.075	41.634	0.187	0.787	0.026
26	02/02/12	2.50	0.162	0.671	0.022	0.855	0.189	0.785	0.026
26	02/02/12	7.50	1.079	4.522	0.152	5.753	0.188	0.786	0.026
27	02/02/12	2.50	0.016	0.068	0.002	0.086	0.186	0.791	0.023
27	02/02/12	12.50	0.452	1.859	0.050	2.361	0.192	0.787	0.021
27	02/02/12	22.50	0.349	1.472	0.044	1.865	0.187	0.789	0.024
7	23 − 26/06/12	2.50	0.879	3.629	0.083	4.591	0.192	0.790	0.018
7	23 − 26/06/12	12.50	1.098	4.533	0.115	5.746	0.191	0.789	0.020
7	23 − 26/06/12	17.50	1.452	6.034	0.172	7.658	0.190	0.788	0.022
15	23 − 26/06/12	2.50	0.387	1.596	0.036	2.019	0.192	0.790	0.018
15	23 − 26/06/12	12.50	0.298	1.228	0.032	1.558	0.191	0.788	0.021
15	23 − 26/06/12	22.50	1.022	4.487	0.152	5.661	0.180	0.793	0.027
21	23 − 26/06/12	2.50	0.574	2.367	0.057	2.998	0.191	0.790	0.019
21	23 − 26/06/12	17.50	1.269	5.233	0.152	6.654	0.191	0.786	0.023
21	23 − 26/06/12	22.50	1.637	6.818	0.211	8.666	0.189	0.787	0.024
*A*3	19 − 23/10/17	2.50	0.078	0.324	0.009	0.411	0.190	0.788	0.022
*A*3	19 − 23/10/17	12.50	0.139	0.588	0.018	0.745	0.187	0.789	0.024
*A*7	19 − 23/10/17	2.50	0.136	0.560	0.016	0.712	0.191	0.787	0.022
*A*7	19 − 23/10/17	17.50	0.040	0.203	0.007	0.250	0.160	0.812	0.028
*A*9	19 − 23/10/17	2.50	0.247	1.022	0.032	1.301	0.190	0.786	0.025
*A*9	19 − 23/10/17	17.50	1.278	6.668	0.232	8.178	0.156	0.815	0.029
*A*11	19 − 23/10/17	2.50	0.040	0.166	0.005	0.211	0.189	0.787	0.024
*A*11	19 − 23/10/17	12.50	1.437	6.916	0.241	8.594	0.167	0.805	0.028

Table S5: Dissolved mercury concentration: comparison between experimental data and theoretical results for all sampling sites. The detection limit (d.l.) for mercury concentration is set at 1.9 ng/l.

		Experimental data		*Theoretical results*	
Station	*Period*	*Depth* $[m]$	$MeHg\ [ng/l]$	*Depth* $[m]$	$MeHg\ [ng/l]$
$A3$	$19-23/10/17$	2.00	0.006	2.50	0.009
$A3$	$19-23/10/17$	17.00	0.017	12.50	0.018
$A7$	$19-23/10/17$	2.00	0.016	2.50	0.016
$A7$	$19-23/10/17$	21.00	0.009	17.50	0.007
$A9$	$19-23/10/17$	2.00	0.017	2.50	0.032
$A9$	$19-23/10/17$	22.00	0.026	17.50	0.232
$A11$	$19-23/10/17$	2.00	0.009	2.50	0.005
$A11$	$19-23/10/17$	21.00	0.016	12.50	0.241

Table S6: Methyl-mercury concentration in seawater: comparison between experimental data and theoretical results for all sampling sites investigated during the oceanographic survey of October 2017.

		Experimental data		*Theoretical results*	
Station	*Period*	*Depth* $[m]$	Hg_D $[ng/l]$	*Depth* $[m]$	Hg_D $[ng/l]$
1	$23-26/05/11$	1.40	3.200	2.50	3.456
1	$23-26/05/11$	6.20	6.700	7.50	4.774
1	$23-26/05/11$	11.20	$\leq d.l.$	12.50	7.757
2	$23-26/05/11$	2.21	$\leq d.l.$	2.50	3.085
2	$23-26/05/11$	6.71	$\leq d.l.$	7.50	3.601
2	$23-26/05/11$	10.65	$\leq d.l.$	12.50	6.228
3	$23-26/05/11$	2.26	$\leq d.l.$	2.50	3.291
3	$23-26/05/11$	4.60	$\leq d.l.$	2.50	3.291
3	$23-26/05/11$	8.40	$\leq d.l.$	7.50	3.937
4	$23-26/05/11$	0.10	$\leq d.l.$	2.50	3.458
4	$23-26/05/11$	3.12	3.200	7.50	3.458
5	$23-26/05/11$	1.00	$\leq d.l.$	2.50	3.988
5	$23-26/05/11$	9.20	$\leq d.l.$	7.50	4.249
5	$23-26/05/11$	15.88	$\leq d.l.$	12.50	4.805
6	$23-26/05/11$	1.98	$\leq d.l.$	2.50	3.412
6	$23-26/05/11$	6.74	$\leq d.l.$	7.50	3.083
6	$23-26/05/11$	13.54	$\leq d.l.$	12.50	2.267
10	$23-26/05/11$	1.00	3.200	2.50	7.769
10	$23-26/05/11$	9.50	14.300	7.50	10.169
10	$23-26/05/11$	19.20	7.300	17.50	12.583
11	$23-26/05/11$	1.42	$\leq d.l.$	2.50	5.295
11	$23-26/05/11$	10.00	$\leq d.l.$	7.50	6.129
11	$23-26/05/11$	18.15	3.300	17.50	11.539
12	$23-26/05/11$	1.63	3.200	2.50	3.461
12	$23-26/05/11$	13.50	3.200	12.50	4.018
12	$23-26/05/11$	23.41	11.800	22.50	8.069
13	$23-26/05/11$	2.40	3.200	2.50	1.788
13	$23-26/05/11$	16.90	8.900	17.50	1.930
13	$23-26/05/11$	29.30	$\leq d.l.$	27.50	1.534
17	$23-26/05/11$	1.20	7.500	2.50	2.772
17	$23-26/05/11$	11.45	19.800	12.50	3.681
17	$23-26/05/11$	21.90	$\leq d.l.$	22.50	7.226
20	$23-26/05/11$	0.50	12.600	2.50	5.354
20	$23-26/05/11$	11.30	14.600	12.50	12.303
20	$23-26/05/11$	16.45	14.600	17.50	14.189
23	$23-26/05/11$	2.40	21.300	2.50	1.976
23	$23-26/05/11$	11.24	$\leq d.l.$	12.50	2.742
23	$23-26/05/11$	20.55	20.300	22.50	7.615
24	$23-26/05/11$	1.00	6.000	2.50	0.856
24	$23-26/05/11$	9.40	8.900	7.50	1.139
24	$23-26/05/11$	16.30	$\leq d.l.$	17.50	2.577
25	$23-26/05/11$	1.60	6.000	2.50	11.555
25	$23-26/05/11$	7.30	14.600	7.50	20.471
25	$23-26/05/11$	12.70	3.200	12.50	41.634
26	02/02/12	2.00	$\leq d.l.$	2.50	0.855
26	02/02/12	8.00	5.550	7.50	5.753
27	02/02/12	2.00	$\leq d.l.$	2.50	0.086
27	02/02/12	11.50	$\leq d.l.$	12.50	2.361
27	02/02/12	27.00	3.550	22.50	1.865
7	$23-26/06/12$	1.00	$\leq d.l.$	2.50	4.591
7	$23-26/06/12$	13.50	$\leq d.l.$	12.50	5.746
7	$23-26/06/12$	21.00	$\leq d.l.$	17.50	7.658
15	$23-26/06/12$	1.00	2.550	2.50	2.019
15	$23-26/06/12$	11.50	4.950	12.50	1.558
15	$23-26/06/12$	26.00	2.350	22.50	5.661
21	$23-26/06/12$	1.00	$\leq d.l.$	2.50	2.998
21	$23-26/06/12$	16.00	6.350	17.50	6.654
21	$23-26/06/12$	22.00	$\leq d.l.$	22.50	8.666
$A3$	$19-23/10/17$	2.00	$\leq d.l.$	2.50	0.411
$A3$	$19-23/10/17$	17.00	$\leq d.l.$	12.50	0.745
$A7$	$19-23/10/17$	2.00	$\leq d.l.$	2.50	0.712
$A7$	$19-23/10/17$	21.00	$\leq d.l.$	17.50	0.250
$A9$	$19-23/10/17$	2.00	9.032	2.50	1.301
$A9$	$19-23/10/17$	22.00	17.785	17.50	8.178
$A11$	$19-23/10/17$	2.00	$\leq d.l.$	2.50	0.211
$A11$	$19-23/10/17$	21.00	6.545	12.50	8.594

Table S7: Dissolved mercury concentration: comparison between experimental data and theoretical results for all sampling sites. The detection limit (d.l.) for mercury concentration is set at 1.9 ng/l.

		Experimental data		*Theoretical results*	
Station	*Period*	*Depth* $[m]$	Hg_T $[ng/l]$	*Depth* $[m]$	Hg_T $[ng/l]$
1	$23-26/05/11$	1.40	9.171	2.50	6.610
1	$23-26/05/11$	6.20	9.171	7.50	8.951
1	$23-26/05/11$	11.20	17.771	12.50	14.262
2	$23-26/05/11$	2.21	$\leq d.l.$	2.50	5.982
2	$23-26/05/11$	6.71	14.871	7.50	6.788
2	$23-26/05/11$	10.65	17.671	12.50	11.415
3	$23-26/05/11$	2.26	$\leq d.l.$	2.50	6.367
3	$23-26/05/11$	4.60	11.971	2.50	6.367
3	$23-26/05/11$	8.40	29.971	7.50	7.422
4	$23-26/05/11$	0.10	$\leq d.l.$	2.50	6.694
4	$23-26/05/11$	3.12	6.271	2.50	6.694
5	$23-26/05/11$	1.00	9.171	2.50	7.731
5	$23-26/05/11$	9.20	7.071	7.50	8.013
5	$23-26/05/11$	15.88	17.671	12.50	8.816
6	$23-26/05/11$	1.98	6.271	2.50	6.365
6	$23-26/05/11$	6.74	3.371	7.50	5.756
6	$23-26/05/11$	13.54	20.571	12.50	4.242
10	$23-26/05/11$	1.00	4.271	2.50	15.422
10	$23-26/05/11$	9.50	15.871	7.50	16.797
10	$23-26/05/11$	19.20	14.871	17.50	23.441
11	$23-26/05/11$	1.42	14.871	2.50	10.010
11	$23-26/05/11$	10.00	14.871	7.50	15.914
11	$23-26/05/11$	18.15	23.471	17.50	22.821
12	$23-26/05/11$	1.63	17.671	2.50	6.312
12	$23-26/05/11$	13.50	3.371	12.50	7.686
12	$23-26/05/11$	23.41	19.271	22.50	15.922
13	$23-26/05/11$	2.40	17.671	2.50	3.241
13	$23-26/05/11$	16.90	12.671	17.50	3.635
13	$23-26/05/11$	29.30	3.371	27.50	2.903
17	$23-26/05/11$	1.20	26.271	2.50	5.006
17	$23-26/05/11$	11.45	129.271	12.50	7.280
17	$23-26/05/11$	21.90	127.071	22.50	14.969
20	$23-26/05/11$	0.50	12.600	2.50	9.620
20	$23-26/05/11$	11.30	23.500	12.50	24.837
20	$23-26/05/11$	16.45	28.200	17.50	30.291
23	$23-26/05/11$	2.40	23.371	2.50	3.541
23	$23-26/05/11$	11.24	20.571	12.50	5.027
23	$23-26/05/11$	20.55	57.771	22.50	14.272
24	$23-26/05/11$	1.00	11.971	2.50	1.533
24	$23-26/05/11$	9.40	18.671	7.50	2.055
24	$23-26/05/11$	16.30	2.271	17.50	4.759
25	$23-26/05/11$	1.60	22.571	2.50	20.562
25	$23-26/05/11$	7.30	31.971	7.50	36.186
25	$23-26/05/11$	12.70	34.871	12.50	73.210
26	02/02/12	2.00	4.554	2.50	1.507
26	02/02/12	8.00	11.054	7.50	10.160
27	02/02/12	2.00	4.554	2.50	0.155
27	02/02/12	11.50	4.804	12.50	4.674
27	02/02/12	27.00	6.104	22.50	3.494
7	$23-26/06/12$	1.00	1.854	2.50	8.724
7	$23-26/06/12$	13.50	9.854	12.50	10.841
7	$23-26/06/12$	21.00	1.750	17.50	14.529
15	$23-26/06/12$	1.00	5.954	2.50	3.647
15	$23-26/06/12$	11.50	8.554	12.50	2.952
15	$23-26/06/12$	26.00	15.687	22.50	11.097
21	$23-26/06/12$	1.00	1.020	2.50	5.383
21	$23-26/06/12$	16.00	14.854	17.50	9.908
21	$23-26/06/12$	22.00	18.090	22.50	17.042
$A3$	$19-23/10/17$	2.00	$\leq d.l.$	2.50	0.801
$A3$	$19-23/10/17$	17.00	$\leq d.l.$	12.50	1.365
$A7$	$19-23/10/17$	2.00	$\leq d.l.$	2.50	1.429
$A7$	$19-23/10/17$	21.00	$\leq d.l.$	17.50	0.470
$A9$	$19-23/10/17$	2.00	12.182	2.50	2.337
$A9$	$19-23/10/17$	22.00	25.132	17.50	18.615
$A11$	$19-23/10/17$	2.00	$\leq d.l.$	2.50	0.375
$A11$	$19-23/10/17$	21.00	12.482	12.50	15.275

Table S8: Total mercury concentration: comparison between experimental data and theoretical results for all sampling sites. The detection limit (d.l.) for mercury concentration is set at 1.9 ng/l.

		Experimental data	*Theoretical results*
Station	*Period*	*Benthic flux* [$\mu g/(\mathrm{m}^2\ \mathrm{d})$]	*Benthic flux* [$\mu g/(\mathrm{m}^2\ \mathrm{d})$]
9	$19-21/09/11$	23.000	35.331
18	$19-21/09/11$	56.000	46.326
22	$19-21/09/11$	8.700	23.039
7	$23-26/06/12$	23.000	19.890
15	$23-26/06/12$	92.000	101.936
21	$23-26/06/12$	21.000	21.052

Table S9: Benthic mercury flux: comparison between experimental data and theoretical results for six sampling sites.

		Experimental data	*Theoretical results*
Station	*Period*	*Atmospheric flux* $[ng/(\mathrm{m}^2\ \mathrm{h})]$	*Atmospheric flux* $[ng/(\mathrm{m}^2\ \mathrm{h})]$
$ST1$	29/11/11	36.000	35.282
$ST2$	29/11/11	14.400	17.655
$ST3$	30/11/11	72.000	43.980
$ST5$	24/06/12	10.800	24.303
$ST6$	23/06/12	7.200	10.627
$ST7$	25/06/12	18.000	15.811

Table S10: Mercury evasion flux: comparison between experimental data and theoretical results for six sampling sites.

Symbol	Interpretation	Year	Unit	Value
O_{Lev_1}	Total mercury outflow from the Levante inlet to the open sea	2005	$Kmol/year$	0.060
O_{Sci_1}	Total mercury outflow from the Scirocco inlet to the open sea	2005	$Kmol/year$	0.119
O_1	Total mercury outflow from the basin to the open sea	2005	$Kmol/year$	0.179
B_1	Dissolved mercury release from the sediment of the basin	2005	$Kmol/year$	3.110
V_1	Gaseous elemental mercury evasion from the basin into the atmosphere	2005	$Kmol/year$	0.022
S_1	Amount of mercury recycled for scavenging within the Augusta basin	2005	$Kmol/year$	0.088
D_1	Total mercury recycled within the Augusta basin	2005	$Kmol/year$	2.911
O_{Lev_2}	Total mercury outflow from the Levante inlet to the open sea	2011	$Kmol/year$	0.050
O_{Sci_2}	Total mercury outflow from the Scirocco inlet to the open sea	2011	$Kmol/year$	0.082
O_2	Total mercury outflow from the basin to the open sea	2011	$Kmol/year$	0.132
B_2	Dissolved mercury release from the sediment of the basin	2011	$Kmol/year$	2.648
V_2	Gaseous elemental mercury evasion from the basin into the atmosphere	2011	$Kmol/year$	0.019
S_2	Amount of mercury recycled for scavenging within the Augusta basin	2011	$Kmol/year$	0.072
D_2	Total mercury recycled within the Augusta basin	2011	$Kmol/year$	2.499
O_{Lev_3}	Total mercury outflow from the Levante inlet to the open sea	2017	$Kmol/year$	0.045
O_{Sci_3}	Total mercury outflow from the Scirocco inlet to the open sea	2017	$Kmol/year$	0.069
O_3	Total mercury outflow from the basin to the open sea	2017	$Kmol/year$	0.114
B_3	Dissolved mercury release from the sediment of the basin	2017	$Kmol/year$	2.451
V_3	Gaseous elemental mercury evasion from the basin into the atmosphere	2017	$Kmol/year$	0.018
S_3	Amount of mercury recycled for scavenging within the Augusta basin	2017	$Kmol/year$	0.066
D_3	Total mercury recycled within the Augusta basin	2017	$Kmol/year$	2.321
O_{Lev_4}	Total mercury outflow from the Levante inlet to the open sea	2054	$Kmol/year$	0.032
O_{Sci_4}	Total mercury outflow from the Scirocco inlet to the open sea	2054	$Kmol/year$	0.050
O_4	Total mercury outflow from the basin to the open sea	2054	$Kmol/year$	0.082
B_4	Dissolved mercury release from the sediment of the basin	2054	$Kmol/year$	1.978
V_4	Gaseous elemental mercury evasion from the basin into the atmosphere	2054	$Kmol/year$	0.014
S_4	Amount of mercury recycled for scavenging within the Augusta basin	2054	$Kmol/year$	0.050
D_4	Total mercury recycled within the Augusta basin	2054	$Kmol/year$	1.884
O_{Lev_5}	Total mercury outflow from the Levante inlet to the open sea	2104	$Kmol/year$	0.027
O_{Sci_5}	Total mercury outflow from the Scirocco inlet to the open sea	2104	$Kmol/year$	0.042
O_5	Total mercury outflow from the basin to the open sea	2104	$Kmol/year$	0.069
B_5	Dissolved mercury release from the sediment of the basin	2104	$Kmol/year$	1.742
V_5	Gaseous elemental mercury evasion from the basin into the atmosphere	2104	$Kmol/year$	0.012
S_5	Amount of mercury recycled for scavenging within the Augusta basin	2104	$Kmol/year$	0.043
D_5	Total mercury recycled within the Augusta basin	2104	$Kmol/year$	1.663
O_{Lev_6}	Total mercury outflow from the Levante inlet to the open sea	2254	$Kmol/year$	0.018
O_{Sci_6}	Total mercury outflow from the Scirocco inlet to the open sea	2254	$Kmol/year$	0.034
O_6	Total mercury outflow from the basin to the open sea	2254	$Kmol/year$	0.052
B_6	Dissolved mercury release from the sediment of the basin	2254	$Kmol/year$	1.385
V_6	Gaseous elemental mercury evasion from the basin into the atmosphere	2254	$Kmol/year$	0.009
S_6	Amount of mercury recycled for scavenging within the Augusta basin	2254	$Kmol/year$	0.032
D_6	Total mercury recycled within the Augusta basin	2254	$Kmol/year$	1.326
A	Input of dissolved mercury from anthropogenic activities		$Kmol/year$	0.000
AD	Atmospheric mercury deposition		$Kmol/year$	$2.210 \cdot 10^{-3}$

Table S11: Mass balance of mercury in the Augusta basin simulated for six different years (2005, 2011, 2017, 2054, 2104, and 2254).

		Experimental data		*Theoretical results*	
Station	*Period*	*Depth* $[m]$	Hg_{pw} $[ng/l]$	*Depth* $[m]$	Hg_{pw} $[ng/l]$
8	$23-26/05/11$	0.11	87.225	0.10	90.129
16	$23-26/05/11$	0.11	98.538	0.10	94.235

Table S12: Mercury concentration in the pore water: comparison between experimental data and theoretical results for the sampling sites investigated during the oceanographic survey of May 2011.